Aus dem Institut für Chirurgische Forschung
(im Walter-Brendel-Zentrum für Experimentelle Medizin (WBex))
der Ludwig-Maximilians-Universität München

Vorstand: Prof. Dr. med. Ulrich Pohl

Functional Characterization of the Transcription Factor Early growth response 1 (Egr1) in Arteriogenesis

Dissertation
zum Erwerb des Doktorgrades der Medizin
an der Medizinischen Fakultät der
Ludwig-Maximilians-Universität zu München

vorgelegt von
Judith-Irina Carola Pagel

aus
Giessen

im Jahr
2014

Mit Genehmigung der Medizinischen Fakultät
der Universität München

Berichterstatter:	PD Dr. rer. nat. Elisabeth Deindl
Mitberichterstatter:	Prof. Dr. med. Jens Waschke
	Prof. Dr. med. Martin Dichgans
	Prof. Dr. med. Christian Schulz
Mitbetreuung durch den Promovierten Mitarbeiter	
Dekan:	Prof. Dr. med. Dr. h.c. M. Reiser, FACR, FRCR
Tag der mündlichen Prüfung:	11.12.2014

Meinen Eltern

Teile dieser Arbeit wurden publiziert in Thrombosis & Hemostasis 2012; 107(3):562-74.

TABLE OF CONTENTS

I INTRODUCTION 1

1 CARDIOVASCULAR DISEASES–A CONTINOUSLY SPREADING EPIDEMIC .. 1
1.1 Cause of disease 1
1.2 New therapeutic strategies 2
1.3 Discovery of a collateral circulation 2

2 FORMATION OF BLOOD VESSELS 3
2.1 Vasculogenesis 3
2.2 Angiogenesis 4
2.3 Arteriogenesis 6

3 MECHANISMS PROMOTING ARTERIOGENESIS 7
3.1 Hemodynamic forces 7
3.2 Monocyte recruitment 9
3.2.1 Monocyte chemoattractant protein 1(MCP-1) 10
3.2.2 Intercellular adhesion molecule 1 (ICAM-1) 10
3.2.3 Urokinase-type plasminogen activator (uPA) 11
3.3 Vascular cell proliferation and differentiation 11

4 THE TRANSCRIPTION FACTOR EARLY GROWTH RESPONSE (EGR1) 12
4.1 Structural properties 12
4.1.1 The Egr1 promoter 12
4.1.2 The EGR1 protein 13
4.2. Function and associated downstream targets 14
4.3 The EGR-family 15

II OBJECT OF THE STUDY 16

III MATERIALS AND METHODS 17

1 MATERIALS 17
1.1 Mice strains 17
1.1.1 C57Bl/6N 17
1.1.2 $Egr1^{-/-}$ 17
1.2 Surgical instruments and expendable material 17
1.3 Chemicals and special equipment 18
1.4 Pharmaceuticals 19
1.5 Primers for qRT-PCR 20
1.6 Special buffers and solutions 21
1.7 Antibodies 22
1.7.1 Primary antibodies 22
1.7.2 Secondary antibodies 23
1.8 Devices 23
1.9 Software 23

2 METHODS 24
2.1 Animal model 24
2.1.1 Anesthesia protocols 24
2.1.2 Femoral artery ligation 25
2.1.3 Isolation of tissue 26
2.2 Laser Doppler perfusion measurements 28
2.2.1 Technical background 29
2.2.2 Measurements 29
2.2.3 Evaluation of flux images 30
2.3 qRT-PCR 31
2.3.1 Total RNA Isolation 31
2.3.2 Agarose gel electrophoresis 32
2.3.3 cDNA Synthesis and qRT-PCR 32
2.4 Western Blot 34
2.4.1 Protein isolation and determination of concentration 34
2.4.2 Sodium dodecyl sulfate-polyacrylamide gel electrophoresis (SDS-PAGE) 34
2.4.3 Blotting 34
2.4.4 Detection of immunoreactive bands 35
2.5 Immunohistochemistry 35
2.5.1 EGR1 staining 35
2.5.2 Leukocyte quantification 36
2.6. Fluorescent activated cell sorting (FACS) 36
2.6.1 FACS analysis of whole blood 36
2.6.2 FACS analysis of whole adductor muscle 36
2.7. Statistical analyses 37

IV RESULTS 38

1 GENERAL OBSERVATIONS 38

2 PARTICIPATION OF EGR1 IN COLLATERAL ARTERY GROWTH 38
2.1 Perfusion recovery in wildtype and Egr1 deficient mice 38
2.2 Egr1 expression in arteriogenesis 40

3 EGR1 INFLUENCES ON CELL COUNTS AND LEUKOCYTE DISTRIBUTION 42
3.1 Leukocyte recruitment 42
3.2 Expression of ICAM-1, MCP-1 and uPA 44

4 PARTICIPATION OF THE OTHER EGR FAMILY MEMBERS 45

5 INFLUENCES ON VASCULAR CELL PROLIFERATION 46
5.1 Cell cycle progression 46
5.2 vSMC phenotype switch 47

V DISCUSSION 49

1 THE MURINE ARTERIOGENESIS MODEL 49
1.1 Why using the murine peripheral femoral artery ligation model? 49
1.2 Comparison to a coronary ligation model 51
1.3 Peripheral arteriogenesis models in different species 51
1.4 The influence of gender 52

2 EGR1 AND ARTERIOGENESIS 53

3 LEUKOCYTE RECRUITMENT 55

4 EXPRESSION OF EGR FAMILY MEMBERS – EVIDENCE FOR COMPENSATION 57

5 CELL CYCLE PROGRESSION AND PROLIFERATION 59
5.1 Expression of cyclins in growing collaterals 59
5.2 vSMC phenotype switch: role of SF-1 and αSM-actin 60

VI PERSPECTIVE: THE PROSPECTS OF CLINICAL ARTERIOGENESIS THERAPY 63

VII SUMMARY 65

VIII ZUSAMMENFASSUNG 66

IX REFERENCES 68

X LIST OF ABBREVIATIONS 77

XI DANKSAGUNG 80

XII EIDESSTATTLICHE VERSICHERUNG 81

I. INTRODUCTION

1 CARDIOVASCULAR DISEASES – A CONTINOUSLY SPREADING EPIDEMIC

Pathologies affecting heart and blood vessels such as coronary heart disease, cerebrovascular disease or peripheral arterial disease, are grouped under the term cardiovascular diseases (CVDs). They remain the major global cause of death representing 30% of the total number of deaths worldwide. Currently, 17.3 million fatal casualties per year are caused by CVDs, among them 7.3 million due to coronary heart disease and 6.2 million due to stroke.[1] These numbers show a strong tendency to enlarge. For 2030, the World Health Organization (WHO) is currently projecting a number of 23.3 million deaths due to CVDs.[1] Therefore, an early case specific medical treatment on the one hand, and prevention on the other hand is and will be vital.

1.1 Cause of disease

In most cases, the etiology and the correspondent histopathologic finding in these patients is atherosclerosis. It is characterized by intima damage resulting from cholesterol deposits into the arterial wall and a subsequent incomplete inflammatory response due to failure of adequate phagocytosis of oxidized cholesterol by macrophages.[2] Their degradation to foam cells and the accumulation of cell debris does not only further chronic vessel wall damage and inflammation but also the hardening of the vessel. The accumulation of foam cells, called atheromatous plaque, can be instable (i.e. vulnerable), and is prone to rupture thus occluding the arterial vessel. The clinical presentation of temporary arterial occlusions is, for example, recurrent episodes of chest pain, transient ischemic attacks or intermittent claudication in peripheral arterial disease.

Prevention is the best form of medicine comprising the reduction of risk factors (RFs) leading to atherosclerosis to reduce the incidence of disease. Due to the high morbidity, CVDs have become a serious burden for every health care system in the western world and are already escalating in newly industrialized countries. Ironically, the alleged advantages of a modern, comfortable lifestyle promote their prevalence. Risk factors are generally classified in modifiable risk factors such as an unhealthy diet, physical inactivity, tobacco abuse, hyperlipidemia, hypertension, diabetes or the metabolic syndrome and non-modifiable RFs like age, sex or genetic predisposition evidencing that not every risk factor for atherosclerosis is in fact controllable.[3] However, 80% of coronary heart disease and cerebrovascular disease are indeed due to the behavioral risk factors physical inactivity, unhealthy diet and tobacco abuse.[1] So although promising, preventive medicine has not been successful to efficiently reduce the prevalence of those behavioral risk factors and the incidence of atherosclerosis related

CVDs in the public. As mentioned before, their prevalence is rather increasing and, accordingly, the demand for a fast, accessible and efficient therapy is also continuously growing.

1.2 New therapeutic strategies

The survival rate for a life threatening acute vessel occlusion such as myocardial infarction is still low with adequate primary care, short transport time ("door-to-balloon time") to a cardiac center providing fast accessible primary percutaneous coronary intervention (PCI) or cardiac bypass surgery being the most relevant factors these days for the outcome of patients ("time is muscle").[4] Although an increasing number of hospitals can provide these procedures, still a considerable percentage of patients cannot be treated this way or the attempted PCI/bypass surgery turns out to be unsuccessful and in 3rd world countries, most patients are unable to gain access to these treatments at all. As already stated, the patients' survival is merely a matter of time-to-treatment in the acute event but distinct structural preconditions in the vasculature can improve the patients' outcome significantly. Therefore, aside from educating the population to a healthier lifestyle and the ongoing technical advances in emergency medicine and PCI techniques, a large field of research is currently exploring new ideas to prevent CVDs and/or treat them from a different point of view. The cardiovascular system has an immense capacity to dynamically adapt to different conditions and pathologies. The door to new therapeutic options lies in the understanding of the dynamics between the molecular processes that promote the progression of disease and the compensatory mechanisms that take place in the living organism. In a recent study, it was shown that well developed preexistent collateral networks are associated with an improved long-term survival of patients after ST-segment elevation myocardial infarction (STEMI).[5] So apart from medical treatment and prevention, distinct anatomical advantages such as an efficient preexistent collateral circulation can apparently cope better with the incidence of a major artery occlusion by maintaining sufficient oxygen supply for the muscle.

1.3 Discovery of a collateral circulation

The recognition of a preexistent collateral network capable of remodeling preceded a 300-years lasting debate. In 1669, the British physician Richard Lower (1631-1691) reported for the first time findings of collateral arteries he had found between the right and the left coronary artery by injecting fluid into one artery and observing its appearance on the other.[6] The Swiss anatomist Albrecht von Haller (1708-1777) described 1757 functional, interarterially connecting vessels in the apex region and in the *sulcus longitudinalis* of the posterior ventricle.[7] In 1785, John Hunter (1728-1793), a Scottish surgeon appointed to King George III, developed a new and modern technique for the treatment of traumatic popliteal aneurysms in patients on the basis of animal experiments using collateral artery growth (see Discussion 1.1).[8] A 100 years later distinguished anatomists like Hyrtl, Henle and Cohnheim denied

the collateral arteries' existence and proposed these vessels to be "simple" end arteries.[9] In the beginning of the 20th century, the works of the anatomist Werner Spalteholz (1862-1940) depicted clearly a coronary collateral circulation.[10] Up until then, pathologists and anatomists used three methods: direct preparation, cast corrosion or radiographs after injection of opaque media, which in those times was still in its infancy. Spalteholz developed a new technique to make specimens transparent after injection of vessels with opaque media, to allow an excellent view inside the organ in its nearly untouched threedimensional structural entity,[11] a method that is still used today with marginal changes. Although Jamin confirmed his findings using X-ray technique,[12] the criticism persisted and it was not until the works of Longland[13] (1953) and Fulton[14] (1965) when the hypothesis of end arteries was finally disapproved. Longland demonstrated that collateral arteries consist of a stem, mid-zone and re-entrant.[13] Fulton described collaterals as anastomoses being detectable in health and disease. He also related distinct vascular growth patterns to the level of ischemic impairment of the myocardium.[14] The relationship between collateralization and the atherosclerotic burden in coronary vessels moved into the center of attention. What did stimulate the development of these networks, why did they develop in some patients suffering from atherosclerosis and not in all of them? And more importantly, could the vessels' growth be stimulated?

2 FORMATION OF BLOOD VESSELS

Tissue homeostasis and vitality is strongly dependent on the adequate oxygen supply maintained by blood within a fine branching vessel network. Blood vessels form not only during the embryonic stages, they adapt in adults in response to changing stimuli, in physiologic and pathologic states. Blood vessel formation and remodeling have been investigated by various disciplines, and different forms of vascular growth have been identified (Figure 1).

2.1 Vasculogenesis

During the early stages of embryonic development, pluripotent hemangioblasts, precursor cells for both hematopoetic and endothelial cells, differentiate from mesodermal cells of the splanchnic layer located in the lateral plate mesoderm.[15] They condense to large cellular aggregates (blood islands).[16] In the inner layer, hemangioblasts differentiate to hematopoetic stem cells whereas in the outer layer, they become angioblasts, which are capable to migrate considerably[17] until they differentiate again to CD34+/CD133+ endothelial precursor cells (EPCs) and form the lining of primary capillary networks (Fig 1A). Growth factors (GF) such as vascular endothelial growth factor (VEGF) and fibroblast growth factor (FGF) 2 mediate vasculogenesis. FGF-2 is required for the differentiation of hemangioblasts from the splanchnic mesoderm and the formation of the blood islands[16] and VEGF and its receptors Flk1 and Flt1 regulate the differentiation of the angioblasts to form endothelial tubes.[18, 19] During

the ongoing embryonic development, the initial networks differentiate to mature vessels that are pruned to a complex network of communicating arteries and veins mostly *via* sprouting mechanisms (see below). Circulating CD34+/CD133+ cells are detectable in the blood of adults, which led to the hypothesis that vasculogenesis might not be restricted to ontogenesis and can be occurring in the adult as well.[17] Whether EPCs might be used as a therapeutic option in CVDs is discussed controversially under current preclinical and clinical investigations.[20]

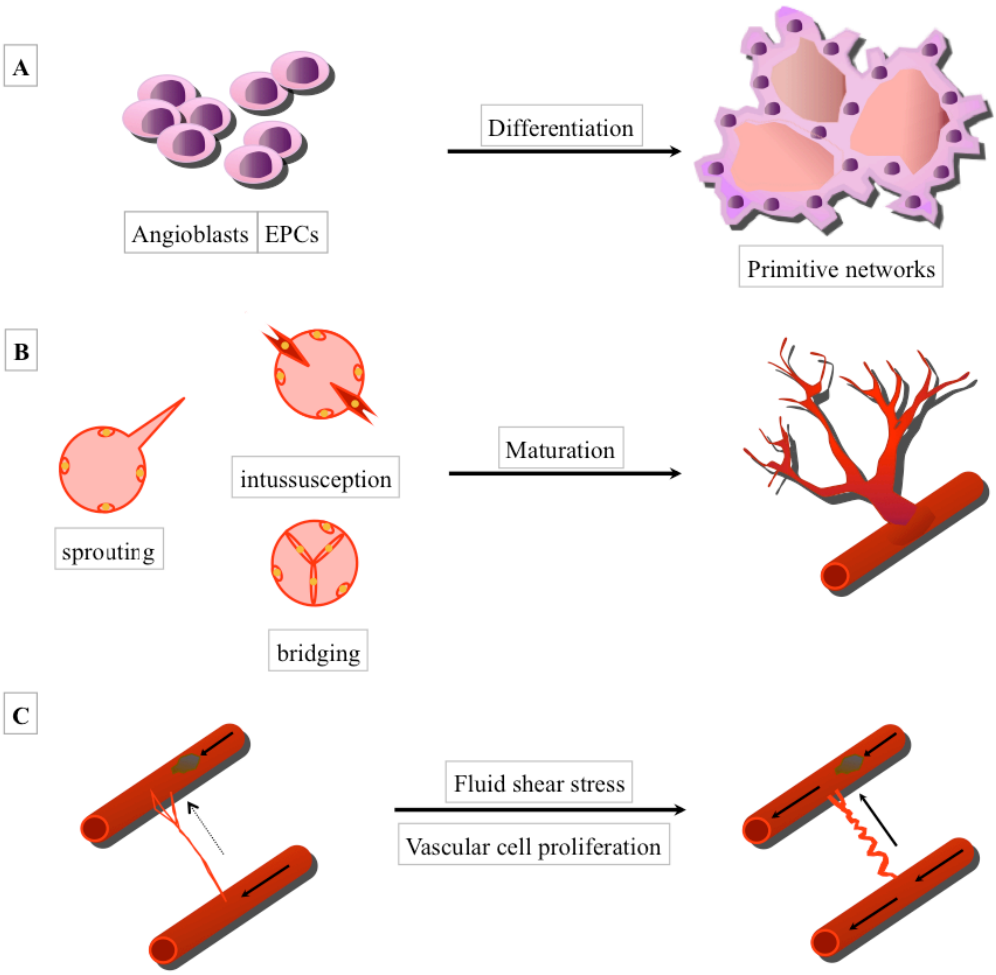

Figure 1: Different types of vascular growth (modified from[17])
A: Vasculogenesis: In situ development of primitive capillary networks from endothelial progenitor cells developed from angioblasts.
B: Angiogenesis: De novo formation of capillary networks from preexisting postcapillary networks. Schematic overview showing the three known mechanisms: sprouting, intussusception and bridging.
C: Arteriogenesis: Shear stress mediated collateral artery growth, forming vessels that are capable to compensate for a stenosis in a major arterial vessel.

2.2 Angiogenesis

Angiogenesis defines the formation of capillary networks from preexisting postcapillary microvessels and is a pivotal element in processes such as wound healing or inflammation. Initially, the term was

introduced 1935 by Hertig to describe the vascular adaptive processes within the placenta during pregnancy.[21] Today, angiogenesis is mostly investigated to explore pathologic states such as inflammation, neoplasia or diabetic retinopathy. Angiogenesis occurs *via* three major mechanisms: sprouting, intussusception and bridging (Fig. 1B). Sprouting terms the extending of sprouts from sides and ends of preexisting vessels and is the process that has been mostly studied. Intussusception forms vessels by longitudinal division out of the preexisting vessel by pillars of peri-endothelial cells and bridging describes the development of transendothelial cell bridges, which then separate into individual capillaries of 5-8µm in diameter.[22] Tissue hypoxia is the initial stimulus that triggers angiogenesis. Activated endothelial cells release nitric oxide (NO) mediating immediate vasodilatation. When pO_2 levels drop, the α-subunit of hypoxia inducible transcription factor -1 (HIF-1α) is stabilized, translocates into the nucleus and forms a dimer with the ß-subunit (HIF-1β). This activates the transcription of HIF-1 target genes, among them VEGF, a very potent angiogenic GF.[23] Apart from transcriptional regulation, augmented VEGF mRNA stability in response to hypoxia promotes the enhanced expression of VEGF.[24] VEGF promotes vasopermeability and subsequently the extravasation of plasma proteins serving as a scaffold for migrating endothelial cells (ECs).[17] The next step is the degradation of the extracellular matrix and the basement membrane by matrix metalloproteinases (MMPs), chymases, heparanases and serine proteases.[22] The urokinase plasminogen activator (uPA) and tissue PA (tPA) convert the plasma protein plasminogen to plasmin, which subsequently activates several MMPs and degrades structural proteins such as laminin and fibronectin.[25] The exposed endothelial cells proliferate and sprout from these regions, directed by chemotactic factors released from fibroblasts, neutrophils, monocytes or mast cells. Angiogenesis is orchestrated by VEGF, FGF, and platelet-derived GF (PDGF) promoting the growing of the new capillary. Antiangiogenic signals prevent an overshooting and undirected proliferation (see below). NO terminates the proliferative actions of growth factors and promotes the formation of vascular tubes.[26] Then, pericytes are recruited along the newly formed structures. Angiopoietin-1 (Ang-1) and its tyrosine receptor kinase Tie-2, stabilize the immature endothelial cell network, attract pericytes and maintain biochemical interactions and vessel integrity and may play an important role in the organization and maturation of vessels. Transforming growth factor-beta 1 (TGF-$ß_1$) strengthens the extracellular matrix and furthers the differentiation and maturation of pericytes.[27] Remodeling and „pruning" of capillary–like vessels eventually results into a structured network of branching capillaries. It's important to note, however, that within the angiogenic formation vascular smooth muscle cells (vSMC) are hardly involved. Capillaries do not hold a vSMC-layer in order to maintain vascular tone as conductance arteries do. For clinicians, angiogenesis is an extremely important mechanism, mostly due to its significance for tumor pathology. Folkmann used the term to describe neovascularization during tumor growth and formed the concept that tumor growth could be controlled by inhibition of angiogenesis. Neoplasia therefore directly depends on an adequate access to the circulatory system in terms of tumor mass enlargement and metastasis.[28] Under physiological cir-

cumstances new vessels mature and become stable. In tumors, vessels do not become quiescent, show unusual, irregular architecture and remain often leaky since the vascular growth is not properly guided. A critical step towards tumor progression is the angiogenic switch where angiogenesis is initiated in the dormant primary tumor nodule to mediate exponential tumor growth and enable metastasis.[29] The difference between physiologic and tumor angiogenesis is that the usually balanced signaling between physiologic proangiogenic (e.g. VEGF, FGF) and antiangiogenic factors (e.g. thrombospondin, angiostatin) becomes destabilized.[30] There is evidence that also EPCs recruited from the bone marrow participate in the angiogenic switch.[31] The discovery of potential targets for an anti-angiogenic tumor therapy targeting especially the initiation of the switch led to the development of antiangiogenic drugs. The appropriate and safe application in terms of a prolonged survival of patients whithout severe side effects is already tested in clinical settings for example for anti-VEGF-A (Bevacizumab [Avastin]) and anti-VEGF-receptor (Cediranib [Recentin]) drugs. Cediranib failed in clinical trials due to inefficiency combined with deleterious side effects[32] whereas Bevacizumab was approved by the U.S. Food and Drug Administration (FDA) for metastatic colorectal carcinoma and glioblastoma multiforme, among others.[33] However, due to severe side effects and high therapy costs this therapy regime does not belong to the standard. So it seems that further investigations are necessary since the inhibition of overall angiogenesis interferes greatly with the physiologic angiogenesis processes and is thus seldom tolerated.

2.3 Arteriogenesis

Arteriogenesis is defined as the process of collateral artery growth, meaning the transformation of preexistent collateral arteries in order to compensate a stenosis of a major arterial vessel. It is a life saving process, not only in the case of myocardial infarction.[5] Coarctation of the aorta is a congenital disease where the aorta is constricted around the area of the *ligamentum arteriosum.* In the case of the postductal coarctation, patients develop an impressive collateral artery network *via* the intercostal arteries leading to notching of the ribs. Without the body's impressive capability to develop these arteries the narrowing of the human body's largest artery would hardly be survivable. Typically, hemodynamic forces such as fluid shear stress (FSS) and circumferential wall stress not ischemia trigger and promote collateral artery growth.[34] Crucial mechanism involve leukocyte, especially monocyte recruitment and proliferation of ECs and vSMCs (see below). The mature, natural bypasses show an increase in diameter and length and therefore develop a typical corkscrew-like morphology. The working group around Wolfgang Schaper rendered important services to the identification of mechanisms regulating collateral artery growth and its differences to angiogenesis. In 1971 they demonstrated for the first time that preexistent arteriolar anastomoses enlarged due to proliferation of vascular cells and not by mere vasodilatation.[35] Whereas the diameter can increase up to 20-times,[36] the capability of remodeling within these vessels is limited to 35 to 40 percent of the origin conductance.[34] Pre-existing

collateral arterioles usually show an internal diameter between 30 and 50µm[37] and are microvascular, thin-walled conduits comprising an endothelial layer, an internal elastic lamina and one or two layers of SMCs.[13] The number and capability of remodeling of these interconnecting vessels varies among species and within individuals[36] and becomes impaired during aging.[38] During the remodeling process, the collateral system prefers few large conduct collaterals instead, resulting in the regression of many small ones, a process called "pruning".[37]

3 MECHANISMS PROMOTING ARTERIOGENESIS

In the past 15 years research has been conducted extensively in the field of arteriogenesis to identify important mechanisms, mediators and signals with the future goal to offer patients the therapeutic alternative of iatrogenic accelerated collateral artery growth.

3.1 Hemodynamic forces

Blood flow through arterial vascular networks is a biomechanical stressor. Different physical parameters influence the homeostasis in the arterial wall: blood pressure, hydrostatic pressure, circumferential wall stress (CWS) and FSS. CWS, endured by the smooth muscle, is directly proportional to the intravascular pressure and inversely proportional to wall thickness and is a 10^6 times stronger force than FSS.[39] After an acute occlusion or severe stenosis of a major artery, a steep pressure gradient between the high-pressure pre-occlusive area and the low-pressure post-occlusive region develops. Blood flow is now redirected along this pressure gradient, thereby recruiting the preexisting collateral network. Shear rate is a gradient of velocity; an increase in the axial blood flow velocity from the vessel wall towards the center of the lumen is defined as simple shear rate in s^{-1}. For a simplified understanding of shear, the rheology of Newtonian fluids (i.e. water) with laminar flow and constant viscosity can be contemplated in this model. For the purpose to describe the basic mechanisms that occur within the collateral vessel, these equations shall be sufficient.

A Newtonian fluid's shear rate $\dot{\gamma}$ at the inner wall of a pipe is defined as:

$$\dot{\gamma} = \frac{8v}{d} \tag{1}$$

Where: $\dot{\gamma}$ = shear rate in s^{-1}, v = linear fluid velocity, d = diameter (= 2 * the radius r) of the pipe.

Along with $v = \frac{Q}{A}$ (Q being the volume flow rate $\frac{dV}{dt}$ in m^3/s) and $A = \pi r^2$ (A being the area cross-section), the formula can be formed to:

$$\dot{\gamma} = \frac{8\left(\frac{Q}{\pi r^2}\right)}{2r} = \frac{4Q}{\pi r^3} \tag{2}$$

As seen in the equations, shear rate is directly proportional to blood flow velocity (1) and inversely related to the third power of the vessel radius (2). Therefore, an increase in blood flow within the collateral network with small vessel diameters ranging from 50µ- 100µm leads to an increase in shear along the collateral endothelium.

For Newtonian fluids, wall shear stress (τ_w) in Pa (former unit used dyn/cm^2) can be related to the shear rate reliant on dynamic viscosity (μ): $\tau_w = \dot{\gamma}^* \mu$

Although the rheology of non-Newtonian fluids (i.e. blood) where pressure, velocity and the fluid's viscosity varies periodically would be more accurate, biological fluid modeling is far from being trivial.[40] More accurate models to describe blood flow and shear within tortuous arterioles are currently in the process of development.[41] The average blood flow in a normal, healthy femoral artery results in shear stress values of $4.8*10^{-3}$dyn/cm^2. After femoral artery occlusion, the FSS within the collaterals increases by nearly 200-fold to $889*10^{-3}$dyn/cm^2, an intense stimulus.[9] The German anatomist Thoma described in his "Law of Histomechanics"[42] the relationship between the size of an artery and the blood flow velocity within. Large vessels with a low flow tend to reduce their lumen, whereas small vessels with a high flow tend to widen it (like collateral vessels).[42] In the works of Langille,[38] Holtz,[43] and Ben Driss[44] it was also shown that changes in arterial blood flow lead to the immediate adjustment of vascular tone and subsequently also a structural reorganisation of the vessel wall in response to a persisting change of blood flow. A sustained increase in fluid shear stress is the stimulus for the activation of the endothelium characterized by swelling and edema and the start for the remodeling process.[39] With the increase in diameter, however, the FSS decreases together with the stimulus to grow. In an experimental setting it was shown that under artificially sustained high FSS within collateral arteries of the hind limb *via* a generated shunt, a 4-fold increase of collateral flow compared with the contra-lateral ligated, but not shunted hind limb could be obtained.[45] FSS does therefore not only trigger arteriogenesis it also maintains the ongoing process. The stimulus is then "translated" into gene activation and expression. This process of mechanotransduction is not entirely understood. ECs detect alterations in FSS and respond with a variety of mechanisms ranging from electrophysical modulation of membrane proteins (second messengers) or ion channels[46] to cellular reorganization of the cytoskeleton,[47] to activation of a number of genes like platelet endothelial cell adhesion molecule 1 (PECAM-1),[48] endothelial NO synthase (eNOS), or intercellular adhesion molecule -1 (ICAM-1).[49] Signal transduction cascades are then activated and transmit the stimulus from surface into the nucleus such as the mitogen-activated protein kinase kinase (MEK) /extracellular signal-related kinase 1/2 (ERK1/2) pathway[50] mediating the subsequent steps towards mature collaterals.

3.2 Monocyte recruitment

The activated endothelium expresses a number of cell adhesion molecules and releases cytokines attracting circulating blood cells.[51] Arteriogenesis strongly depends rather on the recruitment of blood monocytes[52] than on granulocytes or T-cells.[53] However, only 4-8% of all leukocytes comprise monocytes. In response to invasive stimuli and inflammation, their percentage can increase dramatically. Circulating monocytes possess migratory, chemotactic and phagocytotic activities. The attraction of monocytes to the vascular wall is characterized by tethering, rolling and finally the firm adherence at the endothelium.[52] They migrate through the vessel wall (diapedesis), accumulate around the growing arterial vessel and differentiate into tissue macrophages. Their accumulation starts around 12h and cumulates on day 2-3 after the induction of arteriogenesis by femoral artery occlusion.[51] The attachment of monocytes to the collateral endothelium was observed for the first time in the canine heart.[54] Studies using electron microscopy delivered some evidence for a direct transmigration through the arteriolar wall. It is however not entirely proven whether monocytes transmigrate only through the collateral artery or perhaps also through the adjacent venules as the vessels' close proximity suggest (Figure 2). Nevertheless, the presence of monocytes and macrophages has been shown to be important for the development of collateral arteries, since they themselves are the providers of numerous cytokines (e.g. MCP-1), growth factors (e.g. FGFs) and MMPs.[55, 56] Various signaling molecules and cytokines trigger and maintain the transmigration of monocytes.

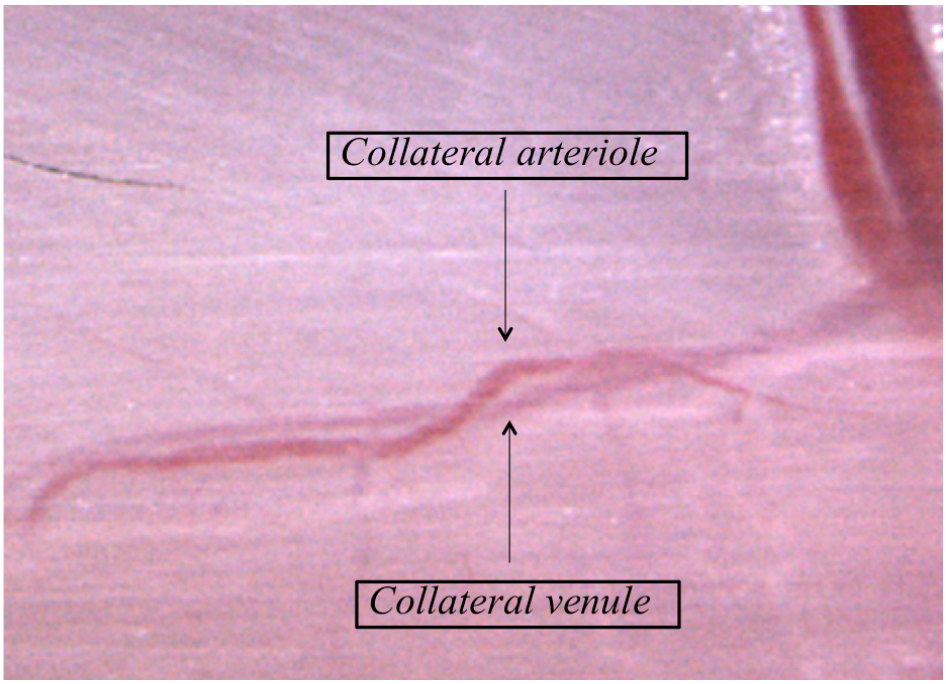

Figure 2: Close proximity of venules and arterioles in the collateral circulation.
Photography shows collateral arteriole (upper vessel) and venule (lower vessel) branching from/to the vasa femoralia in the murine hindlimb.

3.2.1 Monocyte chemoattractant protein 1 (MCP-1)

Chemokines are a heterogenic group of small chemotactic cytokines (8-10kDa) responsible for attraction, migration and activation of leukocytes. They exert their biological function by binding to specific G-protein-linked transmembrane receptors and are divided into four major families according to the spacing of their first two cysteine (C) residues. CC-chemokines contain two cysteine residues adjacent to each other and are responsible for attracting mononuclear cells to sites of inflammation. The other families comprise the CXC-chemokines (C residues separated by one aminoacid) e.g. IL-8, the C-chemokines (with only 2 cysteines), and the CX_3C- chemokine (three aminoacids between the Cysteine residues) with the only member fractalkine.[57] The best-studied chemokines of the CC group are the monocyte chemoattractant proteins (MCPs) 1-5. MCP-1, also known as CCL2 (CC-ligand 2),[58] is a potent chemoattractant for monocytes, T lymphocytes and basophils.[57] Other members of the CC-chemokine family include macrophage inflammatory proteins (MIPs) α, β, γ and RANTES (**R**egulated upon **A**ctivation, **N**ormal **T**-cell **E**xpressed, and **S**ecreted also known as CCL5). The expression of MCP-1 is regulated by growth factors (e.g. VEGF and FGF-2) but also in response to FSS. MCP-1 acts proarteriogenic during arteriogenesis recruiting monocytes to the site of collateral artery growth thereby promoting the remodeling of the vessels.[59] Constant local administration of MCP-1 into the proximal stump of the occluded artery *via* an osmotic minipump resulted in an increase of collateral conductance in the thigh area of the rabbit.[60]

3.2.2 Intercellular adhesion molecule 1 (ICAM-1)

Activated endothelial cells express both intercellular and vascular cell adhesion molecules (ICAM-1 and VCAM-1). They belong to the immunoglobulin superfamily and are cell surface glycopeptides. Their mRNA has been found upregulated at 12h (VCAM-1 and ICAM-1) and 24h (only ICAM-1) during arteriogenesis in the rabbit hindlimb.[51] ICAM-1 is a ligand for the integrins lymphocyte function-associated antigen 1 (LFA-1) and macrophage-1 antigen (Mac-1) on monocytes and fibrinogen and is therefore an important mediator of leukocyte transmigration during arteriogenesis.[60] Integrins are heterodimeric cell surface receptors composed of two trans-membrane glycoproteins: a variable α-chain and a non-variable β-chain; LFA-1 and Mac-1 belong to the β_2-subfamily. Integrins mediate attachment of cells to the matrix, cell-to-cell connections, and regulate intracellular signal transduction.[61] Monocytes bind to the ICAM-1 molecules on endothelial cells by their Mac-1 receptor, invade the vascular wall and accumulate in clusters in the adventitia and the perivascular space of the growing artery. Monocyte attachment and arteriogenesis was shown to be impaired after intravenous infusion of anti-ICAM-1 antibodies.[62]

3.2.3 Urokinase-type plasminogen activator (uPA)

During the recruitment of cells into the perivascular space the extracellular matrix (ECM) has to be degraded to provide space first for the migrating cells, next for the remodeling vessel. ECs, vSMCs and macrophages release matrix-degrading proteinases. The balance between proteolysis and stabilization of the ECM is shifted and the two systems of MMPs and uPA are activated.[63] MMP-2 and MMP-9 have been found upregulated in arteriogenesis.[63] uPA is a serine protease with the substrate plasminogen. By activating plasmin, it triggers proteolysis cascades that, depending on the environment, may lead to thrombolysis or degradation of the extracellular matrix. Monocyte migration *in vitro* critically depends on uPA.[64] Moreover, uPA derived from monocytes can mediate vSMC migration.[65] *In vivo*, the the transmigration of neutrophils[66] as well as the accumulation of monocytes in the perivascular space of growing collaterals[67] also depends on uPA but not on the interaction with its receptor uPAR.

3.3 Vascular cell proliferation and differentiation

Arteriogenesis does critically depend on the proliferation of endothelial and smooth muscle cells.[34, 35] The proliferation phase in the rabbit hind limb begins 24h after arterial occlusion in the mid zone and peaks at day three to seven.[51] During this phase, an increased mitotic and proliferative activity of endothelial cells, smooth muscle cells and fibroblasts can be observed. This time window coincides with the presence of monocytes in the perivascular space. vSMCs demonstrate the most critical change during the maturation of the vessel. First, they increase their tissue mass 3-fold in mice, 10-fold in rabbits 20-fold in canines and more in humans.[68] This is mainly due to the phenotype switch from the contractile to the synthetic type that occurs in vSMCs and which depends critically on the downregulation of the transcriptional repressor splicing factor -1 (SF-1)[69] and of the cytoskeletal protein αSM-actin.[70, 71] The *lamina elastica interna* of the arterial vessel is digested by elastases and is later detectable in form of fragments. Migrating vSMCs loose their contractile apparatus, showing reduced amounts of the cytoskeleton protein alpha-smooth muscle actin (αSM-actin) but abundant amounts of depolymerized actin and depict a prominent rough endoplasmatic reticulum especially around day five to seven.[51] Now accumulated in the intima, they enter the cell cycle and divide. But mitosis also occurs within the media.[35] The filament protein desmin, a marker for contractile vSMCs, disappears during active growth.[71] On day 10 to 14 an irregular neo-intima becomes evident that can persist in the collateral or even lead to complete obliteration of the vessel promoting the previously mentioned pruning. vSMC layers start to revert to the contractile phenotype whereas the ECs still show synthetic activity. The *lamina elastica interna,* restored up to seven layers of vSMCs, can be found in the remodeled vessel. Growth has been described to be almost complete after 21 days.[51]

4 THE TRANSCRIPTION FACTOR EARLY GROWTH RESPONSE (EGR1)

It requires a good coordination to control leukocyte recruitment and vascular cell proliferation within this puzzling disarrangement. Transcription factors (TF) interconnect upstream and downstream signals. In previous studies transcriptional regulators like activator protein 1 (AP-1)[72] or cardiac ankyrin repeat protein (carp)[73] were found upregulated in arteriogenesis. In this study the murine TF Egr1 was investigated to acquire new insights into the molecular regulation of arteriogenesis. Initially, the murine Egr1 was discovered in murine PC12-cells after stimulation with neuronal GF (NGF). It was therefore labeled as nerve GF inducible A (NGFI-A).[74] Later it was also referred to as Zif268,[75] TIS8 or krox-24.[76] The name early growth response 1 was eventually established by Sukhatme et al during studies on stimulated murine and human fibroblasts.[77] Egr1 was found to be rapidly and transiently expressed in response of a heterogenic group of stimuli like GFs, shear stress, hypoxia, (reperfusion) injury and oxidative stress,[78, 79, 80] and therefore participates in an array of signal transduction networks upstream and downstream.[76]

4.1 Structural properties

The murine Egr1 gene consists of two exons and a 700bp intron (between nucleotide position 556 and 557) and maps to 5q23-q31.[81] It encodes a Cys_2-His_2-type of zinc-finger TF with the size of 80-82kDa. It has been shown that the EGR1 protein gets posttranslational modificated i.e. phosphorylated[78, 82] with a high turnover (*in vitro*: 3h detection window).[78]

4.1.1 The Egr1 promoter

In order to understand the regulating mechanism behind Egr1 expression, the murine Egr1 promoter has been investigated and several functional elements have been characterized[83] (Figure 3).

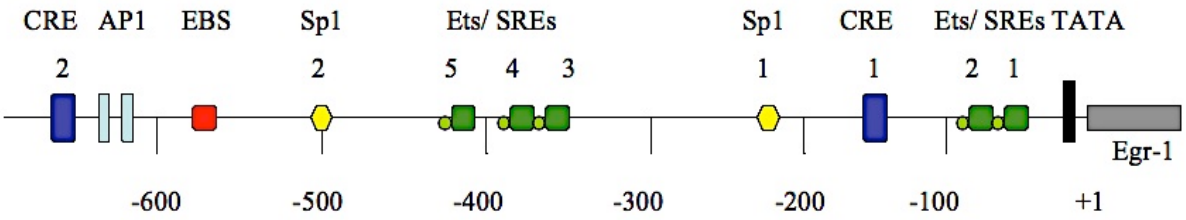

Figure 3: Functional elements on the murine promoter of Egr1

There are five serum response elements (SRE) located at the 3' end of the promoter and next to a TATA box (AAATA, located 26 nucleotides upstream of the transcription start site).[81] Five E-twenty six (Ets) family transcription factor-binding sites are arranged adjacently to these SREs indicating mutual activation. Furthermore, two cyclic adenosine monophosphate (cAMP) response elements

(CREs), an APETALA1 (AP-1) and two gene-specific activator protein 1 (Sp-1) binding sites are located on the promoter.[84] A GC-rich promoter sequence (GCG(G/T)GGGCG),[75] the typical target sequence of the EGR1 protein and therefore named early growth response binding-sequence (EBS), can also be found,[85] making EGR1 capable of binding to its own promoter. Although binding to an EBS actually leads to transcriptional activation of other target genes, EGR1 has been shown to downregulate its own expression in form of a negative feedback loop by binding to its very own EBS.[86] So it appears that there is a lot of own transcriptional control regulating EGR1 expression on the RNA and protein level therefore providing a fine balanced expression profile.

4.1.2 The EGR1 protein

The encoded murine EGR1 protein consists of 533 amino acids and possesses functionally independent components (Figure 4). The human EGR1 protein is only slightly larger comprising 543 amino acids but does not differ significantly concerning amino acid sequence or structural properties.

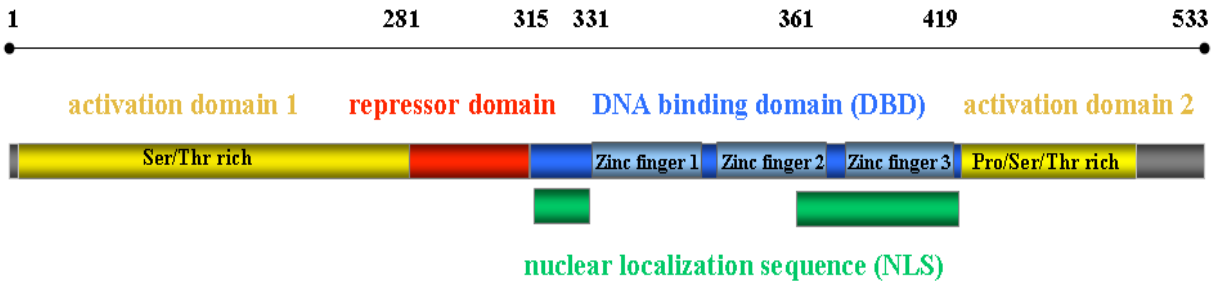

Figure 4: Functional domains of the murine EGR1 protein
Serine/threonine as well as proline/serine/threonine rich sequences are located at the N- and the C-terminal region, respectively. Ser/thr residues are posttranslational phosphorylated. Nuclear translocation is mediated by a bipartite NLS that comprises basic residues in the DBD. NAB regulates EGR1 activity by binding to the repressor domain.

The hallmark of TFs is the DNA binding domain (DBD) to adhere to a specific sequence on the DNA thus regulating transcription. The DBD, from amino acids 331 to 419, is characterized by three zinc-finger motives[87] that characteristically bind to the EBS.[78] Each zinc finger consists of an antiparallel ß sheet and an α–helix arranged around the zinc ion.[87] Nuclear magnetic resonance studies revealed that the zinc fingers are sterically arranged in a semicircular (C-shaped) way thereby fitting into the major groove of DNA where each finger binds to 3bp subsite along one strand of the DNA (the G rich strand)[87] Once synthesized, the EGR1 protein is translocated into the nucleus.[78] It therefore holds a bipartite-type nuclear localization sequence (NLS), 15 amino acids (amino acids 315-330) on the DBD N-terminal flanking region and within the DBD (amino acids 361-419).[88] Basic residues characterize the NLS.[89] The flanking sequence together with all three zinc fingers promotes nuclear localization of the EGR1 protein.[88] The N-terminal region of the protein is an activation domain (3-281) rich in serine and threonine (30%) that can be phosphorylated.[78, 82] This large domain is capable of activating transcription 100-fold. The C-terminal holds a second but weaker activation domain containing additional-

ly proline.[89]There is also a repressor domain, amino acids 281 to 314, where nuclear co-repressors, called NGFI-A binding protein (NAB), adhere to and therefore negatively regulate transcriptional activity of the Egr1 gene.[90, 91] Two different NABs 1 and 2 have been identified in this context.[90, 91] NAB-2, a "late" early response gene, is induced *via* the same stimuli[91] that activate Egr1 expression, but is time-staggered to the latter. EGR1 itself strongly induces expression of the NAB-2 gene by eleven EBS that have been identified in the NAB-2 promoter region.[92] Therefore, any upregulation of Egr1 eventually leads to NAB-2 mediated EGR1 protein repression. NAB-2 effects on Egr1 function are quite well investigated in GF induced proliferation.[93] FGFs are potent Egr1 activators. However, FGF-23 induces NAB-2 at the same time, which eventually suppresses EGR1 mediated transcription activity within the nucleus.[94] Furthermore, a reciprocal expression pattern for NAB-2 and Egr1 has been described; apparently, EGR1 itself prevents an exceeding expression of its own downstream target genes *via* repressors like NAB-2.[92]

4.2 Function and associated downstream targets

Egr1 has been quite extensively investigated, though mainly *in vitro* and in fact, very little is known about its interaction with other Egr family members. Egr1 participates in growth, cell survival programs and apoptosis. Hence, GFs have been shown to induce Egr1 expression. EGR1 again, positively regulates expression of many GF genes by binding to the EBS on their promoters and has also been shown to act as an important cell cycle regulator, controlling mitose progression.[78, 95] EGR1 has previously been described as a master switch for arteriogenesis in mice and rats after femoral artery excision,[96] and it was shown that adenoviral mediated EGR1 delivery improved perfusion recovery[97], however the molecular mechanisms behind this role have not been characterized so far. It has been shown that mechanical forces such as FSS are capable of increasing the mRNA of EGR1 in cultured human ECs *via* MEK/ERK1/2 after 30min of exposure.[50] Cardiac ankyrin protein (carp), described to be upregulated during arteriogenesis *in vivo*, was also shown to induce Egr1 mRNA *via* MEK/ERK *in vitro*.[73] The relation between Egr1 activity and monocyte/macrophage function has also been discussed. Cellular differentiation along the macrophage lineage is an important task of EGR1.[98, 99] Also, EGR1 participates in lipopolysaccharide (LPS) - mediated monocytic activation via MEK/ERK 1/2.[100] Moreover, EGR1 was shown to bind to the promoter of uPA *in vitro*[101] and promoter characteristics of uPA[102] suggest that EGR1 might also be regulating uPA *in vivo.* Due to the expression profiles of MCP-1 and ICAM-1 *in vivo*,[103] these genes are likely EGR1 downstream targets. Cell culture studies revealed that the cell cycle regulator cyclin D1, a key regulator during mitotic progression from G_1- to S-phase, is among the genes lying downstream of Egr1.[104] However, cyclin D1 expression was not impaired in Egr1 deficient mice after partial hepatectomy and therefore these results could not be confirmed *in vivo.*[95] Moreover, there is increasing evidence that Egr1 controls vSMC proliferation. Small interfering RNA (siRNA) molecules targeting the coding region of Egr1 attenuated vSMC prolifera-

tion.[105] As stated before, vSMC phenotype switch is a prerequisite for proliferation and is characterized by downregulation of αSM-actin[70, 71] and SF-1.[69] A recent *in vitro* study showed that downregulation of the latter might be regulated by Egr1.[69, 106] Due to its likely involvement in shear response leukocyte recruitment and vSMC proliferation Egr1 is a specifically interesting candidate to study in arteriogenesis *in vivo*.

4.3 The EGR-family

Egr1 forms a family of Egr TFs together with three other members, Egr2, Egr3 and Egr4. The EGR2 and EGR3 proteins, but not EGR4, also contain a NAB binding site. A 90% homologous three tandem repeat zinc finger domain characterizes this family and differences among them are found mainly outside the DNA binding site.[107, 108] It appears that all Egr-TFs are capable of binding to the EBS on the promoter of target genes to regulate their expression. This raises the question of a possible compensatory mechanism between the Egr family members.

An increasing body of evidence is unraveling the distinct functions of the other factors. Egr2 was shown to regulate hindbrain segmentation and Egr2 deficient mice were reported to be perinatally lethal due to myelination defects in the peripheral nervous system.[109] Egr3 deficient mice are viable but also display various neuronal defects due to Egr3's prominent role in the development of muscle spindles.[110] Egr2 and Egr3 both participate in immunological self-tolerance *via* T-cell anergy induction[111] and act contrariwise to EGR1 and NAB-2 function *in vivo* in T-cell mediated autoimmune disease with Egr3 lying upstream of Egr2.[112] On the other hand, a generated conditional Egr2 knockout (floxed Egr2 allele)[113] has recently been evaluated for CD4 T-cell function and the data suggests that T-cell function might be entirely independent from Egr2 function.[114] It remains therefore to be clarified, whether these results are due to compensatory mechanisms that have not been evaluated in this study. Egr3 has been shown to respond to similar stimuli like Egr1. A recent publication[115] investigated the expression of Egr1/3 in human endothelial cells and found that both can be upregulated *via* VEGF. Interestingly, Egr3 upregulation was found higher and more prolonged than Egr1 and Egr3 was shown to mediate leukocyte adhesion and angiogenesis.[115] The differences in the response to VEGF were due to different upstream signaling cascades being involved in Egr3 and Egr1 expression, respectively. Publications on Egr4 are still very few available. From what is known Egr4 seems to play a crucial role in the developing testis[116, 117] and in male fertility in general, as seen in Egr4 deficient mice.[118] Interestingly, it has been shown that the compensatory function of Egr4 is the reason for fertility of male Egr1 deficient mice[119] in contrast to the observed infertility in female $Egr1^{-/-}$ mice.[120] So it seems, that the other Egr-family-members, which also bind to the EBS, might take over some but not all functions of Egr1 and *vice versa*, but this hypothesis that Egr2 - 4 might be capable to substitute Egr1 function has been proposed but never entirely proven.

II. OBJECT OF THE STUDY

The aim of the study was to provide new insights into the molecular mechanisms of arteriogenesis with the main objective to characterize the functional role of Egr1 in a murine model of peripheral collateral artery growth employing WT and Egr1$^{-/-}$ mice.

The first part of this study aimed to focus on the overall importance of Egr1 for arteriogenesis *in vivo* and its expression in growing collateral arteries. Egr1 has been identified as a "master switch" for arteriogenesis in a murine model of femoral excision,[96] where ischemia and arteriogenesis take place not only at the same time but also in the same anatomical area. Therefore, it has not been investigated, if and how exactly Egr1 furthers the process of collateral artery growth. In order to answer this question, analyses of the Egr1 expression on the RNA and protein level in wildtype animals should be conducted.

The scope of the second part should be dedicated to leukocyte and especially monocyte recruitment in WT and Egr1 deficient mice. Monocyte-counts under baseline conditions and after femoral artery ligation should be counted. The putative Egr1 downstream genes MCP-1 as well as ICAM-1 and uPA were planned to be analyzed *via* quantitative real-time polymerase chain reaction (qRT-PCR) to investigate first of all, whether the expression of these genes was regulated by Egr1 and second of all, whether Egr1 deficiency had an impact on monocyte recruitment under baseline conditions and after femoral artery occlusion.

In the third part, the gene expression of other members of the Egr-family were planned to be analyzed, of which very little is known in the literature. The role of Egr2, -3 and -4 similarly to Egr1 in WT mice has never been characterized in arteriogenesis. It was unclear whether the potential activation of other members was dependent on presence and functionality of EGR1.

The last part should focus on the influences of EGR1 on vascular cell proliferation in growing collateral arteries. The potential participation of key regulators of proliferation such as cdc20 and cyclin D1/E, described as downstream genes of Egr1 *in vitro* could play an important part during arteriogenesis *in vivo*. Moreover, the expression of the EGR1 repressor NAB-2 was planned to be evaluated in this context. The critical vSMC phenotype switch is characterized by downregulation of αSM-actin and the transcriptional repressor SF-1 to further vSMC proliferation. The relationship between Egr1 and the latter two genes has also never been evaluated *in vivo*.

Taken together this study is conducted to better understand the molecular mechanisms regulating arteriogenesis in terms of monocyte recruitment and cell proliferation as well as the potential of other Egr-family members to compensate for Egr1 deficiency.

III. MATERIALS AND METHODS

1 MATERIALS

1.1 Mice strains

1.1.1 C57Bl/6N

C57Bl/6N mice were purchased from Charles River WIGA Deutschland GmbH, Sulzfeld, Germany. Male mice at the age of 8-10 weeks were used as controls with an average weight of 20-25g. These mice were used for practicing the surgical procedures and later for timeline expression studies.

1.1.2 Egr1$^{-/-}$

20 male Egr1$^{-/-}$ mice (B6.129-Egr1 (tm1) Jmi N12) at the age of 6-13 weeks with an average body weight of 20-25g were purchased from Taconic Europe, Tornbjerg, Danmark. This strain was developed in the laboratory of Jeffrey Milbrandt[121] on a 129S6 background and backcrossed to a C57Bl/6N strain for at least 12 generations. Since wild type littermates were not available at Taconic, we compared the results with 20 male wild type C57Bl/6N mice, declared as cage mates by Taconic, with the same age and weight.

1.2 Surgical instruments and expendable material

All surgical instruments	Fine Science Tools (FST), Heidelberg, Germany
Bepanthen® eye- and nasal ointment	Bayer AG, Leverkusen, Germany
Bode Cutasept® F 250ml spray	Bode Chemie GmbH, Hamburg, Germany
CaliBRITE™ beads (unlabeled, FITC, PE)	BD Becton Dickinson GmbH, Heidelberg, Germany
Disposable scalpels (type 20)	Feather Safety Razor Co., Osaka, Japan
Eppendorf tubes 1.5ml	Eppendorf AG, Hamburg, Germany
Ethicon Vicryl® 6-0	Johnson & Johnson GmbH Norderstedt, Germany
Falcon cell strainer nylon 70µm	BD Becton Dickinson GmbH, Heidelberg, Germany
Falcon tubes 40ml	BD Becton Dickinson GmbH, Heidelberg, Germany
Filter paper	Whatman GmbH, Dassel, Germany
Fine bore polyethylene tube (58mm/96mm)	Smiths Medical International Ltd, Hythe, Kent, UK
LightCycler® capillaries (20ml)	Roche Diagnostics GmbH, Mannheim, Germany
Lysis Tubes P	Analytik Jena (bio solutions), Jena, Germany
MaXtract High Density 200x 2ml tubes	Quiagen GmbH, Hilden, Germany
Microtiter plate (96-well)	Quiagen GmbH, Hilden, Germany
Nitrocellulose membrane	Whatman GmbH, Dassel, Germany
Nunc CryoTube™ vials 1,8ml	Fisher Scientific GmbH, Schwerte, Germany
Pipette tips	Eppendorf GmbH, Hamburg, Germany
Shandon cover plates	Thermo Fisher Scientific Inc., Waltham, MA, USA
Silk braded suture (metric 1 US 5/50)	Pearsalls Ltd., Taunton, UK
Sterile cannulas (3G11/4“ and 20G11/2“)	BD Becton Dickinson GmbH, Heidelberg, Germany
Sterile syringes (1 and 5ml)	BD Becton Dickinson GmbH, Heidelberg, Germany
Sutupak Perma Hand®-Silk Suture 4-0	Johnson & Johnson GmbH, Norderstedt, Germany
Three-way stop cocks	B.Braun, Melsungen AG, Germany

1.3 Chemicals and special equipment

1st Strand cDNA Synthesis Kit	Roche Diagnostics GmbH, Mannheim, Germany
Acetone	Merck KGaA, Darmstadt, Germany
Adenosine	Fluka Chemie, Buchs, Switzerland
Agarose, LE, analytical grade	Promega GmbH, Mannheim, Germany
BCA Protein Assay Kit	Thermo Fisher Scientific, Bonn, Germany
Bovine serum albumin (BSA)	Sigma Aldrich GmbH, Seelze, Germany
Blotting grade non-fat–dry milk	Bio-Rad Laboratories GmbH, Munich, Germany
Bromphenol blue sodium salt	Sigma Aldrich GmbH, Seelze, Germany
Chloroformisoamylalcohol (25:24:1)	Sigma Aldrich GmbH, Seelze, Germany
Collagenase II	GibcoBrl, Invitrogen, Karlsruhe, Germany
Complete Mini Protease Inhibitor Cocktail	Roche Diagnostics GmbH, Mannheim, Germany
D*Sucrose	Fluka Chemie GmbH, Buchs, Switzerland
3,3′-diaminobencidine (DAB)	Sigma Aldrich Chemie GmbH, Munich, Germany
Dispase	GibcoBrl, Invitrogen, Karlsruhe, Germany
Dithiothreitol (DTT)	AppliChem GmbH, Darmstadt, Germany
6x DNA loading dye	Fermentas GmbH, St. Leon-Rot, Germany
dNTP Mix (10mM each)	Eppendorf AG, Hamburg, Germany
Ethylenediaminetetraacetate (EDTA)	AppliChem GmbH, Darmstadt, Germany
Ethyleneglycoltetraacetate (EGTA)	Sigma Aldrich Chemie GmbH, Munich, Germany
Formaldehyde 37%	Sigma Aldrich Chemie GmbH, Munich, Germany
GelRed Nucleic Acid Stain, 10000x in DMSO	Biotrend, Chemikalien GmbH, Köln, Germany
GeneRuler™ 100 bp DNA Ladder	Fermentas GmbH, St. Leon-Rot, Germany
Glycerol 100% solution	AppliChem GmbH, Darmstadt, Germany
Glycine	AppliChem GmbH, Darmstadt, Germany
Guanidine thiocyanate	AppliChem GmbH, Darmstadt, Germany
HCL 1M	Merck KGaA, Darmstadt, Germany
Hyaluronidase	Sigma Aldrich Chemie, Taufkirchen, Germany
Isopropanol	Sigma Aldrich GmbH, Seelze, Germany
Laemmli buffer (10x)	Serva Electrophoresis GmbH, Heidelberg, Germany
Latex, flexible mold compound	Chicago latex, Crystal Lake, IL, USA
2-Mercaptoethanol	Sigma Aldrich GmbH, Seelze, Germany
Methanol	AppliChem GmbH, Darmstadt, Germany
Methylbutane	Sigma Aldrich Chemie GmbH, Munich, Germany
NaOH 1M	Merck KGaA, Darmstadt, Germany
N-Laroylsarcosine sodium salt	Sigma Aldrich GmbH, Seelze, Germany
Normal goat serum	Vector, Burlingame, CA, USA
PageRuler^{TM} Prestained Protein Ladder	Fermentas GmbH, St. Leon-Rot, Germany
Paraformaldehyde 4%	AppliChem GmbH, Darmstadt, Germany
Phenol	Sigma Aldrich GmbH, Seelze, Germany
Phenylmethanesulfonyl fluoride (PMSF)	Calbiochem, La Jolla CA, USA
Ponceau S Solution	Sigma Aldrich Chemie GmbH, Munich, Germany
Potassium chloride (KCL)	Merck KGaA, Darmstadt, Germany
Potassium dihydroxyphosphate (KH2PO4)	Merck KGaA, Darmstadt, Germany
Random nonamers	Hoffmann- La Roche, Mannheim, Germany
RBC Lysis buffer	eBiosciences, Frankfurt, Germany

RQ1 RNase-Free DNase 1000U, 1U/µl	Promega GmbH, Mannheim, Germany
Sodium acetate	Sigma Aldrich GmbH, Seelze, Germany
Sodium citrate tribasic dihydrate	Sigma Aldrich GmbH, Seelze, Germany
Sodium chloride (NaCl)	Sigma Aldrich GmbH, Seelze, Germany
Sodium dodecyl sulfate (SDS)	AppliChem GmbH, Darmstadt, Germany
Sodium fluoride (NaF)	Sigma Aldrich Chemie GmbH, Munich, Germany
Sodium hydrogen phosphate (Na2HPO4)	Merck KGaA, Darmstadt, Germany
Sodium orthovanadate (Na3VO4)	Sigma Aldrich Chemie GmbH, Munich, Germany
SSYBR Green I Kit, Light Cycler® - FastStart DNA MasterPlus	Hoffmann- La Roche, Mannheim, Germany
SuperSignal West Femto Maximum Sensitivity Substrate	Thermo Fisher Scientific, Bonn, Germany
ToPro3 nucleus dye	Invitrogen GmbH, Darmstadt, Germany
TAE 50x	Eppendorf AG, Hamburg, Germany
Tris-buffer	AppliChem GmbH, Darmstadt, Germany
Tris-glycine Gel 4-20%	Serva Electrophoresis, Heidelberg, Germany
Triton X-100	Sigma Aldrich GmbH, Seelze, Germany
Tween 20	AppliChem GmbH, Darmstadt, Germany

1.4 Pharmaceuticals

Drug	Brand name	Company
Atipamezolhydrochloride	Revertor®	CP-Pharma GmbH, Burgdorf, Germany
Buprenophine	Temgesic®	Essex Pharma GmbH, Munich, Germany
Fentanyl	Fentanyl-Curamed®	CuraMED Pharma, Karlsruhe, Germany
Flumazenil (0.5mg/5ml)	Flumazenil-hameln®	Hameln Pharma GmbH, Hameln, Germany
Heparin-Na 25.000 I.E./5ml	Heparin-natrium-25000-ratiopharm®	Ratiopharm GmbH, Ulm, Germany
Isoflurane	Forene®	Dräger Medical, Lübeck, Germany
Ketamine hydrochloride	Ketavet®	Pfizer/ Pharmacia GmbH, Karlsruhe, Germany
Medetomidine-hydrochloride	Dormitor®	Pfizer Pharma, Berlin, Germany
Midazolam	Midazolam-ratiopharm®	Ratiopharm GmbH, Ulm, Germany
Naloxone hydrochloride (0.4mg/ml)	Naloxon Inresa	Inresa Arzneimittel GmbH, Freiburg, Germany
Xylazine 2%	Rompun®	Bayer AG, Leverkusen, Germany

Table 1: List of pharmaceuticals used in this study

1.5 Primers for qRT-PCR

All primers (salt free) were purchased from eurofins mwg operon, Ebersberg, Germany and ordered *via* the website: www.eurofinsdna.com/home.html

Target	Primer	Sequence	Product length, annealing temp.
Egr1	Forward Reverse	5'-CGAACAACCCTATGAGCACCTG-3' 5'-CAGAGGAAGACGATGAAGCAGC-3'	270bp, 64°C
Egr2	Forward Reverse	5'-CGTATCCGAGTAGCTTCG-3' 5'-GATACCTTCTGGATAGCAG-3'	116bp, 56°C
Egr3	Forward Reverse	5'-CAGATGGCTACAGAGAATG-3' 5'-CACTCATGAGGCTAATGATG-3'	181bp, 54°C
Egr4	Forward Reverse	5'-GACTTAACAGACTCCTGC-3' 5'-CAGACATGAGGTTGAGAG-3'	136bp, 56°C
MCP-1	Forward Reverse	5'-CTCAAGAGAGAGGTCTGTGCTG-3' 5'-GTAGTGGATGCATTAGCTTCAG-3'	182bp, 62°C
ICAM-1	Forward Reverse	5'-GAAGTCTGTCAAACAGGAG-3' 5'-CAGTACTGGCACCAGAATG-3'	142bp, 58°C
uPA	Forward Reverse	5'-CTGCTATCATGGAAATGGTGACTC-3' 5'-CTAGGCTAATAGCATCAGGTCTG-3'	136bp, 62°C
cyclin D1	Forward Reverse	5'-GAAGGAGACCATTCCCTTGA-3' 5'-GTTCACCAGAAGCAGTTCC-3'	100bp, 60°C
cyclin E	Forward Reverse	5'-CTCGGGTGTTGTAGGTTGCT-3' 5'-CTGTTGGCTGACAGTGGAGA-3'	111bp, 63°C
cdc20	Forward Reverse	5'-GAGCTCAAAGGACACACAGC-3' 5'-GCCACAACCGTAGAGTCTCA-3'	99bp, 62°C
ki67	Forward Reverse	5'-GAGTGAGGGAATGCCTATG-3' 5'-GCTGTGAGTGCCAAGAGAC-3'	145bp, 58°C
SF-1	Forward Reverse	5'-CAACGCCAAGATCATGATTC-3' 5'-CTCCATCGTATTGGCAGTG-3'	127bp, 56°C
aSM-actin	Forward Reverse	5'-GAGCATCCGACACTGCTG -3' 5'- GTACGTCCAGAGGCATAG -3'	146bp, 58°C
18S	Forward Reverse	5'-GGACAGGATTGACAGATTGATAG–3' 5'-CTCGTTCGTTATCGGAATTAAC–3'	108bp, 64°C

Table 2: List of primers and their corresponding product length and annealing temperature

1.6 Special buffers and solutions

Adenosine buffer (IHC)
100ml PBS
250mg BSA
100mg adenosine pH 7.4

Loading buffer (WB)
250mM Tris (12.5ml) pH 6.8
8% SDS (20ml)
100% glycerol (20ml)
0.02% bromphenol blue (10mg)
400mM mercaptoethanol (1.7ml)

Phosphate buffered saline (PBS) 10x
80g NaCl
2g KCL
14.4g Na_2HPO_4
2.4g KH_2PO_4
aqua dest ad 1L pH 7.4

Probe buffer PBS+BSA 2% (WB)
45ml aqua dest.
5ml 10 x PBS
1g BSA

Protein isolation buffer (WB)
20mM Tris–HCl
250mM sucrose
1mM EDTA
1mM EGTA
1mM DTT
0.1mM Na_3VO_4
10mM NaF
0.5mM PMSF pH 7.4

Sodium acetate solution (RNA isolation)
2M Na-acetate ($NaCH_3COO$) (16.4 g)
dH_2O ad 100ml pH 4.0

Solution A (RNA isolation)
50ml dH_2O
4M guanidine thiocyanate (23.63g)
25mM sodium citrate tribasic dihydrate (367.6 mg) pH 7.0
0.5% N-lauroylsarcosine sodium salt (0.25g)
0,1M 2-mercaptoethanol (348.7 µl)

Solution for muscle tissue digestion (FACS)
Collagenase II 1mg/ml
Hyaluronidase 0.5mg/ml
Dispase 1mg/ml
BSA 0.6mg/ml
PBS ad 50ml pH 7.4

10x TBS (WB)

24.2g Tris
80g NaCl
165ml HCL 1N
835ml aqua dest. pH 7.6

Transfer buffer (WB)
2.9g glycine
5.8g Tris
0.37g SDS
200ml methanol
aqua dest ad 1L pH 8.3

Washing buffer (WB)
1x TBS
0.1% Tween-20

1.7 Antibodies

Tables 3 and 4 display the primary and secondary antibodies, respectively, as well as their dilution and the application for which they have been used.

1.7.1 Primary antibodies

Target	Dilution/Application	Company
Rabbit anti-mouse-EGR1	1:500 (WB) 1: 50 (IF)	Santa Cruz Biotechnology, Heidelberg, Germany
Mouse anti-mouse αSM-actin (clone:1A4)	1:200 (IF)	Abcam, Cambridge, MA, USA
Rat anti-mouse Mac-3 mAb (Clone: M3/84)	1: 100 (IHC)	BD Pharmingen™, Heidelberg, Germany
anti-mouse CD11b mAb Phyco-erythrin (PE)-conjugated	1:10 5µl in 50µl (FACS)	Beckman-Coulter, Krefeld, Germany
anti-mouse CD45 mAb-FITC-conjugated	1:10 5µl in 50µl (FACS)	Beckman-Coulter, Krefeld, Germany
Anti-mouse CD3 mAb, FITC-conjugated	1:10 5µl in 50µl (FACS)	Beckman-Coulter, Krefeld, Germany
Anti-mouse-CD19 mAb PE-conjugated	1:10 5µl in 50µl (FACS)	Beckman-Coulter, Krefeld, Germany

Table 3: List of conjugated and unconjugated primary antibodies, their dilution and application
(WB = Western Blot, IF = immunofluorescence, IHC =conventional immunohistochemistry, FACS = fluorescence activated cell sorting, mAb = monoclonal antibody)

1.7.2 Secondary antibodies

Target	Dilution/ Application	Company
Alexa Fluor®546 goat anti-mouse IgG (H+L)	1:200 (IF)	Invitrogen GmbH, Darmstadt, Germany
Alexa Fluor® 488 goat anti-rabbit IgG (H+L)	1:200 (IF)	Invitrogen GmbH, Darmstadt, Germany
Donkey anti-rat IgG HRP conj.	1: 500 (IHC)	Dianova GmbH, Hamburg, Germany
Goat-anti-rabbit-IgG HRP conjugated	1:5000 (WB)	Santa Cruz Biotechnology, Heidelberg, Germany

Table 4: List of secondary antibodies, their dilution and application

1.8 Devices

All pipettes	Eppendorf AG, Hamburg, Germany
BioPhotometer	Eppendorf AG, Hamburg, Germany
CM 3000 cryomicrotome	Leica GmbH, Wetzlar, Germany
Confocal microscope Leica TCS SP5	Leica GmbH, Wetzlar, Germany
Electrophoresis power supply E301	Amersham Biosciences GmbH, Freiburg, Germany
ELISA Plate Reader	Bio-Tek instruments, Winooski, USA
FACS CaliburTM	BD Becton Dickinson GmbH, Heidelberg, Germany
Heating pad and rectal probe	FHC, Bowdonham, ME, USA
Incubator	Haraeus, Hanau, Germany
Laser Doppler Imager LDI2 V5.1	Moor Instruments Ltd., Devon, UK
Light Cycler 1.5	Roche Diagnostics GmbH, Mannheim, Germany
Magnetic stirrer	IKA®-Werke GmbH & CO. KG, Staufen, Germany
Micro 200 R centrifuge	Hettich Zentrifugen, Tuttlingen Germany
Microinjection syringe	Hamilton Bonaduz AG, Bonaduz, Switzerland
Microwave	Siemens AG, Munich Germany
Orca CCD Camera	Hamamatsu PHOTONICS GmbH, Herrsching, Germany
Speed mill	Analytik Jena (bio solutions), Jena, Germany
Stereomicroscope DV4 Spot – with cold light source KL1500 LCD	Carl Zeiss AG, Göttingen, Germany
Thermomixer compact	Eppendorf GmbH, Hamburg, Germany

1.9 Software

Adobe® Acrobat ® Professional	Adobe Systems Inc., San Jose, Ca, USA
Endnote® X4.01	Thomson Reuters, New York, NY, USA
FACSComp software	BD Becton Dickinson GmbH, Heidelberg, Germany
Leica Application Suite AF lite	Leica GmbH, Wetzlar, Germany
Light Cycler Data Analysis (Version 3.5.17)	Hoffmann- La Roche, Mannheim, Germany
Microsoft® Excel®, Word® PowerPoint® 2003	Microsoft Corp., Redmond, Washington, USA
Moor LDI2 V5.1 software	Moor Instruments Ltd., Devon, UK
Sigma Plot® 11.0	Systat software inc., Chicago, IL, USA
Wasabi software	Hamamatsu PHOTONICS GmbH, Herrsching, Germany

2 METHODS

2.1 Animal model

All animal experiments were conducted according to the German law of animal protection and were approved by the Government of Oberbayern, Munich, Germany. Only mice were used for experiments in this thesis. After arrival at the institute, all mice were kept in standardized cages with a regular 12h day and night cycle and received food and water *ad libitum*.

2.1.1 Anesthesia protocols

2.1.1.1 *Ketamine/ Xylazine*

Ketamine 100mg/ml, Xylazine 2 % and 0.9 % isotonic saline-solution were combined in a 1:1:2 mixture and injected intraperitoneally (i.p.). Initially, this standard anesthesia protocol was used during the establishment of the surgical procedures and some pilot experiments. When better anesthesia combinations were available (see below), ketamine/xylazine was not used anymore.

2.1.1.2 *Triple combination anesthesia (MMF)*

The combination of midazolam (5.0mg/kg), medetomidine (0.5mg/kg) and fentanyl (0.05mg/kg) (MMF) is a modern anesthesia protocol. The advantages are an improved analgesia and reduced anesthesia induced cardiodepression. Furthermore, there is the option to antagonize the narcotics and therefore limit the duration of anesthesia by application of flumazenile (0.5mg/kg), naloxone (1.2mg/kg) and atipamezole (2.5mg/kg) (FNA). Although the common opinion is to inject anesthesia i.p., I applied these substances by subcutaneous injection (s.c.) into the skin fold at the neck, which worked out extremely well. Here, mice were not subject to the risk of incidental damage of important structures, vessels or organs and the induction is not significantly delayed when compared to i.p. injection. Initially, mice were given a little amount of isoflurane for a short inhaled narcosis (30 sec) to reduce the stress of the injection.

2.1.1.3 *Isoflurane/O_2*

Isoflurane (1.5Vol%) combined with 100% O_2 (1L/min flow) was used for the Laser Doppler perfusion measurements beginning on day 3 and prior to s.c. injection of narcotics (see above). Since analgesia was not necessary for LDI, the good hypnotic potential of isoflurane and the fast induction and waking up period made it ideal for this application.

2.1.1.4 *Postoperative analgesia*

For postoperative analgesia buprenophin (1.2mg/kg per day) was used. Mice received 100µl of buprenophin s.c. 10min prior to ending of general anesthesia as well as on day 1 and 2.

2.1.2 Femoral artery ligation

2.1.2.1 *General preparation*

Induction of anesthesia was performed by s.c. injection of triple combination anesthesia MMF. Adequate surgical tolerance was established when the toe reflex of both hind limbs could not be triggered anymore. In order to protect the eyes from drying-out, bepanthene eye-ointment was then applied to the eyes of animals. Subsequently, mice were placed in a supine position on a heating pad and a rectal probe was inserted in order to monitor the body temperature and maintain readings of 37°C. Then both inguinal skin areas were cleaned with disinfection spray and were cautiously shaved with a scalpel blade.

2.1.2.2 *Surgical procedure*

All surgical procedures were conducted using a stereomicroscope and a cold light source. Skin incisions of 5mm were performed on each leg at the inguinal area. The superficial adipose tissue was removed carefully to reach the femoral artery, vein and nerve (Figure 5).

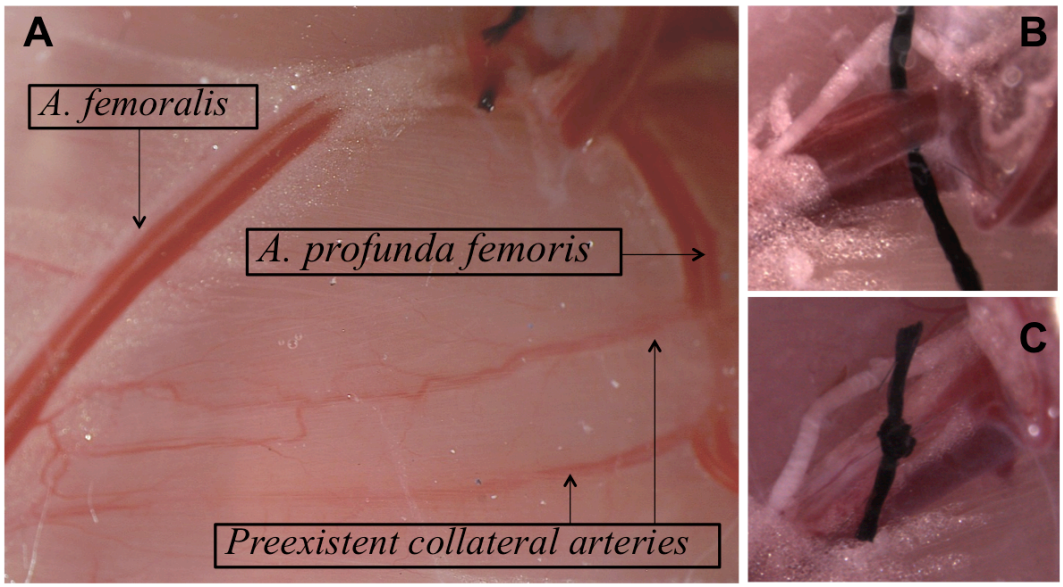

Figure 5: Ligation of femoral artery
A: Anatomical overview showing the arteria (A.) femoralis & profunda femoris as well as the collateral arteries.
B: Ligature site: Suture placed between the distal A. genu descendens and the proximal A. circumflexa
C: View of the nod, the perfusion of the distal part of the femoral artery is suspended.

The latter was dissected from the artery and finally the femoral artery and vein were carefully separated without producing any bleeding of a vessel. Distal of the branching of the circumflex artery and

proximal to the branching of the *A. genu descendens*, a piece of braded suture (7/0) was placed under the femoral artery of both hindlimbs. On the right side, three nods were tied for ligation of the femoral artery. On the left side, the sham side, the suture was only placed under the vessel but no nod was tied. The suture remained at the site. Finally the skin was sutured using 6/0 Vicryl and anesthesia-antagonizing mixture FNA was injected into the mice.

2.1.3 Isolation of tissue

2.1.3.1 *Catheterization of abdominal aorta*

Each blood cell carries a distinct amount of RNA and protein that could naturally "contaminate" the gene expression analyses of isolated collateral arteries among animals. Thus, the collateral arteries needed to be perfused to reduce the amount of blood inside the vessels before harvesting the tissue at different timepoints after femoral artery ligation to prevent this natural bias. Therefore, the aorta catheterization technique was adapted from the arteriogenesis rabbit model and applied to mice (Figure 6).

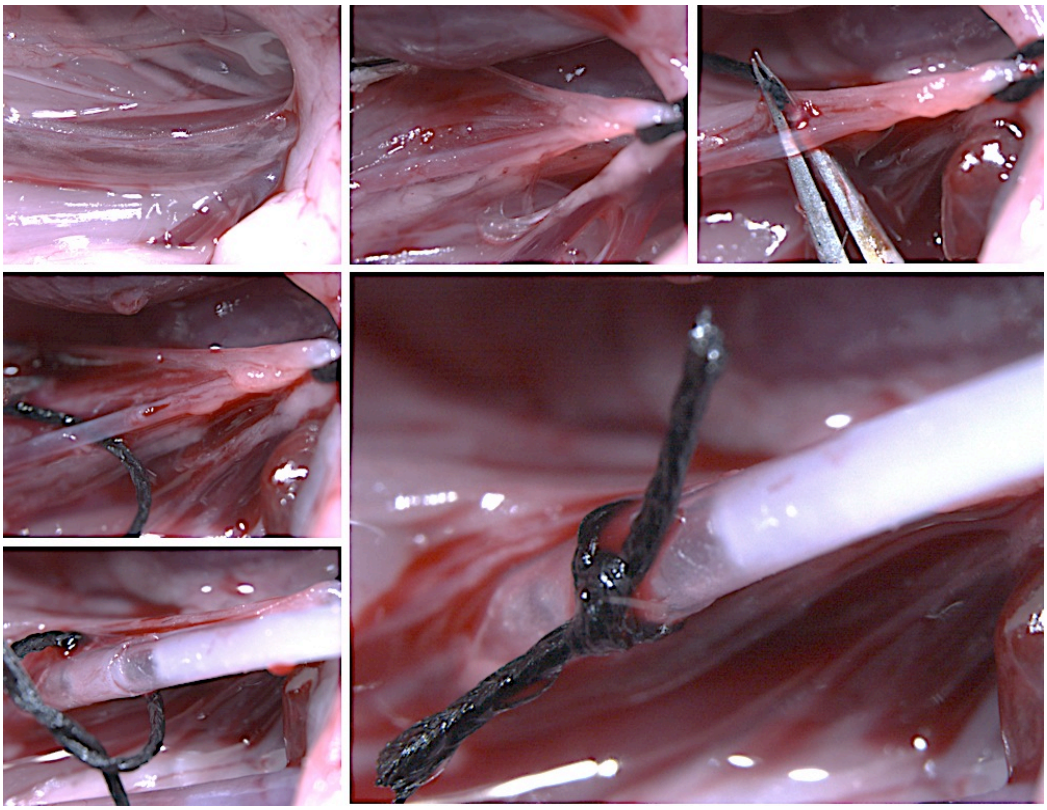

Figure 6: Catheterization of murine aorta (from top left to lower right)
The inferior vena cava and the aorta (upper left panel) are mobilized (upper middle panel) and the aorta is separated from the vein (upper right panel). A small incision is made (middle left panel) and the catheter is inserted (lower left panel) and fixed with a double nod (middle right panel).

The catheter was composed of a piece of tubing (outer diameter: 58mm, inner diameter: 38mm) that was placed onto a canula (size 14, tip cut off) connected to a three-way stopcock. Prior to insertion,

the catheter was rinsed with 0.9% saline solution. After commencing of the surgical tolerance phase by inducing anesthesia with MMF, the mouse was given 0,1ml of heparin and was placed transversely on a heating pad monitoring body temperature. A broad midline laparotomy from the xiphoid process to pubic area was performed and major parts of the intestine were mobilized and placed on the right of the mouse on a gauze compress to gain access to the abdominal aorta and the inferior vena cava. Both vessels were loaded on a curved forceps and a piece of Perma Hand silk suture was wound around both vessels right below the outlet of both renal vessels. Both ends of the suture were fixed with a Halstedt-Mosquito hemostat under cranial traction. The traction is particularly important to reduce blood flow and pressure within both vessels in order to facilitate the insertion of the catheter. Next, the abdominal aorta is freed from annexing fascia and separated from the inferior vena cava and another piece of suture was wound around the vessel and a provisional single nod was tied. Usually, the inferior vena cava ruptures, which is necessary to establish an artificial outflow for the perfusion solution and to prevent an overload of volume. Due to the first suture, the bleeding was controllable. Using fine spring scissors a small cut was conducted as close as possible to the first suture, the catheter was inserted carefully without tearing the aorta and advanced in caudal direction. The provisional nod was tied and a second nod placed on top to ensure stable positioning.

2.1.3.2 *Isolation of tissue for qRT-PCR and Western Blot*

After inserting the catheter, the distal vascular system was rinsed with 5ml saline solution until both paws appeared to be free from blood. After perfusion, however, the collaterals were hardly distinguishable from the surrounding muscle tissue; therefore a contrast medium had to be infused for tissue isolation (Figure 7).

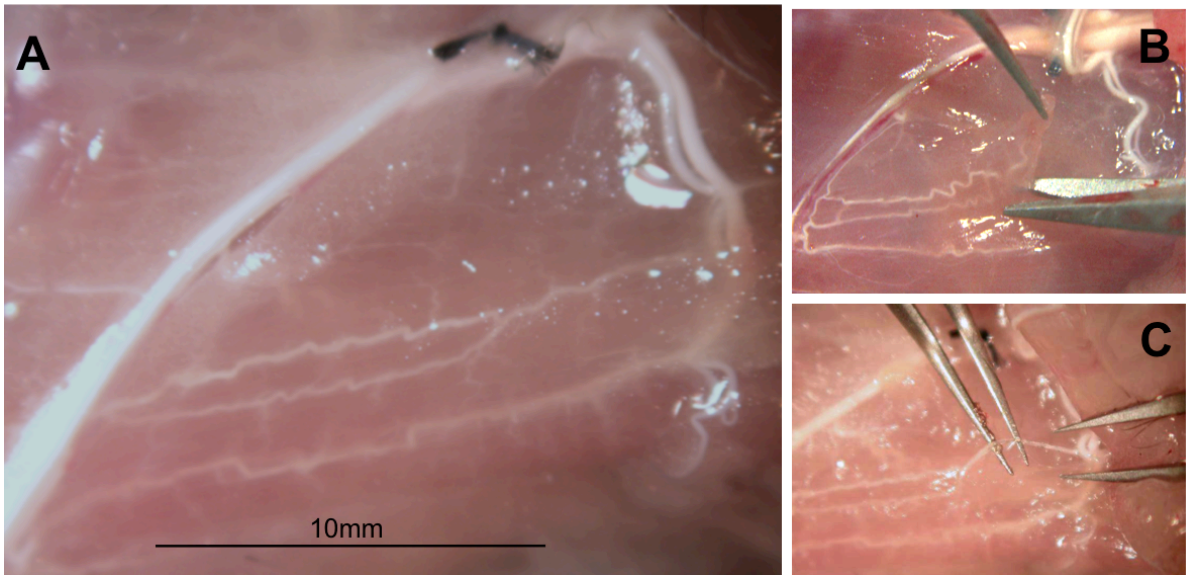

Figure 7: Isolation of collaterals for qRT-PCR and Western Blot
A: Photography showing collaterals perfused with latex.
B: The two superficial collateral arteries were dissected in a standardized size.
C: Latex made also a very fine preparation of these collaterals possible

Latex has excellent characteristics for this issue. The white color enables a good contrast to the muscle and the flexible texture permits the clear preparation of very small arterioles. 1ml was infused slowly into the vessels *via* the lying catheter. After preparation of skin and fascia from both hindlimbs, the two superficial collateral arteries were very good visible and easily isolated. Brain tissue and bone marrow was harvested 12h after ligation. For bone marrow sampling, both femurs per animal were flushed with physiologic saline solution and the cell suspension was collected in Eppendorf tubes. All samples were snap frozen in liquid nitrogen and stored at -80°C until further processing for qRT-PCR or Western blot.

2.1.3.3 *Tissue sampling for immunohistological analyses*

Three days after femoral artery occlusion, aorta was cannulated as described above and the vascular system of both hindlimbs was perfused with 3ml of adenosine buffer. For the detection of macrophages, the vasculature was perfused with 4% PFA to fix the tissue immediately. By touching both legs and tail, the grade of fixation could be estimated. After perfusion, the adductor muscles of both hindlimbs (occluded and non-occluded) were dissected. The muscles were isolated in a triangle-like shape comprising the collateral vessels in the front area. Proximal to the *A. profunda femoris* the base was cut. One side of the tip was cut laterally from the *A. femoralis* towards the knee and the natural anatomical border of the adductor muscle built the third side. Then the samples were placed in a tube containing 40ml of 10% glucose solution at 4°C over night. This hyperosmotic solution dehydrated the muscles and they dropped down to the bottom of the tube. The next day, the tissue was transferred into 40ml of 20% glucose solution and stored over night at 4°C. For cryopreservation, the muscles were placed upright on cork plates, covered with TissueTek® and then frozen immediately in 100ml of cold methylbutane (-150°C). This was done to cool down the tissue more slowly and reduce the amount of air entrapped. Then the samples were submerged in liquid nitrogen (-180°C) and stored at -80°C. For the detection of Egr1, samples without PFA fixative were used. Adductor muscles were harvested after perfusion with adenosine buffer placed face down in intermediate sized cryomolds and covered with TissuTek®. Samples were frozen on dry ice and stored at -80°C until further processing.

2.2 Laser Doppler perfusion measurements

The laser Doppler technique is a commonly used method to measure perfusion in the microcirculation. There are basically two principles: first there is the laser Doppler perfusion monitor where optical fiber light guides transmit light to the tissue and back to a probe that usually requires direct tissue contact. Second, there is the laser Doppler imaging (LDI) where the tissue remains untouched by the detector. For this study, the moorLDI2 was used to measure perfusion in the right and left leg prior to ligation, directly after and on day 3, 7, 14 and 21. Before using the device, I learned the technique at the Max-Planck-Institute in Bad Nauheim, Germany and established the method at our laboratory.

2.2.1 Technical background

The LDI equipment consists of a laser head that generates a low power laser beam in conventional technique *via* stimulated emission in an optic resonator. A moving mirror deflects the emitted beam in that way that a single beam is scanning a defined area in this study both mice hind limbs. The infrared wavelength of the beam does not only penetrate better through darker pigmented skin than a red wavelength, it also gives a higher weighting to blood flow in the deeper dermis. The laser beam is scattered by moving blood in vessels of the hindlimbs and by static tissue. Motion shifts the light in frequency (so called "Doppler" effect) whereas static tissue is non-shifting. The difference of shifting and non-shifting light is detected at two square-law detectors (receiver module) in form of intensity fluctuations, processed and displayed as color-coded pixels (flux image). Flux arbitrary units are proportional to the blood flow. Absence of blood flow, however, does not lead to "zero" flux. The residual interstitial movements are detected as well (resting tissue bias) and need to be subtracted during the data evaluation (see below).

2.2.2 Measurements

Prior to ligation, mice were anesthetized as described above and placed in a supine position (Figure 8).

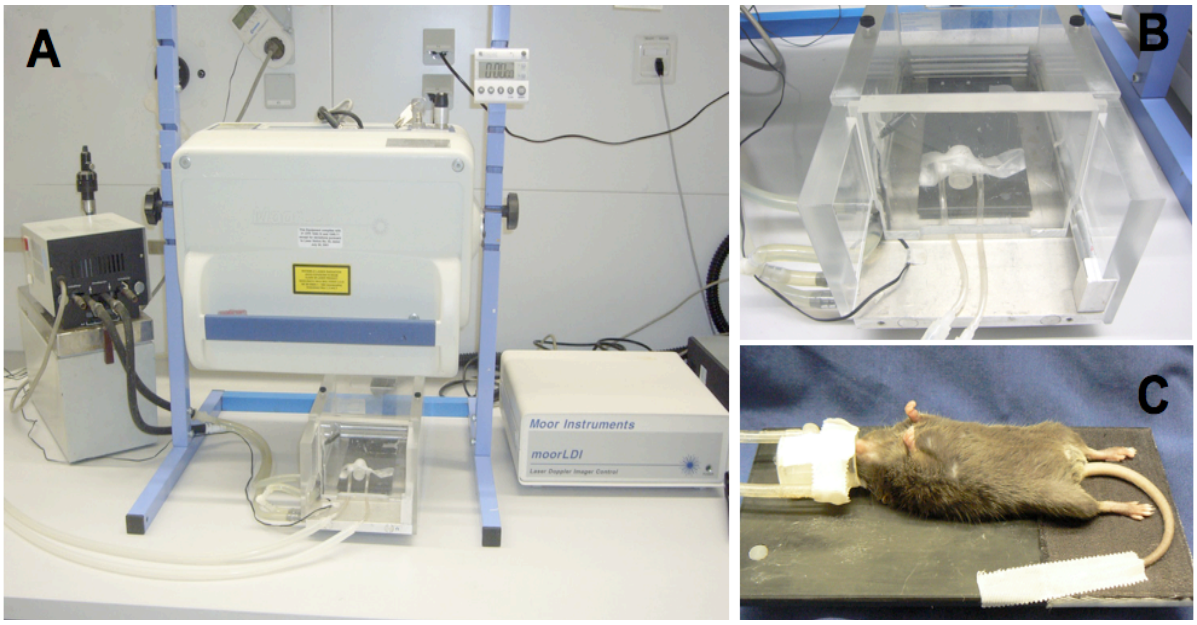

Figure 8: LDI setup
A: Laser Doppler equipment with a water bath regulating constantly the temperature of a heating chamber underneath the laser beam.
B: Close up of heating chamber with gas mask for inhalative anesthesia. Distilled H_2O was heated in the water bath and directed into the chamber using plastic tubing connected to acrylic glass tubes within the chamber.
C: Positioning of mouse on stage including the facemask. This stage can be moved and is placed inside of the heating chamber.

For all measurements a constant ambient temperature had to be provided. For this reason, a heating chamber connected to a water bath was constructed in our laboratory. The temperature was set to 37°C at the water bath and constantly monitored using a temperature probe within the chamber in all experiments. Both hind limbs were fixed with double-faced adhesive tape placing the sole of paws towards the laser beam. It was taken care that both hind limbs weren't overstretched. After 7min in the heating chamber the scan of both hind limbs was started. The scanning region was defined with a pixel resolution of 138 x 90 and a scan speed of 4 ms/pixel for a 1.7 x 3 cm area. If the scan took place on a later date, for example day 3, mice were anesthetized with an isoflurane/ O_2 gas mixture. Anesthesia was maintained *via* a facemask attached to the evaporator. The use of inhalative agents at later time points was chosen due to the fast wash-in/wash-out times of isoflurane. Furthermore, analgesia was not required for the measurements per se. After regaining consciousness the mice were put back into their cages.

2.2.3 Evaluation of flux images

Flux images were evaluated with the moor software „image review". A defined region of interest (ROI) was drawn over each hind limb from ankle to toes (Figure 9). Both areas were chosen equal in size (0.55cm^2) in all animals and groups. The software processes a flux mean value. These mean values were arranged as a right-to-left-ratio (relative perfusion). The reflection of resting tissue needs to be subtracted from the mean values to eliminate the occurring tissue bias. This background value was gained by post mortem LDI measurements.

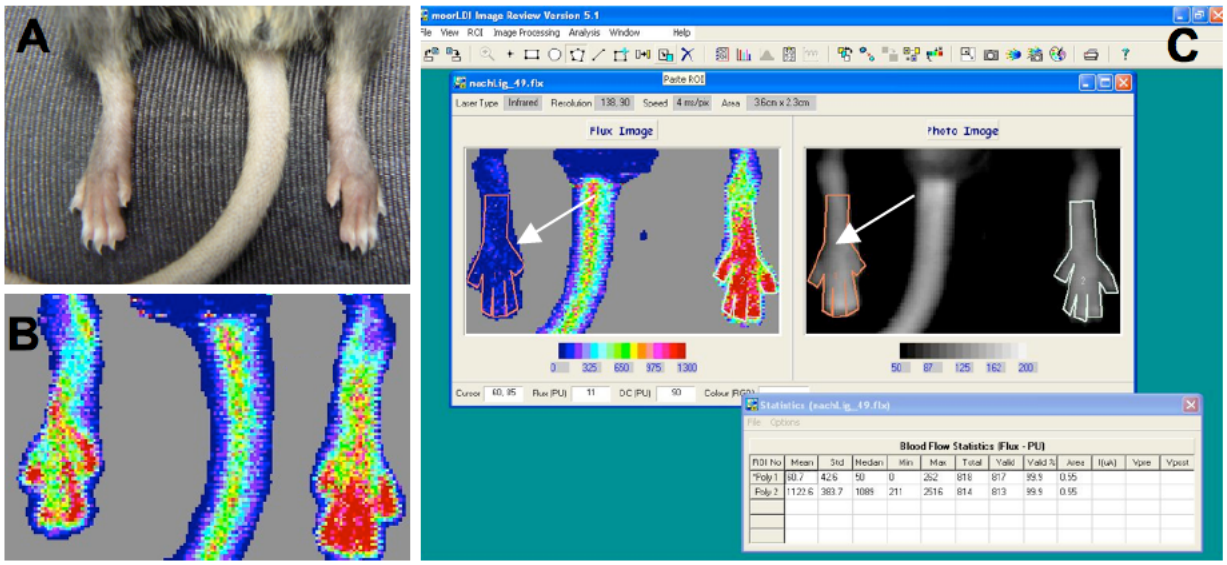

Figure 9: Perfusion transferred to flux values
A: Both hind limbs were taped in parallel to each other with the plantar side down, so that the back of the foot was exposed to the laser beam.
B: Representative flux image
C: Screenshot showing flux image and photo image, the drawn ROI (white arrow) and processed flux statistics as given by the software.

2.3 qRT-PCR

2.3.1 Total RNA isolation

Total RNA was extracted from isolated collateral arteries according to the *single-step* method of Chomczynski and Sacchi.[122] Two isolated collaterals per mouse per side were placed in lysis tubes, 300µl of solution A was added and the probe was homogenized in a speed mill for two minutes. Subsequently, 60µl 2M sodium acetate (pH 4.0), 600µl phenol and 120µl chloroform/isoamylalcohol (49:1 v/v) were added, the probe was vigorously shaken for one minute, transferred into MaXtract High Density tubes and placed on ice for 15min. Then the probe was centrifuged at 12000g at 4 °C for 2 minutes and the supernatant was transferred into a new 1,5ml reaction tube. To remove residual genomic DNA, 6µl 10x reaction buffer as well as 6µl DNase (both RNase-Free DNase Set) were added and the probe was incubated at 37°C for 30 minutes. Phenol and chloroform/isoamylacohol were added to the probe (49:1 v/v) and again the probe was shaken vigorously for one minute, transferred into 2ml MaXtract High Density tubes, placed on ice for 15 minutes and centrifuged at 12000g at 4°C for 2 minutes. The supernatant was transferred into a new 1,5ml tube, 1µl glycogen and 600µl isopropanol were added and incubated for 1 hour at -20°C or over night. Then the probe was spun down at 10,000g at 4°C for 30min, the pellet washed twice in 70% ice-cold ethanol and again centrifuged at 10,000g for five minutes. The resulting pellet was taken up in 90µl of Solution A, resuspended in 90µl isopropanol and the probe was kept at -20°C for over at least an hour or over night. After spinning down at 10,000g for 25 minutes, the pellet was washed two times with 70% ice-cold ethanol and centrifuged at 10,000g for 5 minutes. The pellet was let dry, then resuspended in 100µl ddH_2O and placed in a shaker at 64°C for 10-15 minutes. The concentration was determined in 2-4µl aliquots *via* measurement of the optical density (OD) in a spectrophotometer at 260nm (absorption spectrometry) according to the formula:

$$c(\mu g\ RNA/\mu l\ H_2O) = (OD_{260}*V*F)/1000$$

Where:

c = concentration of undiluted RNA sample
OD_{260} = absorption at 260nm
F = multiplication factor (40 µg/ml for an RNA probe)
V = dilution factor in sample
OD_{260} values in the range of 0.1 and 1.0 were considered reliable.

The purity of the probe (exclusion of contamination) was determined with the OD ratio OD_{260}/OD_{280}, absorption values at 260nm and 280nm, and values in the range of 1.8-2.0 were accepted.

2.3.2 Agarose gel electrophoresis

The qRT-PCR product and the quality of total RNA, respectively, were confirmed by gel electrophoresis on a 1.2% agarose gel using GelRed staining. 1.2g agarose and 100ml 1x TAE buffer were placed for 2 min at 600Watt in a microwave, placed on a magnetic stirrer until it was lukewarm. 5µl of Gel Red dye was added while stirring. The mixture was filled in the gel chamber and allowed to solidify during 30min at 4°C. 3µl loading dye was added to 10µl of the probe in ddH_2O (final volume of qRT-PCR products or 1µg of RNA, respectively) and spun down for 1min at 7300g. Probes were carefully pipetted in the slots of the gel and 1x TAE was filled in the tank. To evaluate the qRT-PCR generated DNA amplicon, a 100bp DNA ladder, a negative control (RNA instead of cDNA was used for qRT-PCR) as well as ddH_2O ran on the gel along with the qRT-PCR products. The gel was allowed to run at 70mA//40-60V for 1.5-2h. Documentation was performed using a cooled CCD camera and Wasabi software.

2.3.3 cDNA-Synthesis and qRT-PCR

1µg of RNA was reverse transcribed into cDNA with random nonamers and the 1st Strand cDNA Synthesis Kit for qRT-PCR. 1µg of total RNA was diluted to a Volume of 7.8µl and 12.2µl of the reaction kit (Table 4) was added. The reaction kit was composed of the following components:

Reagent	**Volume/1 sample**	**Final concentration**
10x reaction buffer	2.0µl	1x
25mM $MgCl_2$	4.0µl	5mM
Deoxynucleotide Mix	2.0µl	1mM
Random Primer $p(dN)_6$	2.0µl	0.08 A_{260} units (3.2µg)
RNase Inhibitor	1.0µl	50 units
AMV Reverse Transcriptase	0.8µl	≥20 units
Gelatin	0.4µl	0.01mg/ml
Total	12.2 µl	

Table 5: Reaction mix for cDNA synthesis

The mixture with the total volume of 20µl was briefly vortexed and centrifuged to collect the sample at the bottom of the tube, then the mixture was incubated at 25°C for 10min (annealing), at 42°C for 60min (reverse transcription), at 99°C for 5min (denaturation of reverse transcriptase) followed by a

cooling down at 4°C for 5min. Finally 80µl ddH_2O were added to the tube and cDNA was stored in eppendorf tubes at -20°C.

qRT-PCR was performed on a Light Cycler 1.5 using a SSYBR Green I Kit - Light Cycler® FastStart DNA Master^{Plus} in a reaction volume of 10µl according to the manufacturer's protocol. Each PCR reaction had a reaction volume of 10µl and was composed according to the manufacturer's protocol:

1µl of cDNA,

1µl of primer mixture (50pmol of each forward and reverse primer),

2µl "reaction mix" (contains FastStart Taq DNA Polymerase, reaction buffer, $MgCl_2$, SYBR Green I dye, dNTP)

6µl dH_2O (PCR grade, provided by the manufacturer)

Cycling parameters were:

95°C for 10 minutes (initial denaturation)

95°C for 10 seconds (40 cycles of denaturation)

5 seconds of annealing (primer specific temperatures are listed in materials 1.5, table 2),

72°C for 15 seconds (extension)

Melting curve: from 65°C to 95°C, ramp rate 0.1°C/sec

Cooling 30s at 40°C

At least three independent qRT-PCR reactions were performed on each template. Results were analyzed using Light Cycler Data Analysis (Version 3.5.17). The specificity of the amplification products was confirmed by analyzing their melting curves (no additional peak was visible).

For generation of a standard curve, dilutions from 10^5 to 10^{10} were generated. The resulting slope and crossing point (Cp) for targets (CpT) and reference gene (CpR) were established. Slope values were used for calculation of efficiency using the following formula:

E= 10^(-1/slope)

Since "typical" housekeeping genes like glyceraldehyde-3-phosphate dehydrogenase (GAPDH) and beta3-actin are subject to a greater variance in expression levels dependent on experimental treatment conditions and are indeed differentially expressed in this model, they could not serve as internal standards.[123] Therefore, results were normalized to the expression levels of the 18S rRNA[123] with the following formula according to the method of method of Pfaffl.[124]

$$\text{Normalized ratio} = \frac{E_T^{\,CpT(C) - CpT(S)}}{E_R^{\,CpR(C) - CpR(S)}}$$

Where:
E_T = Efficiency of target, E_R = Efficiency of reference (here: 18S rRNA)
C_pT = Crossing point of target (cycle number at detection threshold)
C_pR = Crossing point of reference (cycle number at detection threshold)
R = Reference
S = Sample
C = Calibrator (tissue from untreated animals was used as calibrator probe)

2.4 Western Blot

2.4.1 Protein isolation and determination of concentration

To isolate total protein, tissue samples were placed on ice in 3ml total protein isolation buffer and homogenized using a Teflon-glass pestle. After incubation of 30min on ice, the probe was centrifuged at 14,000g for 30min at 4°C. The total protein concentration was measured in the supernatant using a bicinchoninic acid (BCA) assay kit. The assay is based on two reactions. Peptide bonds in proteins reduce Cu^{2+} ions to Cu^{1+} so that the quantity reduced Cu^{2+} is proportional to the amount of protein present in the solution. Then, two molecules of BCA are able to chelate with one Cu^{1+} ion thereby forming a purple complex that can be detected at the wavelength of 562nm. In order to create a standard curve for the protein quantification, wells of a 96-well plate were filled with the following concentrations of BSA (in mg): 0 (baseline), 0.05, 0.1, 0.25, 0.5, 0.75, 1.0 and 2.0 in a reaction volume of 10µl. The kit's reagents were mixed according to the manufacturer's instructions and 200µl of the mixture was added to each well. After incubation of approximately 30min at room temperature, the OD_{562} was measured using the ELISA reader. The OD of the buffer was measured as well to subtract its background value from the probe values. The results for BSA were plotted to a standard curve and the protein concentration of test samples was determined accordingly.

2.4.2 Sodium dodecyl sulfate-polyacrylamide gel electrophoresis (SDS-PAGE)

4x loading buffer was added to the sample according to the determined concentration of the sample (4:1), followed by incubation of 5min at 95°C in a mixer for denaturation of proteins and was then placed on ice. Laemmlie buffer was filled in the tank. Equal amounts of probes (10mg) and the molecular weight marker (Page Ruler Prest. Protein Ladder marker) were filled in the slots of a 4–20% Tris-glycine gel using a Hamilton syringe. The running conditions were 10mA for 10min and subsequently 25mA for 70-90min (discontinuous method established by Laemmli[125]).

2.4.3 Blotting

For electrophoretic transfer of sample proteins to a nitrocellulose membrane, chromatography filter paper and membrane were cut according to the size of the gel (7x8cm). Filter paper, membrane, gel and another piece of filter paper were incubated with transfer buffer for 5min and placed in the transfer assembly. Current values were calculated according to the size of the filter paper ($I[mA] = A[cm^2]$ x 0.8) and the transfer ran for over 1h. After the transfer, proteins were stained with Ponceau S solution (1:9 dilution in H_2O bidest). To do so, the membrane was covered entirely with the working solution, gently shaken and subsequently the solution removed. Then fresh working solution was added to the membrane, placed on a shaker and incubated for 5-10min at room temperature. Finally the mem-

brane was washed with washing buffer until bands were visible and scanned for documentation. The membrane was washed until the bands disappeared, blocked in 5% non-fat dry milk (NFDM) for 1h and washed again 3 times (each washing procedure lasted 5min).

2.4.4 Detection of immunoreactive bands

For EGR1 protein detection, the polyclonal rabbit anti-mouse- EGR1 antibody was diluted (1:500) in 5% BSA, added to the blot and incubated over night at 4°C. The next day, the blot was washed 3 times with washing buffer for 10min. The secondary HRP-conjugated goat-anti-rabbit-IgG antibody was diluted in 5% NFDM (1:5000) and incubated for 1 hour at room temperature followed by washing three times (10min each) of the membrane. In the meantime, the chemiluminescent substrate (Super-Signal-Femto-West) was prepared according to the manufacturer's protocol. Then the membrane was incubated with the substrate (0.1ml/cm^2) for 5min to visualize the immunoreactive bands and placed in a plastic wrap. The blot was imaged on a cooled CCD camera using wasabi software. Results are displayed in concordance with the Ponceau staining since typical housekeeping genes are not applicable for this model[123].

2.5 Immunohistochemistry

2.5.1 EGR1 staining

7µm sections were cut on a cryomicrotome, placed on SuperFrost Menzel slides, allowed to dry for one hour and stored in -80°C until further processing. On the day of the staining, slides were placed in ice-cold acetone for 20min for fixation. Then the slides were mounted on Shandon coverplates® in a humid chamber and 100µl PBS/0.3%Triton (P/T) (v/v) was added to each slide. Subsequently, slides were blocked with 5% normal goat serum in P/T (v/v). Slides were washed once with P/T and then incubated with a mixture containing the rabbit anti-mouse EGR1 (1:50) and the anti-aSM Actin antibody (1:100) diluted in P/T over night at 4°C. After rinsing for 5min with P/T, the slides were incubated with a mixture containing the secondary antibodies Alexa fluor488-conjugated goat anti-rabbit and Alexa fluor562-conjugated goat anti-mouse IgG (each 1:200 in P/T) for 1 hour at room temperature protected from light. Subsequently, the slides were rinsed twice with P/T and incubated with ToPro3 (1:400) diluted in P/T (v/v) for 10min to stain nuclei. Sections stained whithout the primary or the secondary antibody served as negative controls. Slides were removed from the cover plates, and coverslipped using Vectastain mounting medium and immediately analyzed on a Leica confocal microscope using the Leica application suite software.

2.5.2 Leukocyte quantification

Histological quantification of the number of activated macrophages in the adductor muscle was performed in Egr1$^{-/-}$ and WT mice (*n*=3/ per group). From every adductor, 6 cryosections (7µm) were obtained; 2 from the medial, 2 from the middle and 2 from the lateral part. The distances between the sections remained the same for every sample. Sections were air-dried, washed with PBS, incubated with 3ml H_2O_2 in 180ml methanol (10min) for quenching of endogenous peroxidase activity. For detection of macrophages, slides were incubated with a monoclonal rat anti-mouse Mac-3 antibody (over night at 4°C, 1:100) and subsequently incubated with horseradish peroxidase conjugated donkey anti-rat IgG (1h, 1:200). Again, sections stained whithout the primary or the secondary antibody served as negative controls. The immunoperoxidase signal was visualized with the chromogen 3.3′-diaminobencidine (DAB). The total number of Mac-3 positive cells accumulated in the adventitia and perivascular space of collateral arteries was counted per slide.

2.6 Fluorescence activated cell sorting (FACS)

2.6.1 FACS-analysis of whole blood

Whole blood from Egr1$^{-/-}$ and WT mice (n=9 per group) was drawn from the left ventricle by intracardiac puncture. Mice under anesthesia were given 0.1ml of heparin (500IU), placed on their back and the skin of the thorax was carefully removed. The third or fourth intercostal space was punctured using a 1ml syringe and a fine canula. The collected blood was diluted in an equal volume using 0.9% saline and red blood cell lysis was performed according to standard protocols. 30µl of the resulting cell suspension was incubated with 10µl of an anti-mouse CD11b PE-conjugated mAb. Before sorting, remaining erythrocytes were lysed according to standard procedures (fixation in 2% PFA for 10min and incubation with 0.1% Triton X-100 in PBS for 30 minutes at room temperature). Granulocyte and monocyte populations were identified by fluorescence and scatter light characteristics. Absolute monocyte and granulocyte counts were calculated from the numbers of analyzed monocytes and fluorescent standard beads that were added to the probe.

2.6.2 FACS-analysis of the whole adductor muscle

In order to detect cells within muscle tissue, the adductor muscles of Egr1$^{-/-}$ and WT mice (n=6 per group), were perfused with PBS *via* cannulation of the aorta to eliminate the blood, harvested, weighed (each weighed 2mg±0.05) and placed in small cell culture dishes. Next the homogenization of the tissue was executed by cutting the tissue into small pieces with a sterile scalpel and by inducing digestion with the digestion solution. The dishes were softly shaken and placed in an incubator at 37°C for over an hour. In between the suspension was resuspended using a 500µl pipette to facilitate ho-

mogenization. Then the homogenisate was filtered through a 70µm cell strainer together with PBS and 2% BSA, spun for 10 min at 95g and the supernatant discarded. The resuspended pellet was washed by centrifugation again at 95g for 5min and finally resuspended in 100µl PBS and 2% BSA. The samples were incubated with one of the following combinations of two monoclonal antibodies: 10µl CD 11b PE/ CD 45 FITC or CD 3 FITC/ CD19 PE for 20min at 4C°. The solution was washed three times by centrifugation at 95g for 5 minutes and finally resuspended in 100µl PBS and 2% BSA. Fluorescent standard beads were used to calculate the absolute numbers of cells per µl of cell suspension.

2.7 Statistical analysis

Statistical analysis was carried out with SigmaPlot® 11.0. All experimental values are stated as mean ± SEM. The data was first tested for normality (Kolmogorov-Smirnov-Test). Analyses between two groups were performed using unpaired student's t-test or Mann-Whitney rank sum test, respectively. Analyses between two or more groups were performed using one-way-ANOVA and subsequent Holm Sidak correction. Results were considered to be statistically significant with p values of <0.05.

IV. RESULTS

1 GENERAL OBSERVATIONS

Prior to surgery no obvious differences or an apparent phenotype were observed in WT or Egr1 deficient mice. All initial surgical procedures were conducted without complications (arterial, venous or neuronal damage) and were well tolerated by Egr1 deficient and control mice; none of the animals showed an increased tendency of vessel fragility during the surgical procedure or died during or after the procedure. No anatomical variations in the hindlimb vasculature such as differences in branching or caliber of the vessels were observed in Egr1 deficient mice when compared to control mice and no bleeding occurred. Already 1h after surgery, animals of both groups moved around in cages and started grooming and cleansing their fur. No wound infections, skin color changes, ischemic gangrenes or a significant motor impairment of the hind limbs were observed. Food intake and water consumption were normal in both groups.

2 PARTICIPATION OF EGR1 IN COLLATERAL ARTERY GROWTH

2.1 Perfusion recovery in wildtype and Egr1 deficient mice

Egr1 has previously been studied in a femoral artery excision model,[96] where angiogenesis and arteriogenesis occur in the adductor muscle at the same time. In order to evaluate the role of Egr1 during arteriogenesis only, the unilateral femoral artery ligation model was used in WT and Egr1 deficient mice (n=7 per group). The time course of perfusion recovery was monitored by LDI perfusion measurements over the time period of 21 days. Prior to femoral artery ligation (baseline measurement), no significant differences in right-to-left blood perfusion ratio between the WT (0.99±0.02) and the Egr1 deficient group (1.0±0.02) were detected. Immediately after ligation, the blood flow ratio (ligated/non-ligated) dropped by 90% in both groups with the WT group showing a ratio of 0.11±0.01 and the Egr1 deficient mice showing a mean value of 0.10±0.02. On day 3, the group of the Egr1 deficient mice showed a slight tendency for a delay in perfusion recovery (0.2±0.04) when compared to the WT group (0.31±0.03). This difference, however, was not statistically significant (p=0.06). On day 7, statistically significant differences in $Egr1^{-/-}$ (0.46±0.05) vs. WT (0.73±0.04) became apparent and persisted also at day 14 (0.65±0.02 $Egr1^{-/-}$ vs. 0.88±0.04 WT) and day 21 (0.79±0.03 $Egr1^{-/-}$ vs. 0.96±0.02 WT), the end of the observation period (Figure 10).

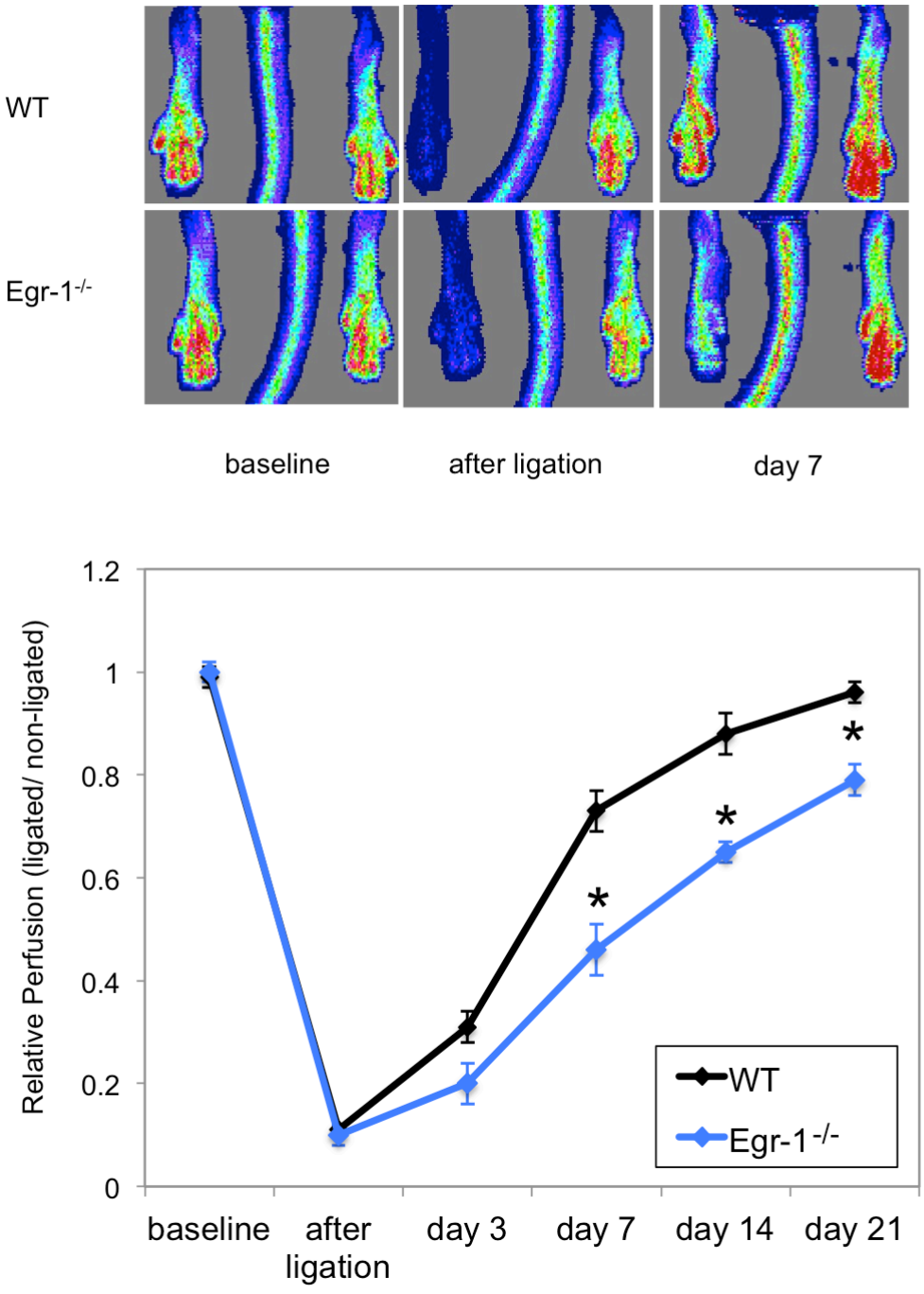

Figure 10: LDI analyses in Egr1$^{-/-}$ and WT mice after femoral artery ligation
Top: Representative laser Doppler images of both groups prior to, directly after ligation and on day 7.
Bottom: Line plot showing right-to-left (occ/sham) flux ratios during an observation period of 21 days, n=7, mean±SEM, *p<0.05 vs. control.

2.2 Egr1 expression in arteriogenesis

The collateral arteries of C57Bl/6 mice were harvested at timepoints 3h, 6h, 12h, 24h, 48h and 3d after femoral artery ligation from the occluded and the sham side and qRT-PCR was performed for Egr1 levels. Quantification in relation to 18S revealed significant differences between the occluded and the sham side at 12h, 24h, 36h and 48h. (Figure 11**A**) Accordingly, protein levels of Egr1 in collateral arteries were increased on the occluded side when compared to sham at 24h, 36h and 48h after femoral artery ligation. (Figure 11**B**)

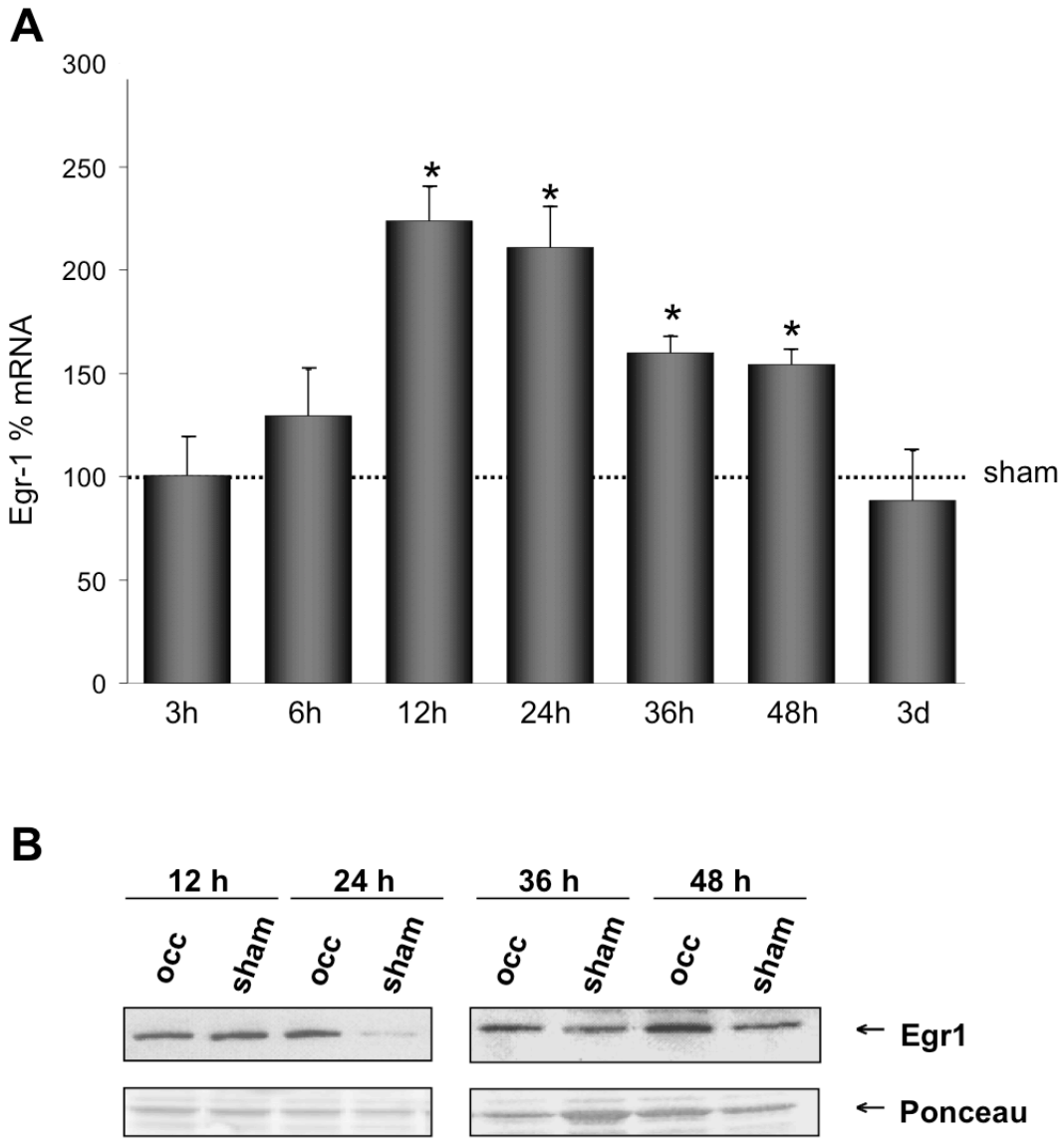

Figure 11: Egr1 Expression in growing collateral arteries
A: Vertical bar chart showing the timeline of Egr1 mRNA levels expressed in isolated growing collaterals of WT mice at various time points after femoral ligation. Vertical dot line represents Egr1 mRNA levels detected on the sham side which was set to 100% to calculate the relative expression, mean±SEM, *p<0.05 vs. sham.
B: Representative Western Blot of EGR1 protein (top) isolated from collateral arteries 12h, 24h, 36h and 48h after ligation. Bottom: Ponceaustaining performed to control equal loading.

Immunofluorescence staining for EGR1 48h after femoral artery ligation evidenced a localization of EGR1 in ECs, vSMCs and perivascular cells of growing collaterals as well as in venules and nerves (Figure 12). When focusing closer on the distinct layers of the arterial collateral vessel, EGR1 stained to the activated bulging endothelium and to cells adherent to ECs. Focusing at the smooth muscle cell layer, EGR1 co-stained with αSM-actin and was also detected in perivascular cells.

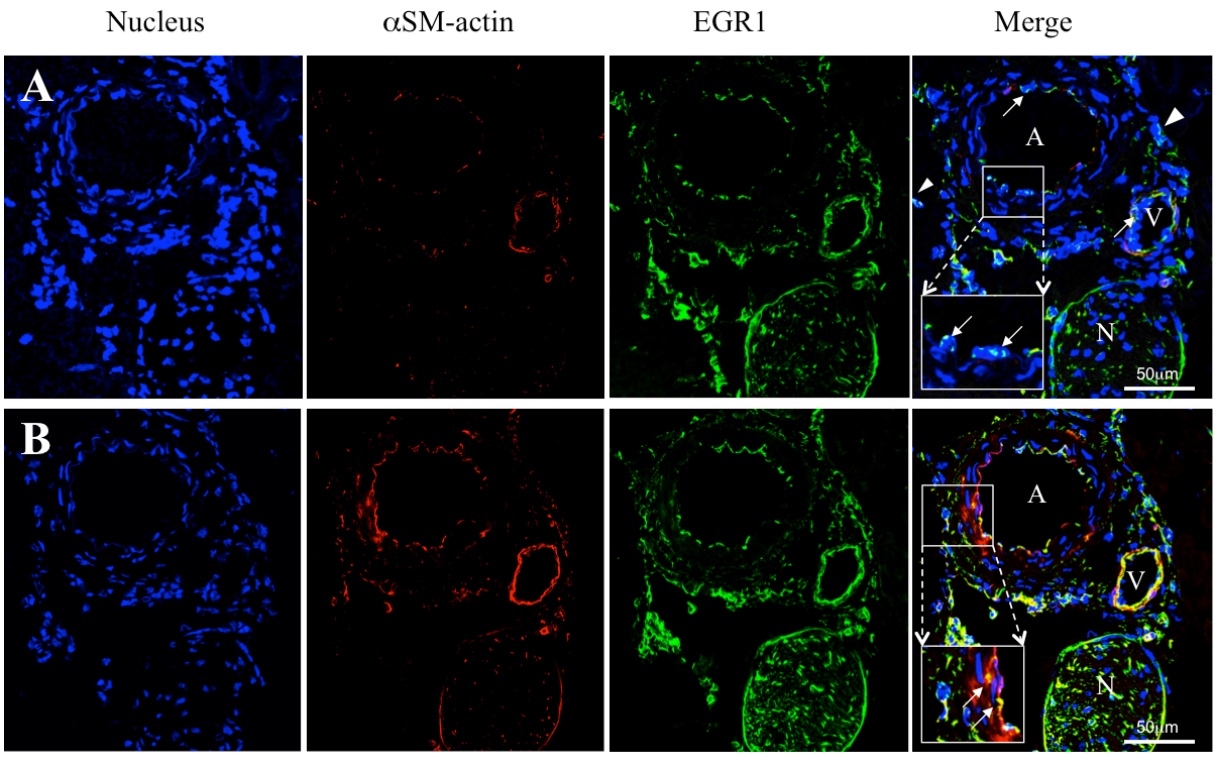

Figure 12: Immunohistochemical detection of EGR1 in growing collateral arteries
Crossectional view of collateral vessels in the adductor muscle 48h after ligation showing single stain (nucleus = blue, aSM-actin = red, EGR1= green) and merged images
A: Overview over collateral artery (A), vein (V) and nerve (N) in a crossection focusing on the endothelial layer: EGR1 (green) stains to the activated bulged endothelial of the collateral arteriole and venule (arrows). The insert contains a magnification showing nuclei of endothelial cells staining positive for EGR1. EGR1 was also detected in nerves and perivascular cells (arrow heads). Scale bar = 50µm
B: Overview over collateral artery (A), vein (V) and nerve (N) in a crosssection focusing on the smooth muscle cell layer: The insert shows a magnification of EGR1 stained to the smooth muscle cell layer together with αSM-actin (arrows). Scale bar = 50µm

3 EGR1 INFLUENCES ON CELL COUNTS AND LEUKOCYTE DISTRIBUTION

3.1 Leukocyte recruitment

It has been previously reported that Egr1 deficiency might affect cell maturation and cell numbers; however no data on baseline monocyte counts were available for these mice. In order to analyze the baseline monocyte and granulocyte counts of Egr1$^{-/-}$ and WT mice, FACS analyses of the whole blood in non-ligated animals were performed. The data showed significantly increased amounts of monocytes in Egr1$^{-/-}$ mice (521.89±52.88 cells/µl) when compared to WT mice (326.57±22.04 cells/µl). Accordingly, higher amounts of granulocytes were also detected in Egr1$^{-/-}$ mice (811.79±76.96 cells/µl) compared to the WT group (559.80±34.57 cells/µl) (Figure 13).

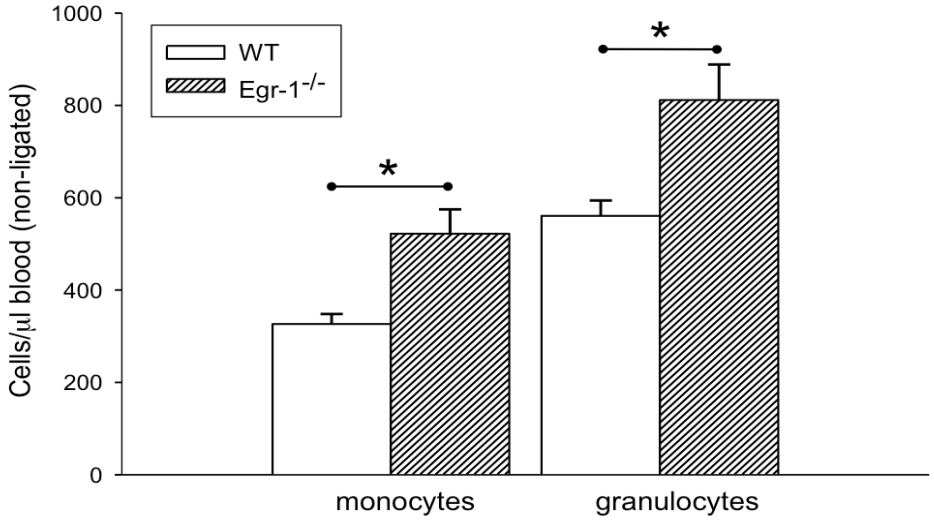

Figure 13: Baseline leukocyte counts in Egr1$^{-/-}$ and WT mice
Vertical bar chart showing FACS blood cell counts of monocytes and granulocytes in WT and Egr1$^{-/-}$ mice; mean±SEM, *p<0.05.

Next, it was investigated whether increased amounts of blood monocytes might as well result in increased numbers of macrophages in the adductor muscle in the baseline situation (sham condition) and after imposing a stimulus for transmigration (femoral artery ligation). Therefore adductor muscle tissue samples were collected after femoral artery ligation on the sham and the occluded side. Using immunohistochemistry, the number of macrophages accumulated in the perivascular area of growing collateral arteries (occluded side) and sham arteries was counted per arteriole per slide. The quantification revealed significantly more cells in the perivascular space of the occluded side of Egr1$^{-/-}$ mice (8.10±0.99 per vessel) when compared to WT (6.12±0.45 per vessel) 3 days after femoral ligation. When the sham sides of both groups were compared, Egr1$^{-/-}$ mice showed significantly fewer macrophages (1.87±0.16 per vessel) than WT mice (3.91±0.44 per vessel). These data indicate that monocyte recruitment is significantly impaired in Egr1$^{-/-}$ mice under baseline conditions (Figure 14).

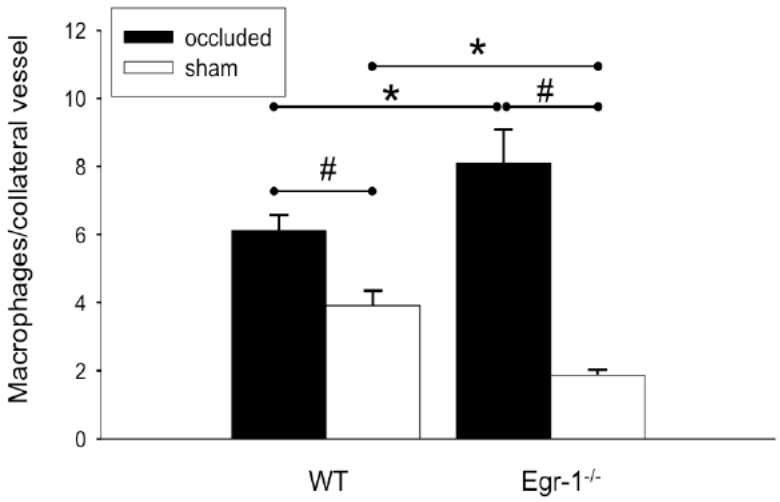

Figure 14: Stimulus directed leukocyte recruitment in Egr1$^{-/-}$ and WT mice
Vertical bar chart displaying macrophage counts per collateral vessel in adductor muscles of WT and Egr1$^{-/-}$ mice on day 3 after femoral ligation. Baseline leukocyte recruitment into the perivascular space seems impaired whereas stimulus driven recruitment is overcompensated in Egr1 deficient mice. Mean±SEM, *P<0.05 vs. WT control, # p<0.05 occ vs. sham.

According to the data obtained from the histological quantification of macrophages, FACS of the whole adductor muscle of non-ligated animals revealed fewer resident monocytes in Egr1$^{-/-}$ (18.14±2.73 cells/µl) than in WT mice (51.22±4.38 cells/µl). Moreover, the total number of leukocytes was reduced in Egr1$^{-/-}$ when compared to WT mice (552.45±75.79 cells/µl vs. 768.48±76.22cells/µl), corroborating the findings for baseline leukocyte recruitment. When looking at other cell populations, reduced numbers of T-cells (9.21±1.33 cells/µl in Egr1$^{-/-}$ vs. 76.64±30.1 cells/µl in WT) and B-cells (144.00±19.36 cells/µl in Egr1$^{-/-}$ vs. 392.49±44.33 cells/µl in WT) could be detected (Figure 15).

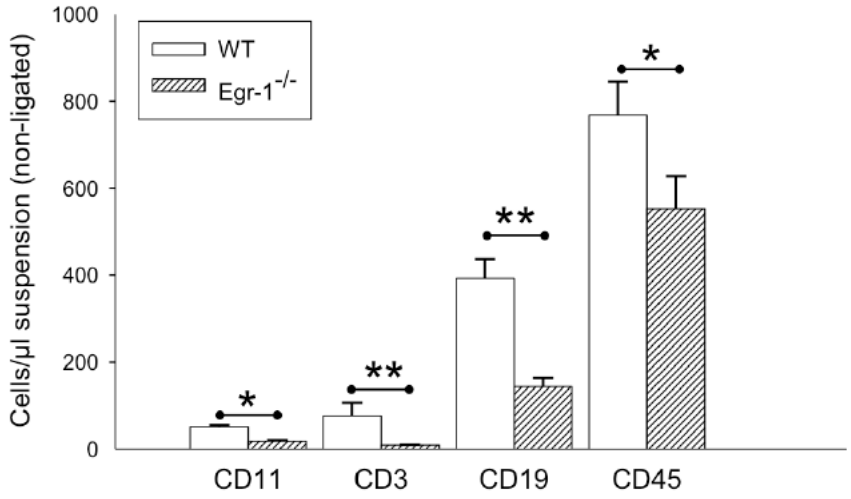

Figure 15: Baseline cell transmigration
Vertical bar chart of FACS cell count data gained from digested whole adductor muscle tissue of unligated WT and Egr1$^{-/-}$ mice. Investigated cell types: CD11 = monocytes, CD3 = T-cells, CD19 = B-cells, CD45 = leukocytes. Mean±SEM, *p<0.05, **p<0.001 vs. WT.

3.2 Expression of ICAM-1, MCP-1 and uPA

After having observed the differences in leukocyte number and distribution under baseline and stimulated conditions, it was interesting to look at typical mediators of chemotaxis, adherence and transmigration of leukocytes that previously been shown to be involved in arteriogenesis, and were also discussed as Egr1 downstream targets. Therefore, the mRNA levels of the potential Egr1 downstream genes MCP-1 (Figure 16A), ICAM-1 (Figure 16B) and uPA (Figure 16C) were assessed using qRT-PCR in growing collateral arteries at 12h and 24h after femoral artery ligation. An upregulation of

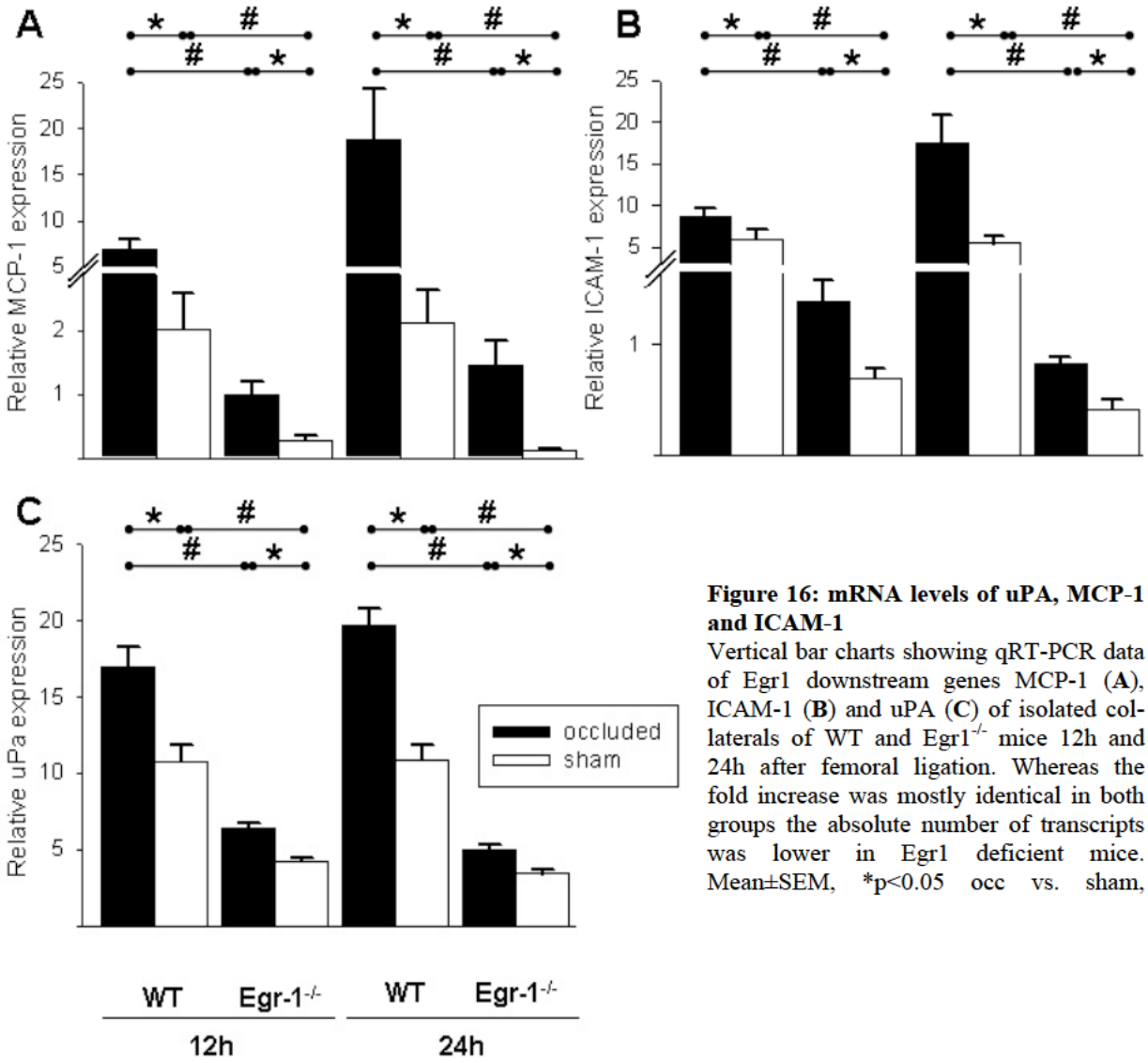

Figure 16: mRNA levels of uPA, MCP-1 and ICAM-1
Vertical bar charts showing qRT-PCR data of Egr1 downstream genes MCP-1 (**A**), ICAM-1 (**B**) and uPA (**C**) of isolated collaterals of WT and Egr1$^{-/-}$ mice 12h and 24h after femoral ligation. Whereas the fold increase was mostly identical in both groups the absolute number of transcripts was lower in Egr1 deficient mice. Mean±SEM, *p<0.05 occ vs. sham,

mRNA was found in WT mice for MCP-1 (7.57fold), ICAM-1 (1.44fold) and uPA (1.61fold) at the 12h timepoint. Egr1$^{-/-}$ mice also showed an upregulation at the same timepoint (MCP-1: 7.51fold, ICAM-1: 3.1fold and uPA: 1.52fold). This increase was furthermore detectable at 24h in WT (MCP-1: 8.53fold, ICAM-1: 3.26fold and 1.9fold) and Egr1$^{-/-}$ mice (MCP-1: 10.88fold, ICAM-1: 3.11fold and

uPA: 1.51fold). Both animal groups showed even a further increase for MCP-1 and ICAM-1 at the timepoint 24h. Interestingly, the relative fold increase (differences occluded vs. sham) was roughly consistent within both groups but the overall absolute amount of transcripts was decreased at all timepoints in Egr1 deficient mice compared to WT mice.

4 PARTICIPATION OF THE OTHER EGR FAMILY MEMBERS

In order to evaluate the role of Egr family members in arteriogenesis and their capability to maintain transcription of important EGR1 target genes under Egr1 deficiency, the mRNA-levels of Egr family members Egr1-4 in growing collateral arteries were assessed in WT and Egr1$^{-/-}$ mice (Figure 17).

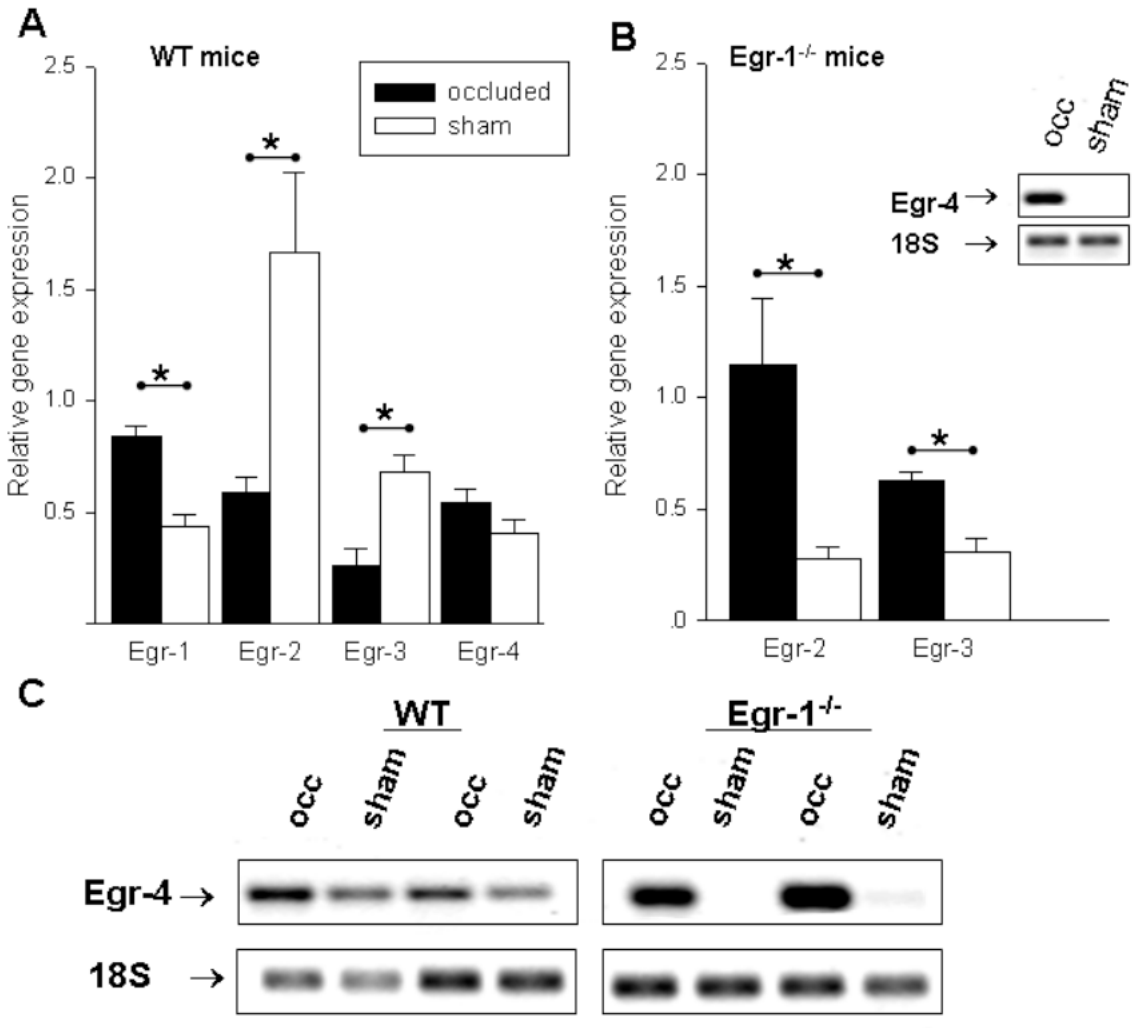

Figure 17: qRT-PCR of Egr2, Egr3 and Egr4 in Egr1$^{-/-}$ and WT mice 12h after ligation
A: Vertical bar chart of Egr1, Egr2, Egr3 and Egr4 mRNA levels detected via qRT-PCR in collateral arteries of WT mice 12h after ligation. Mean±SEM, *p<0.05 occ vs. sham
B: Vertical bar chart of Egr2-3 mRNA detected in Egr1$^{-/-}$ mice 12h after ligation. Figure insert: representative agarose gel showing Egr4 expression (upper panel) and 18S (lower panel) in Egr1 deficient mice. Mean±SEM, *p<0.05 occ vs. sham. **C**: Representative agarose gel comparing Egr4 expression (upper panel) of WT and Egr1 deficient mice, lower panel displaying 18S to evidence that qRT-PCR ran efficiently. In WT mice only a trend to upregulation of Egr4 was observed, however in Egr1 deficient mice, a very pronounced expression was detected compared to sham.

In WT mice, Egr2 and Egr3 levels were significantly downregulated at 12h after femoral ligation (Egr2: 0.35fold occ vs. sham and Egr3: 0.44fold, respectively). Egr4 mRNA levels evidenced a trend towards upregulation on the occluded side; however, no significance could be detected. By contrast, $Egr1^{-/-}$ mice displayed a significant upregulation of Egr2 and Egr3 mRNA on the occluded side (Egr2: 2.14fold occ vs. sham and Egr3: 1.20fold, respectively). Egr4 was found significantly upregulated on the occluded side but in collaterals on the sham side, Egr4 was barely detectable *via* qRT-PCR.

5 INFLUENCES ON VASCULAR CELL PROLIFERATION

5.1 Cell cycle progression

In order to evaluate mitotic progression, mRNA levels of Egr1 downstream genes and important cell cycle regulators cyclin D1, E and cdc20 were analyzed by means of qRT-PCR. Cyclin D1, cyclin E and cdc20 showed no differential expression pattern in WT mice (Figure 18). In contrast, cyclin E (1.3fold) and cdc20 (2.0fold) were significantly upregulated and in growing collaterals of $Egr1^{-/-}$ mice, however, cyclin D1 could not be detected anymore neither in collaterals of the occluded nor the sham operated side *via* qRT-PCR.

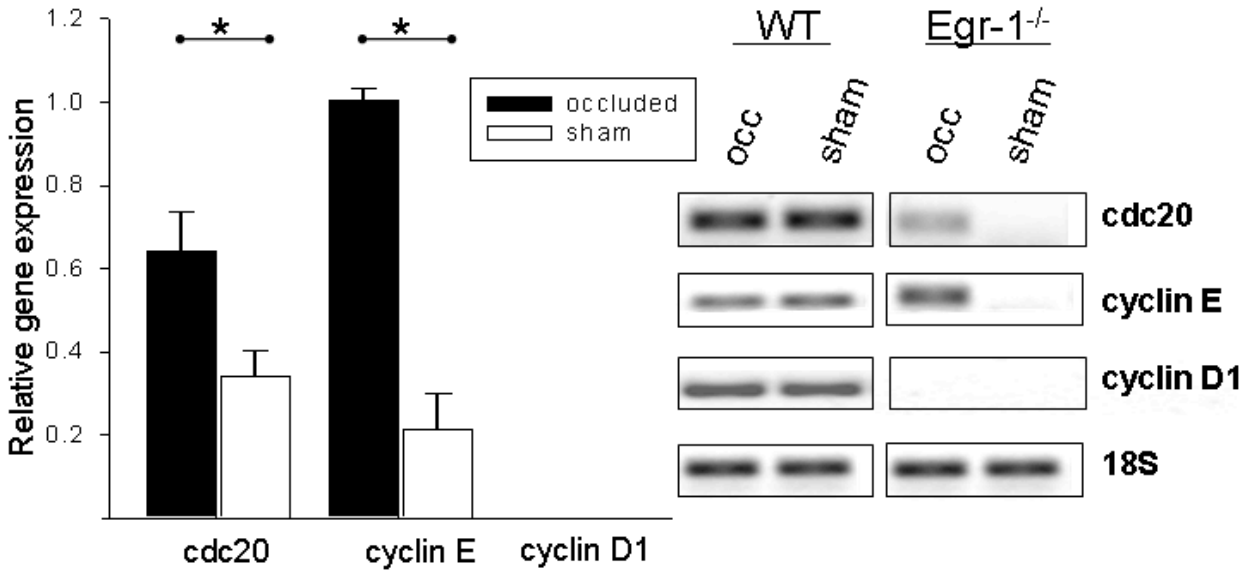

Figure 18: Assessment of cell cycle progression *via* qRT-PCR
On the left side, vertical bar chart displaying cdc20, cyclin E and cyclin D1 mRNA in $Egr1^{-/-}$ mice 12h after femoral artery ligation. Representative agarose gels (right side) showing cdc20, cyclin E and cyclin D1 qRT-PCR products of collateral arteries of WT and $Egr1^{-/-}$mice 12h after ligation (upper 3 panel), lower panel displaying 18S showing that qRT-PCR ran efficiently. For cyclin D1 no signal was detected in $Egr1^{-/-}$ mice either on the occluded or the sham side, mean±SEM, *$p<0.05$ occ vs. sham.

To test whether the loss of cyclin D1 expression was an overall phenomenon or whether this was only true for vessels, cyclin D1 expression was tested in other organs (brain and bone marrow) of Egr1 WT

and deficient mice (Figure 19). Interestingly, cyclin D1 was detectable in both groups in tissues with a higher mitose turnover such as brain and bone marrow. Still the data evidenced that in collateral vessels of Egr1 deficient mice cyclin D1 expression dropped below the detection limit.

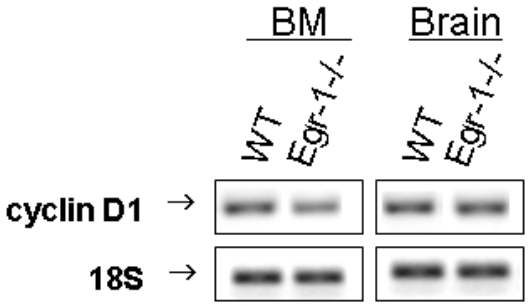

Figure 19: Cyclin D1 expression in other organs of Egr1$^{-/-}$ mice
Representative agarose gels displaying detectable cyclin D1 expression (upper panels) in bone marrow (BM) and brain of WT and Egr1 deficient mice. Lower panels displaying 18S to confirm that qRT-PCR ran efficiently.

5.2 vSMC phenotype switch

The data obtained from cell cycle regulators cdc20, cyclin E and D1 showed that there was a significant difference in mitose progression between Egr1 deficient mice and wildtypes. Since cell cycle progression was likely to be impaired in the vasculature, expression of vSMC phenotype switch markers, such as SF-1 and αSM-actin, as well as proliferation marker ki67 were investigated in Egr1$^{-/-}$ and WT mice 12h after femoral artery ligation (Figure 20). On the occluded side of WT mice, SF-1 (0.55fold occ vs. sham) as well as αSM-actin (0.46fold occ vs. sham) were found to be downregulated showing that already at 12h after ligation vSMCs start switching their phenotype, a prerequisite for vSMC proliferation. By contrast, on the occluded side of Egr1$^{-/-}$ mice, SF-1 was found upregulated (1.60fold occ vs. sham). Moreover, the previously described downregulation of αSM-actin was not detectable in Egr1 deficient mice. There was rather a tendency for upregulation detected in Egr1 deficient collateral vessels which was however not significant. Since Egr1 deficiency apparently did interfere with the phenotype switch, the range of proliferation was investigated in both groups. In WT mice, proliferation marker ki67 was found 1.65fold upregulated after ligation, showing a start in vascular cell proliferation as early as 12h, whereas in Egr1$^{-/-}$ mice, no difference in occ vs. sham was detected.

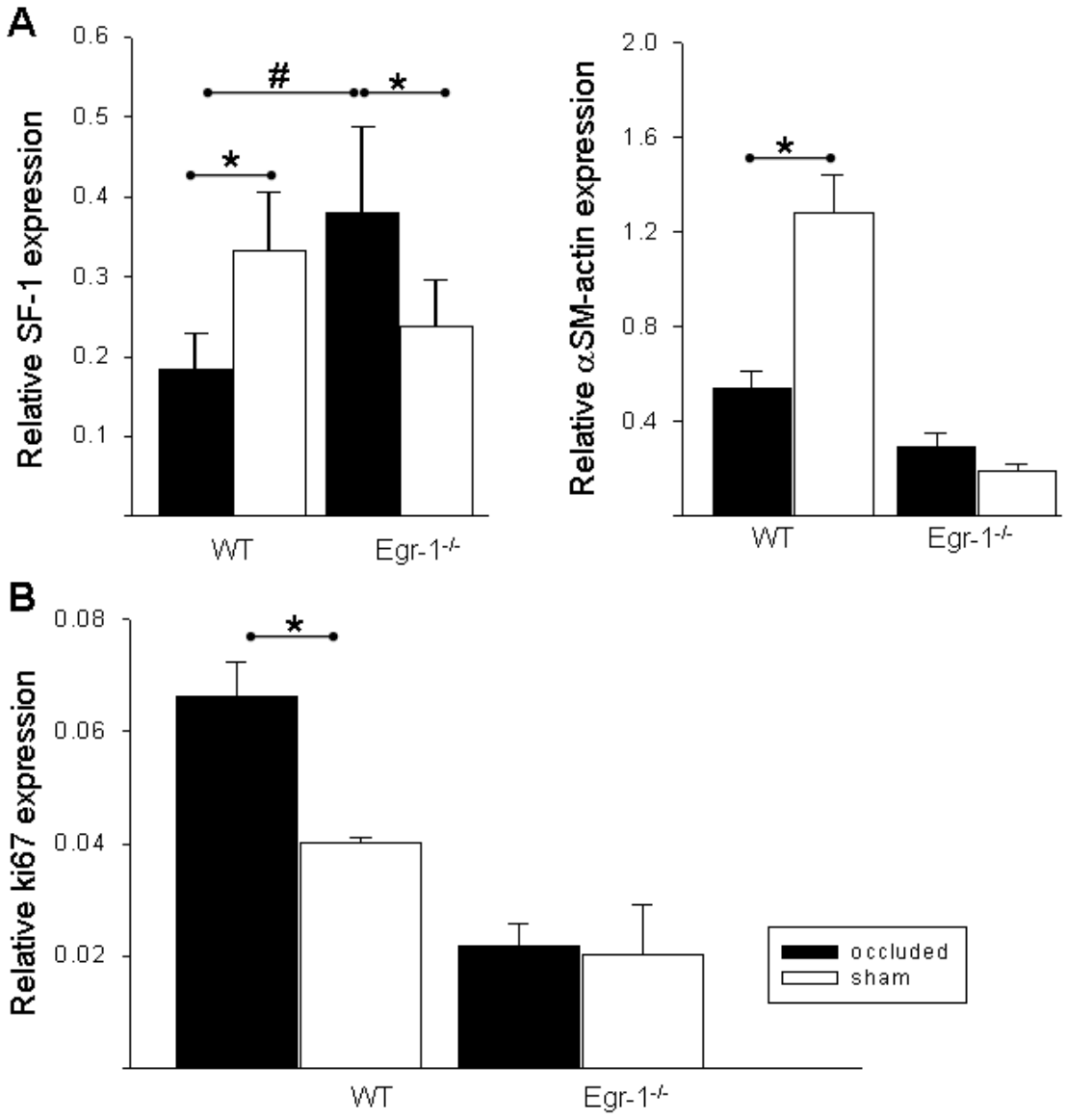

Figure 20: Asessment of vSMC phenotype switch and proliferation in collateral arteries of Egr1$^{-/-}$ and WT mice

A: Vertical bar chart showing mRNA levels of SF-1 (on the left) and αSM-actin (on the right) 12h after femoral artery ligation in Egr1$^{-/-}$ and WT mice, mean±SEM, *p<0.001 occ vs. sham, #p<0.05 WT vs. Egr1$^{-/-}$.

B: Vertical bar chart displaying ki67 mRNA levels detected in growing collateral arteries12h after femoral artery ligation, mean ±SEM *p<0.05 occ vs. sham.

V. DISCUSSION

In the present study, the function of Egr1 in terms of leukocyte recruitment and vascular cell proliferation *in vivo* was investigated in a murine hindlimb model of arteriogenesis. The data showed that collateral artery growth is associated with increased expression of Egr1 on the mRNA and the protein level. Egr1 deficient and WT mice displayed increased expression levels of MCP-1, ICAM-1 and uPA on the site of arteriogenesis being important for leukocyte recruitment and extravasation. Whereas relative upregulation was similar to WT mice, the overall amounts of transcripts were significantly lower in Egr1 deficient mice. This indicates that in Egr1 deficient mice probably other members of the Egr family or other transcription factors compensate the function of EGR1, yet not efficiently. Under baseline conditions (sham side and unligated mice), reduced numbers of leukocytes were found in Egr1 decficient mice, whereas after femoral artery ligation, increased numbers of perivascular leukocytes were detected. Cell cycle genes cyclin D1, cyclin E and cdc20 were not differentially expressed in WT mice. In Egr1 deficient mice cyclin E and cdc20 were found significantly upregulated, however, cyclin D1 was not detectable anymore in the vasculature, conferring EGR1 a unique role as transcription factor regulating cyclin D1 expression during vascular remodeling. Moreover, the delay in proliferation could be explained by a disturbance in the critical vSMC phenotype switch in Egr1 deficient mice as revealed by aberrant αSM-actin and SF-1 expression, which could not be counterbalanced in Egr1 deficient mice.

1 THE MURINE ARTERIOGENESIS MODEL

There is a large variety of experimental models to study the range of vascular remodeling. The differences within protocols are on the one hand due to different species used such as mice,[126] rats,[127] rabbits,[128] dogs[35] or pigs[45] thereby applying different techinques to different anatomical settings and on the other hand due to different vascular supply areas (coronary,[35] mesenteric,[129] cerebrovascular[130] or peripheral[126] model) to choose from. The advancing knowledge and the recognition of the differences between angiogenesis and arteriogenesis, regarding gene expression for example, has shown that it is particularily interesting to study these processes selectively, independent from each other.

1.1 Why using the murine peripheral femoral artery ligation model?

Arteriogenesis differs decisively from angiogenesis in terms of initiation, regulation and purpose. The differences are mainly the initial trigger (FSS vs. ischemia), the fact that preexistent vessels develop and remodel instead of a new sprouting of vessels and the functional compensation of a stenosis, which is not possible with angiogenesis alone.[39] Arteriogenesis is not ischemia related and can restore

adequate vessel conductance *via* collateral artery growth to transport oxygen-saturated blood to ischemic tissue.[131] Angiogenesis and arteriogenesis, however, can occur at the same time in the same area. Since the role of Egr1 in arteriogenesis separately from angiogenesis had to be investigated, an animal model had to be chosen where arteriogenesis occurs solely and locally separated from ischemia-triggered angiogenesis. When focusing on peripheral arteriogenesis, there are basically two principle models: the femoral artery excision model associated with ischemia and the femoral artery ligation model.[126] Due to the fast procedure, the femoral artery ligation model offers first an uncomplicated, second a very specific way of studying arteriogenesis and has a long tradition. John Hunter (see Introduction 1.3) conducted artery ligation experiments already in 1785. While hunting and observing deer in the royal Richmond Park, he became interested in the growth of antlers and investigated collateral artery growth in growing antlers after ligation of the external carotid artery.[8] In a translational approach from his studies, he continued with femoral artery ligation in the dog before finally transferring the acquired operating technique to patients. In dogs, he wanted to gain evidence that the development of bypasses also occurs in a different species and in a different anatomical area.[8] A new rabbit femoral excision model associated with ischemia in the hindlimb was published in 1992 to study angiogenesis.[132] Schaper, who has been studying arteriogenesis by coronary artery ligation in the canine and porcine heart since the 1960s adapted and modified this model to generate a peripheral arteriogenesis model that separates angiogenenesis and arteriogenesis anatomically clear from each other.[128] Femoral artery ligation offers the advantage to specifically study the molecular regulation of arteriogenesis in the *m. adductor, semitendinosus* and *gracilis* without interference from angiogenesis related factors.[128, 131] By omitting a partial excision and performance of the nearly atraumatic ligature, it is excluded that vascular growth occurs due to wound healing or tissue necrosis.[128] Ischemia does not occur within that area and ischemia related metabolites (e.g. ATP, ADP, AMP) did not differ within the ligated and non-ligated side.[131] An upregulation of HIF-1α could neither be detected.[128] VEGF and its receptor Flt-1 were not found upregulated nor did external application of VEGF in high concentrations alter collateral conductance in a large range. The observed minor effects occurred rather *via* indirect activation of monocytes,[133] expression of integrins and increased transmigration since monocytes do express Flt-1. The murine model, used in this study, permits to study angiogenesis in the thigh muscles separated from the adductor collaterals. Hence the ischemic area is clearly separated from the adductor area where arteriogenesis occurs and both processes can be studied separately without interference from each other but within the same animal. Furthermore this model is suited as functional model for exercise experiments.[134] The murine femoral artery ligation model is more specific for the purpose of characterizing Egr1 function during arteriogenesis and superior to the femoral artery excision model.

1.2 Comparison to a coronary ligation model

In principle, the process of arteriogenesis can occur and therefore be studied mechanistically in every organ or anatomical area of the body.[35, 129, 130] The surgical procedure of peripheral arteriogenesis models is usually well tolerated with adequate postoperative analgesia making dropouts very rare. This is naturally not the case in a coronary model where the left anterior descending (LAD) coronary artery of the heart is ligated. This model is attended by a large variety in mortality (7-25%) and defect in cardiac function correlating with the variety in infarct size (8-65%, dependent on the study) and anatomical placement of the suture.[135] But apart from mortality there are also some structural differences, which also have to be considered. The hearts of different animals (pigs, dogs, guinea pigs, humans) differ decisively in terms of the formation of interconnecting arteriolar networks. The range of tissue damage after myocardial infarction as well as the induced collateral artery remodeling strongly relies on the structural morphology of the preexisting collateral network. In the guinea pig hardly any myocardial infarction develops but maximal infarct size can be observed in the pig and rat heart. Whereas the pig depicts a quite similar three coronary vessel anatomy like humans, the dog shows typically two vessels. In the porcine heart, the collateral circulation is hardly developed whereas the canine epicardial collateral circulation is well developed making it very sustainable even to multiple vessel occlusions.[136,] So dependent on the studied animal the vascular anatomy is very variable. Moreover, angiogenesis in the myocardium cannot be separated from arteriogenesis. Ischemia is induced at the time of ligation within the heart muscle and necrosis does occur. Since the aim of this study was to analyze the role of Egr1 for arteriogenesis strictly separate from angiogenesis, the use of a coronary model was not feasible. There are methods to gradually occlude a (coronary) vessel, which comes quite close to the typical clinical situation. Ameroidconstrictors, made of hygroscopic material, are placed around a coronary artery and within 1-3 weeks the artery is occluded due to moisture expansion.[137] However, the grade of occlusion is variable and therefore the grade of stenosis is hardly predictable. These constrictors are associated with a variable incidence of myocardial infarction and mortality rate therefore reducing reliability even more. With further development of this method and the adaptation to other "clinical scenarios" such as chronic ischemic heart failure, it might serve as a very suitable model to simulate pathologies of the human heart.

1.3 Peripheral arteriogenesis models in different species

Aside from the murine model, other femoral artery ligation models in the peripheral circulation are well established. There are the rat,[127], rabbit,[128] and the porcine[45] model. The rabbit femoral artery ligation model is the earliest and best characterized arteriogenesis model existing. Arteriogenesis models investigating the porcine circulation permit the transferal of achieved results into the human

patient. The clinically known Bland-White-Garland syndrome is a rare congenital anomaly, where the left coronary artery branches from the pulmonary artery and blood flow is therefore directed from the right coronary artery *via* collateral vessels to the left coronary artery and from there into the pulmonary artery following to pressure levels. Inspired from this condition, the working group around Schaper established a shunt model in the porcine hind limb, in which shear stress is always maintained in the collateral circulation,[45] allowing to dissect FSS stimulated effects from other mediators of arteriogenesis. Research using the rat model is less frequent than using a murine model. Yet a simple advantage makes this model very attractive for basic research. A rat is evidently bigger than a mouse providing a larger quantity of tissue sample of collateral tissue isolated from the adductor muscle. Moreover, more advanced surgical (i.e. the transferal of the arterio-venous shunt arteriogenesis model into the rat) and imaging methods can be applied.[134] This widens the range of study designs to choose from and eases gene expression studies. However, knockout and transgenic models are barely available until now but might be on hand in the future.

Mice represent good research animals due to their short generation time and large variety of genetically engineered strains, such as transgenic or knockout models, as used in this study. Here the negative influences of deficiency can be studied. The control mice on a C57Bl/6 background, shows the best performance in collateralization when compared to other standard control strains such as the sv129S or the Balb/C mouse.[138, 139] The latter exhibited the lowest collateral flow immediately after femoral artery occlusion (C57Bl/6 has been shown to have a 7 fold higher acute collateral flow) resulting in severe ischemia of the lower extremity and a slower perfusion recovery. On day 21, when C57Bl/6 mice have a fully developed collateral circulation (100% compared to sham), the Balb/C strain exhibits only 50% of perfusion recovery.[138] Therefore a reduction in arteriogenesis due to application of certain inhibitor substances or gene loss of function is studied best in the C57Bl/6 background, whereas therapeutically designed studies should be studied in Balb/C or sv129S. Due to the higher operating expenses, large animal experiments are reserved for preclinical experiments whereas small animal models dominate basic research.

1.4 The influence of gender

An additional word might be added to the role of gender in arteriogenesis. In animal studies mostly male animals are used since the range of influence of the female hormone cycle (i.e. positive effects of estrogen) is barely evaluated in this model. A publication of 2003 found no differences in angiogenesis or arteriogenesis between male and female rabbits after femoral artery excision[140], however oophorectomized females displayed a defect in recovery most likely due to the loss of estrogen. A more recent publication studying mice also after femoral artery excision started to shed light on basic mechanisms and came to the conclusion that females performed less well in terms of functional perfusion recovery and angiogenesis *in vivo* as well as vascular cell proliferation and capillary sprouting *in vitro*. [141] This

relates quite well to clinical data showing a higher prevalence of PAD in women, which however tended to be older suggesting once more a positive influence of estrogen.[142] It brings some difficulties to evaluate a larger group (>5) of female mice since housing would have to be in one cage to ensure timely equalized hormone cycles in all animals or one is forced to use oophorectomized animals, which is a severe intervention without a true correlation to the desired study aims. But the clinical treatment will focus more and more on personalized medicine, which requires a profound knowledge on gender differences in health and disease and will therefore challenge researchers to acquire more knowledge especially in this field.

2 EGR1 AND ARTERIOGENESIS

Arteriogenesis, the growth of pre-existing collateral arteries into functional arteries relies on the proliferation of ECs and vSMCs[143, 144] and is strongly dependent on perivascular accumulation of leukocytes, in particular monocytes, supplying the growing vessel with growth factors and cytokines.[55, 56, 145] Egr1 has been shown to participate in these processes at least *in vitro* and therefore renders the peripheral arteriogenesis a powerful tool to analyze Egr1 function in terms of vascular cell proliferation and leukocyte recruitment *in vivo*.

There is an increasing body of evidence that after femoral artery occlusion, flow alterations in small preexisting collateral arteries lead to increased shear stress, which subsequently activates the collateral endothelium and triggers the whole process.[45, 68, 130] It appears that elevated fluid shear stress is the universal and prime initial stimulus for arteriogenesis not only in muscle tissue[51] but also in brain[130] or heart. It is not clear, however, how this elevated shear is sensed by the EC, coded to information and transmitted to vSMCs for example. PECAM-1 has been proposed to form part in such a shear sensing mechanotransductory complex in ECs *in vitro*.[48] During arteriogenesis PECAM-1 deficient mice exhibited a different EC morphology, i.e. smaller size, resulting in a delay in perfusion recovery.[146] But so far, the role as a mechanosensing receptor could not be entirely proven *in vivo.* Similarly, various *in vitro* studies found Egr1 rapidly expressed in ECs after exposure to shear stress.[79] The acquired results indicate that this might also be the case *in vivo.* In own preliminary intra vital microscopy experiments (n=5), where the femoral artery of C57Bl/6 mice was ligated while focusing on one of the superficial collateral arteries, the vessel showed immediate vasodilatation after ligation, which started from the entry point close to the *a. profunda femoris* and within 5min the whole vessel vasodilated and remained this way until the end of the observation period which was 30min after ligation (data not shown). Moreover, velocity measured with fluorescent micro beads increased dramatically. Baseline velocities were 8824.72±583.59µm/s (*a. profunda*) and 2288.98±205.56µm/s (collateral artery). Directly after ligation the velocity did not increase significantly in the *a. profunda femoris* (9109.05±940.75µm/s, $p=0.75$) but velocity in the collateral vessel nearly adapted the speed of the larger vessel (7248.15±542.06µm/s, $p<0.00005$). High shear stress induced vasodilatation in rat mes-

enteric resistance arteries has been shown to be nitrous oxide (NO) and reactive oxygen species (ROS) dependent.[147] Despite its well-described anti-inflammatory and anti-proliferative active profile, there are studies that notice in NO a contributor to arterial outward remodeling.[148] Moreover, Egr1 belongs to the NO early responding genes.[149,] How NO affects collateral artery growth still remains under discussion. It has been shown, that constantly increased amounts of oxidizing agents activate various signaling pathways aiming at the promoter of "redox sensitive" genes. One of these genes is Egr1. Hydrogen peroxide at non-toxic doses has been shown to rapidly induce Egr1 mRNA and protein expression.[150] Moreover, previous studies described that the DNA binding capacity of EGR1 is redox regulated *in vitro*. Cystein residues within the DNA-binding domain of the protein are oxidized and severely reduce the DNA binding capacity of EGR1 whereas under reducing conditions DNA binding is enhanced [151]. Under non-toxic ROS levels, the EGR1 binding ability is rescued by activation of an apurinic/apyrimidinic endonuclease 1 (APE-1).[80, 151] APE-1 is a DNA repair enzyme with nuclear redox activity.[152] In various cell types, ROS induce nuclear translocation of APE1, which in turn induces DNA binding of transcriptional regulators. APE-1 restores EGR1 DNA binding by direct protein – to protein interactions and even enhances its transcriptional activity *in vitro* and *in vivo*. Moreover, evidence for a positive auto regulatory loop between APE-1 and Egr1 exists,[80] mutually maintaining their transcriptional activity under non-toxic redox conditions. To prevent a never-ending activation between APE-1 and EGR1,[85 86, 153] both factors are capable to downregulate their own expression *via* a negative feed back mechanism. Our data gathered from WT mice evidenced that after femoral artery ligation, when FSS and very likely high ROS levels occur, Egr1 is upregulated in growing collateral arteries in a time dependent manner. On the mRNA level, Egr1 was found to be upregulated as early as 12h after femoral artery ligation, which persisted until 48h after ligation. Accordingly, the protein levels of EGR1 were found upregulated on the occluded side starting at 24h after ligation and were also detectable at 36h and 48h. Proliferation and adaptation of collateral vessels to the altered FSS start rapidly. And it is the timely decrease in FSS inversely related to the enlargement of the collateral diameter that eventually stops the remodeling process, as seen in the previously discussed shunt model.[45] This makes a shear stress dependent upregulation of EGR1 very likely, since at day 3, when leukocyte infiltration and proliferation peak, EGR1 was not found differentially expressed anymore. Egr1 deficient mice exhibited a strong delay in perfusion recovery over 21 days as shown by Laser Doppler analyses. These results are in line with the previously reported findings of impaired collateral artery growth in $Egr1^{-/-}$ mice after whole femoral artery excision.[96] Therein it has been shown that the morphology of large and small vessels as well as the number of capillaries was similar in WT and deficient mice. However, they documented that Egr1 deficient mice showed fewer number of arterioles in the adductor muscles. Furthermore, Egr1 deficient mice showed severe gangrene whereas in the present study this was not observed. This is very likely due to the excision of the femoral artery, which already induces ischemia in the adductor muscle leading to a more severe ischemic damage in the calf

muscle.[96] Apart from this study it has been shown, that adenoviral gene transfer of Egr1 accelerates perfusion recovery. [97] However, the authors focused mainly on the mechanistic insights into angiogenesis of the calf muscle and tallying with previously reported findings, Egr1 overexpression greatly enhances angiogenesis.[154]. In this study the focus lied on the role of Egr1 during arteriogenesis, a subject, which has not been covered by the previous reports.

3 LEUKOCYTE RECRUITMENT

Leukocyte (especially monocyte) recruitment into the perivascular space of growing collateral arteries is a critical mechanism during arteriogenesis.[53, 145] Monocytes derive from the bone marrow and pass through several developmental stages (hemocytoblast, common myeloid progenitor, myeloblast, monoblast, promonocyte) until they transmigrate and mature to macrophages in the tissue. The maturation process is controlled by growth factors. Differentiation from pluripotent stem cells to myeloid progenitor cells is mediated by interleukin (IL-3). Further differentiation to monocyte/macrophage lineage is mediated by macrophage colony-stimulating factor (M-CSF) and granulocyte macrophage colony-stimulating factor (GM-CSF). Thus, the intermittent or continuous infusion of GM-CSF increased arteriogenesis in a pig model of femoral artery ligation.[155] It has been described that monocytes and neutrophils express EGR1,[156, 157] and it has been shown that EGR1 is crucial for development of hematopoietic stem cells along the macrophage lineage.[158]

Under baseline conditions in unligated animals, Egr1 deficient mice evidenced higher cell counts of granulocytes and monocytes in the peripheral blood compared to WT mice. Accordingly, fewer leukocytes in particular macrophages, T- and B-lymphocytes could be detected in the whole digested adductor muscle of $Egr1^{-/-}$ mice in comparison to WT mice. After femoral artery ligation, however, the number of perivascular-accumulated macrophages increased dramatically in $Egr1^{-/-}$. On the sham side of the latter, there were still reduced numbers of macrophages matching nicely with the reduced baseline cell counts within the muscle. It appears that Egr1 is crucial for the differentiation of a variety of cells along the macrophage lineage, not only for WT- myoblasts but also for leukemia cells or hematopoietic stem cells. [98, 158] Moreover, it has been shown that Egr1 also participates in B-cell development[159] and T-cell differentiation.[160] It could therefore be argued that the increased baseline blood levels of leukocytes and monocytes in $Egr1^{-/-}$ mice reflect an impairment of cell maturation, which leads to an overproduction of cells by the bone marrow. This is an effect, which can be frequently observed in myeloid leukemias. Moreover, it has been reported for different knockout models associated with a defect in leukocyte recruitment that they evidence an increase of leukocyte cell counts in the blood.[161] The reduced cell number found in the whole adductor muscle and on the sham side of $Egr1^{-/-}$ mice furthermore strongly suggests an impairment of cell recruitment under baseline conditions. Stimulus directed migration, however, appeared to be still working, since we could detect macrophages in the perivascular area of growing collaterals. We even found a higher number than in WT

mice. It seems that after the induction of a strong stimulus, the degree of leukocyte transmigration occurs mediator dependent and in accordance with the respective circulatory level of such cells accounting for the elevated number of perivascular cells in Egr1 deficient mice after femoral artery ligation. The constitutive expression of EGR1 in monocytes and neutrophils most likely reflects the ability to quickly respond to inflammatory stimuli.[156] However, it was reported that monocytes isolated from the blood and from various tissues of $Egr1^{-/-}$ mice showed no defect in activation upon stimulation.[162] EGR1 is crucially involved in the transcriptional control of many genes involved in monocytic activation and differentiation[163] so that it seems nearly unlikely that an Egr1 loss of function should have no effect on monocyte function. This might also be due to a compensatory effect of EGR2, which plays a major role for leukocyte function, especially during T-cell[112] and monocyte activation[98] and might compensate for Egr1 gene loss of function. Nevertheless, activation of leukocytes seemed to be working, whereas it was the baseline function and recruitment that evidenced defects. It might therefore be that accordingly to the constitutive expression of EGR1 in monocytes, EGR1 is especially responsible for the continuous recruitment whereas in acute inflammatory reactions, where a fast response is necessary, many other TFs as well as other Egr family members are capable of recruiting these cells into the site of inflammation.

Recruitment of leukocytes into the perivascular space cannot be undertaken without the help of cytokines, adhesion molecules and proteinases. Therefore, the mRNA levels of distinct effector genes involved in the recruitment of leukocytes were analyzed (MCP-1, ICAM-1 and uPA) that might represent EGR1 dependent downstream genes, due to their promoter characteristics[102] or expression profiles.[103] Reduced mRNA levels of all three transcripts on the sham and the occluded side of $Egr1^{-/-}$ mice in comparison to WT mice were found. The lower expression under sham conditions in Egr1 deficient mice further supports the data from the whole tissue digestion experiments and the sham side of ligated animals where reduced numbers of leukocytic cells were detected in the tissue. Interestingly, the upregulation of MCP-1, ICAM-1 and uPA in response to femoral artery ligation was not impaired since their relative expression (occ vs. sham) was similar in $Egr1^{-/-}$ and WT mice also at a later timepoint (24h after ligation). It still appears, that all three transcripts might be accounting for the higher number of perivascular leukocytes. Here again the role of other members of the Egr family in terms of similar function or compensatory mechanisms has to be considered since all of the members are capable of binding to EBS but the data on these members are only few. It has, however, previously been described that EGR3 and -4 are able to upregulate ICAM-1 *in vitro* by interacting with NFκB p65.[164] This might also be the case in this model *in vivo*. Moreover, targeted disruption of the MCP-1 receptor, CCR-2, almost abolishes collateral artery growth due to impaired monocyte recruitment.[165] Hence, MCP-1 seems to be the superior cytokine in mediating arteriogenesis.[53] It is therefore more than likely that other transcription factors or also members of the Egr family might be able to upregulate MCP-1 without the presence and proper function of EGR1. The LDI perfusion data revealed a

significant delay in perfusion recovery but not a near abolishment of collateral artery growth meaning that MCP-1 was exerting its functions in Egr1 deficient mice.

4 EXPRESSION OF EGR FAMILY MEMBERS – EVIDENCE FOR COMPENSATION

Egr1 forms a family of Egr TFs together with three other members, Egr2,[107] Egr3[166] and Egr4.[167] All of them show the characteristic three tandem repeat zinc finger structure and differences are mainly outside the DNA binding area.[107, 108] Accordingly, all Egr-TFs bind to the EBS of Egr target genes. In WT mice, a downregulation of Egr2 and Egr3 at 12h and 24h after femoral artery occlusion was detected compared to the sham side. These data are in line with findings in T-cells showing that Egr2 and 3 were regulated contrariwise to Egr1.[112] In Egr1 deficient mice, however, Egr2 and 3 were upregulated and the expression levels of Egr4, which were already upregulated in growing collaterals of WT animals, were further increased in $Egr1^{-/-}$ mice. Egr1 deficient mice are viable and display a quite mild phenotype considering all the essential processes Egr1 is involved in. These mice do not show any obvious defects in cellular differentiation.[121] Nevertheless, female knockout mice are sterile due to the loss of Egr1 mediated mRNA transcription of luteinizing hormone (LH) in the gonadotropin-releasing hormone (GnRH)-LH axis.[120] Egr2 deficient mice however are embryonically lethal[109] whereas $Egr3^{-/-}$ are viable but with a striking phenotype.[168] So it seems that Egr1 loss of function can be tolerated quite well most likely due to compensation in between the family, as already proven for Egr4.[119] It has been shown in Egr1 deficient mice that Egr2 is capable to execute the function of Egr1 in B-lymphocyte development.[159] Moreover, Egr2 has been described to be responsible for monocytic activation on an equal level with Egr1, though in an *in vitro* setting.[98] For EGR3 and especially for EGR2 functions this seems to be not the case. An important issue, if one discusses the idea of compensatory mechanisms within the Egr family, is the internal activation and transcription control between their members. When EGR1 binds to its own promoter this does not result in a further upregulation as binding of EGR1 to an EBS normally does. It results in a downregulation of Egr1 in order to control enduring activation (negative feedback mechanism[86] of Egr1). What remains unclear is how this downregulation is controlled or mechanistically resolved and - if this were a special characteristic feature of the EBS of Egr promoters – what functional element might be the reason for that. Moreover, if we look at the expression of Egr2 and Egr3 in WT mice after femoral artery ligation, might it not be feasible to hypothesize that EGR1 after upregulation also binds to the promoters of Egr2 and 3 and downregulate their transcription in the same way? Up to now there is no data proving this theory, and *in vitro* studies planned to answer this question will be quite extensive. But it seems logical that EGR1 binding to the Egr-family's own EBS leads to a downregulation in order to prevent an overshoot expression. We know that Egr family members are activated by similar stimuli.[115] Therefore a typical activating stimulus (such as shear stress) should actually result in the upregulation of more than one Egr family member at and over the same time, however this is rarely the case.[115] Therefore there has to be a control

mechanism involved preventing needless redundancy of gene activation, which is also important to protect the surrounding tissue of simultaneous gene activation at the same time point which might result in an Egr-related „expression storm“. So looking back at the data, the downregulation of Egr2/3 is quite well explained with this hypothesis. Another interesting player in this inter-family control scheme is NAB-2. As already mentioned NAB-2 is induced by EGR1 in a time-staggered way. Interestingly, a recent study could show that not only EGR1 but also EGR2 and EGR3 are capable of binding on the promoter of NAB-2, thereby establishing a triple negative feedback.[169] Therefore, if Egr1 is activated by an upstream signaling cascade (e.g. MEK/ERK) and induces NAB-2, this repressor will eventually bind to Egr2 and Egr3 since their promoters also exhibit a NAB-2 binding site. This will result in a downregulation by NAB-2 whereas Egr1 levels will remain constantly upregulated until the upstream activation signal is silenced. The control of upstream signaling cascades on distinct members of the family under similar stimuli conditions has already been described for Egr1 and Egr3.[115] It was shown in the very same study that upregulation of Egr3 was longer than that of Egr1 due to different upstream signaling cascades but during the same stimulus driven conditions. So when the upstream activation signal shuts down, this results in an important stop signal. NAB-2, induced by one still activated Egr member, will eventually stop the other members, presenting a powerful and fast expression control mechanism. However if the upstream signal does not shut down, for example due to an aberrant activation in cancer, the negative feedback loop cannot work and the more upstream cascades are deregulated the higher the probability to activate all Egr resulting in ongoing, uncontrolled mitosis.

For Egr4, the regulation might be slightly different, since Egr4 does not exhibit a NAB-2 binding site. Moderate activation of Egr4 was already seen in WT mice, which then was further pronounced in Egr1 deficient mice. Egr4 plays a major role in male fertility[116, 117] and it is Egr4 that protects male Egr1 deficient mice from infertility.[119] Therefore, not surprisingly, Egr4 deficient mice are infertile.[118] As stated before, all Egr family members bind to the EBS, however, EGR4 has been shown to display a threefold lower DNA affinity compared to EGR1 to -3.[170] Once again one might argue that Egr1 is missing at the promoter of Egr4 thereby stopping the inhibition. However, it has been described that EGR4 acts as a transcriptional repressor *via* binding to its own promoter.[171] In the same *in vitro* study it was shown that EGR1 did not negatively alter Egr4 promoter activity but the binding site on the Egr4 promoter is not described as typical EBS, rather as a large section of GC sequences. So it remains unclear how much of the EGR1 protein can actually bind to Egr4. Nevertheless, it seems that Egr4, which overtakes important functions in Egr1 deficient mice, is „missing“ at the GC rich binding site of its own promoter thereby stopping the very own transcriptional repression leading to high levels of EGR4 protein in Egr1 deficient mice. These data together with our data strongly indicate that other members of the Egr family are capable to overtake the tasks of Egr1 and compensate its loss of function in terms of monocyte recruitment and activation. However, further studies are necessary to confirm this and to assign individual functions to distinct members of the Egr family in order to unravel

which signal transduction cascade targets which promoter, and which member can activate which downstream gene as an alternative to Egr1 activity.

5 CELL CYCLE PROGRESSION AND PROLIFERATION

5.1 Expression of cyclins in growing collaterals

Cyclin D1 and cyclin E promote cell cycle progression from G_1 to S-phase.[95] Cyclin D1 binds to cyclin-dependent kinases CDK 4 and CDK6 forming active holoenzymes that can phosphorylate the retinoblastoma protein (Rb). Upon phosphorylation, Rb releases the transcription factor E2F, which in turn activates genes essential for G_1–S transition and S-phase.[172] Cyclin D1 can also control cellular functions in a CDK-independent way through direct interaction with transcriptional regulators and nuclear receptors.[173] Cyclin D1 differs from other cyclins due to the fact that it is induced by mitogens such as growth factors and integrins as a delayed early gene in G_1 phase.[174] EGR1 influences on different key regulators of proliferation such as cdc20, cyclin D1/E, Cdk4 and proliferating cell nuclear antigen (PCNA) have been described for *in vitro* settings.[175] The relationship of Egr1 and cyclin D1 is quite frequently analyzed in the context of tumor progression. In prostate cancer cells, for example, it has been shown that the MEK/ERK1/2 pathway mediated upregulation of Egr1 led to an activation of cyclin D1.[175] In the current study the analyses of cell cycle regulators revealed no differential expression pattern of cdc20, cyclin E and D1 in WT mice at the timepoint 12h after ligation. Apparently the amount of protein synthesized from these genes was present in sufficient amounts for baseline (sham side) cell cycle progression as well as after femoral artery ligation. $Egr1^{-/-}$ mice expressed lesser amounts of cyclin E and cdc20 under sham conditions. However, after femoral artery ligation, these genes evidenced a differential expression pattern and as such were strongly upregulated. Cyclin D1, on the other hand was below the detection limit in collateral arteries in Egr1 deficient mice either on the occluded or the sham operated side. In brain and bone marrow tissue, however, cyclin D1 was found to be expressed in equal amounts in WT and $Egr1^{-/-}$ mice. The data tally with findings showing that Egr1 silencing in primary rat carotid vascular smooth muscle cells employing Egr1 decoy oligodeoxynucleotides[176] resulted in significantly reduced expression levels of cyclin D1. The close relationship between Egr1 and cell cycle regulators and the range of their expression seems to be tissue dependent as the different expression patterns seen in collateral artery tissue compared to brain or bone marrow tissue indicate. This seems also be true for hepatic tissue. During hepatocellular mitosis it has been shown that Egr1 deficient mice failed to progress from metaphase to anaphase, which was due to a lack of cdc20 induction a key regulator promoting anaphase progression. However, here the authors were able to detect cyclin D1 and E in Egr1 deficient mice.[95] It is again most likely that the signaling cascades involved in the pathological and physiological processes that govern mitosis and cell cycle progression also rule over the associated Egr1 downstream genes. Which type of cell cycle regulator is

involved depends apparently on the tissue, the stimulus and the participating genes. As for arteriogenesis, cyclin E and cdc20 can be upregulated when cyclin D1 is missing, but nevertheless adequate cell cycle progression and proliferation requires cyclin D1 in growing collateral arteries which in turn requires activation of Egr1, an effect which could not be compensated efficiently by other transcription factors.

5.2 vSMC phenotype switch: role of SF-1 and αSM-actin

Vascular smooth muscle cell differentiation from the contractile to the synthetic type is a critical process during arteriogenesis and a prerequisite for proliferation. During this change in phenotype, typical cytoskeletal proteins such as desmin, calponin and vinculin are downregulated, the abundant actin filaments disappear[143] and a prominent rough endoplasmatic reticulum can be observed.[51] Therefore, vSMC proliferation and phenotype switch in arteriogenesis are strongly dependent on downregulation of αSM-actin[70, 71] and the transcriptional repressor SF-1.[69] To investigate whether αSM-actin is downregulated in wildtype and also in Egr1 deficient mice and whether Egr1 might regulate SF-1 downregulation not only *in vitro*[106] but also *in vivo* accounting for the synthetic type of SMCs, αSM-actin and SF-1 expression was analyzed. And indeed, SF-1 and αSM-actin were found downregulated in growing collateral arteries of WT animals at 12h after femoral artery ligation but not in Egr1 deficient mice. Moreover, SF-1 was significantly upregulated in Egr1 deficient mice on the occluded side when compared to the sham side. These data strongly indicate that the switch from the contractile to the synthetic phenotype is at least attenuated in Egr1 deficient mice. This is an Egr1 effect that again cannot be substituted for by other transcription factors to promote vSMC proliferation. Actin is a 42kDa cytoskeletal protein found in microfilaments and thin filaments, which are part of the contractile apparatus. Hence, actin is important for maintenance of cell shape, contraction, cell motility, organelle movement and cell signaling. There are three isoforms, alpha, beta and gamma wherein the alpha actins are found in muscle tissue and in the contractile apparatus. Beta and gamma forms mostly mediate internal cell motility.[177] Another quite well known member of cytoskeletal proteins is Ras homologue gene family (Rho) member A (RhoA). It is a small guanosine triphosphatase (GTPase) participating together with its effector Rho-associated coiled-coil containing protein kinase (ROCK) in stress fiber formation and cell cycle progression.[177, 178] RhoA is upregulated in growing collaterals and long term inhibition of ROCK *via* Fasudil strongly inhibits arteriogenesis.[34] If one takes a closer look at the upstream signaling cascades that target the Egr1 promoter an interesting relationship between αSM-actin and Egr1 becomes apparent.[76] As already mentioned, MEK/ERK1/2 lies upstream of Egr1 and is easily activated in response to alterations in FSS.[46] Activated ERK translocates into the nucleus and promotes binding of Ets-family transcription factor Elk-1 to the DNA. On the promoter of Egr1, in close proximity to the SREs, binding sites for Elk-1 (GGAA/T**)** are localized indicating reciprocal activation. SRF is classically dependent on binding of ternary complex factors (TCFs) Elk-1, Sap-1 and Sap-2, to acti-

vate transcription.[179] And in fact, Elk-1 and SRF form a ternary complex and synced activate transcription[180] combining the MEK/ERK pathway with SRF associated gene regulation. Myocardin, a SRF cofactor is specifically expressed in cardiac and smooth muscle cells. It powerfully stimulates SRF-dependent transcription in a variety of cell types and is critical for vSMC differentiation *in vivo*.[181] Myocardin-related transcription factor (MRTF) A (also known as MAL/MKL1) and –B (MKL2) have been described to act similar to Myocardin.[182] MRTFs are expressed more widely and are differentially regulated by subcellular localization. In a resting state, MRTF-A remains in the cytoplasm when bound to monomeric globular actin (G-actin) *via* its RPEL motif.[183] Rho has been described to promote translocation of MRTFs into the nucleus, an important step in stimulating vSMC-specific gene expression.[184] Upon activation of the Rho/ROCK cascade, G-actin levels drop and MRTF-A, dissociated from G-actin, translocates into the nucleus to enhance SRF activity.[185] The low levels of G-actin, responsible for MRTF-A translocation and SRF mediated transcription, are due to LIM-kinase-1 (LIMK-1) mediated cofilin inactivation. LIMK-1 a serine/threonine kinase found to lie downstream of Rho, inactivates cofilin *via* phosphorylation both *in vitro* and *in vivo*.[186] Cofilin is known to be a potent regulator of actin filament dynamics and is able to bind and depolymerize actin. Cofilin was found upregulated EC and vSMCs during arteriogenesis.[45, 70] Rho activates LIMK-1, which inactivates cofilin thus generating low G-actin levels. As stated before, SRF activation is highly supported by either Elk-1 or myocardin/MRTFs. So it seems that it is not SRF but rather the co-enhancer families Ets and MRTFs that recruit and compete for SRF to promote transcription of their respective downstream genes, i.e. Egr1 or cytoskeletal proteins. This means, that during arteriogenesis, Egr1 is upregulated likely *via* MEK/ERK1/2 and SRF binding on the promoter. SRF then is missing at the promoter of cytoskeletal genes such as αSM-actin eventually resulting in a downregulation, which was seen in WT but not in Egr1 deficient mice. Using electron microscopy in a rat model of balloon-injured arteries, it has recently been shown that Egr1 decoy oligodeoxynucleotides inhibit the switch from the contractile to the synthetic phenotype of vSMCs.[176] Failure to switch to the synthetic phenotype will inhibit proliferation of vSMCs, which also might explain the delay in collateral artery growth as seen in the LDI perfusion measurements of Egr1 deficient mice.

Ki67 is expressed in all cell phases except in G_o - phase, can be found in all proliferating cells and is therefore a well-known proliferation marker. At 24h after ligation ki67 was found upregulated in growing collaterals of WT mice, whereas in $Egr1^{-/-}$ mice, no difference was detected. This result goes inline with the results of Vazquez-Pardon et al[187] who performed ki67 staining on iliac artery tissue samples and found that Egr1 silencing prevented nicotine-enhanced neointimal formation in the rat balloon injury model. Moreover, previous studies *in vitro* with human aortic smooth muscle cells (HASMC) after transfection with small interfering RNA targeting EGR1[105] and *in vivo* with Egr1 deficient mice showing impaired recovery from partial hepatectomy[95] support the findings that Egr1 is an important factor for cell cycle progression and proliferation and decisively regulates phenotype switch

during arteriogenesis, a function that can not be entirely counterbalanced by other transcription factors.

In summary the data show that Egr1 regulates the recruitment of leukocytes especially monocytes into the perivascular space. However, this can also be achieved by other TFs such as the other Egr-family members (Egr2, Egr3 and Egr4). Cyclin D1 controlled proliferation and mitotic progression in the vascular bed *in vivo* is dependent on Egr1 since loss of function could not be compensated efficiently by another transcription factor. Egr1 controls the critical phenotype switch of vSMCs during arteriogenesis, a prerequisite for proliferation. Therefore, vascular remodeling in arteriogenesis directly relies on EGR1 function controlling more than one aspect in this multifaceted process. Therefore, EGR1 might be an important intercept point for therapeutic applications in patients in the future.

VI. THE PROSPECTS OF CLINICAL ARTERIOGENESIS THERAPY

Over the past years new information has been gathered to unravel how the process of arteriogenesis works and several factors such as GM-CSF or FGF have been identified that might work as treatment option for patients. GM-CSF has been clinically tested in the coronary[188] as well as in the peripheral[189] circulation, however, these trials showed no or only little success and in some cases were accompanied with severe side effects that led to premature termination of these trials. FGFs have also been quite extensively studied in clinical settings[190] *via* single or multiple infusions in the coronary circulation and even using an adenoviral gene transfer.[191] Common problems with most of the trials is that very few are conducted under true double blind placebo-controlled conditions, the fact that different primary end-points are set and methods for the evaluation of collateral growth and/or angiogenesis are used inconsistently. Seiler et al established new quantitative methods for the assessment of the coronary collateral circulation in humans during routine PTCA.[192] Hence a low pressurederived collateral flow index (CFIp) (measured using a pressure guidewire) has been shown in a 10-year follow-up study to be an independent prognostic factor for cardiovascular mortality.[193] Moreover, this study evidenced that a collateral coronary circulation is life saving. In a different approach the arteriogenesis network trial 2, a prospective, controlled, proof-of-concept study,[194] analyzed the effects of external counter pulsation (ECP) collateral flow. ECP describes a noninvasive technique employing three pairs of pneumatic cuffs wrapped around the lower extremities. ECG triggered cuff inflation at the onset of the diastole and deflation at the beginning of the systole augments diastolic blood flow volume and blood pressure and decreases systolic pressure.[195] ECP was able to improve fractional flow reserve and CFIp.[196] Pushing collateral artery growth in patients using the initial stimulus has been proven to be effective. The identification of pro-arteriogenesic factors and their translation into clinical practice might as well further enhance the mechanical support given by ECP. However, the quite disappointing results of highly anticipated clinical studies using single molecules, which have been proven to be very beneficial in preclinical trials, showed that controlling a very complex mechanism such as arteriogenesis with one single molecule does not seem feasible.[189] The true complexity of vascular remodeling is the reason why the application of a single growth factor cannot improve the patients' outcome in a clinical setting. The present work focused on Egr1 and its role in promoting arteriogenesis. Egr1 is important for smooth muscle cell proliferation in arteriogenesis and when Egr1 is found in the biopsies taken from aneurysms and aortic plaques of patients, it would not be prudent to rate this as a poor prognosis or pathogenesis factor just because of its presence.[197] Egr1 is important for the "daily-routine- mitosis" and it appears that in most cases Egr1, as well as other TFs, is reigned by transcription cascades that mediate its action and control its power.[76] Although Egr1 has become a very well known player in tumor biology, it has never been understood whether it is friend or foe. It rather de-

pends on the specimen that was investigated whether it was *in vivo* or *in vitro* and what kind of signaling cascades have been studied in this context.[76] It seems obvious that stimulation of Egr1 promoted growth in patients simply by entirely overexpressing Egr1 is neither the path to resolve the problem nor is it very wise due to the side effects that might occur such as uncontrolled proliferation leading inevitably to cancer. Looking ahead to the future of iatrogenic arteriogenesis therapy in patients, can Egr1 therefore be a drug target at all? The answer might be found in the identification of upstream signaling cascades that play a role in arteriogenesis and are specifically capable of switching on and switching off genes thereby controlling the process. The coordination of the many different cell types participating in vascular remodeling requires a broad range of signal transduction cascades activated simultaneously in different "vascular compartments". As an example for the different signal transduction cascades, the MEK/ERK1/2 pathway has been shown to participate in arteriogenesis. ERK 1/2 is activated in response to increased FSS[34] and lies upstream of Egr1.[76] *In vitro,* MEK inhibition abolished the typical desmin downregulation during vSMC transformation and led to cell cycle arrest.[198] So in this case MEK/ERK1/2 was the "on-switch" for the vSMC phenotype switch. The identification of signaling cascades lying upstream of Egr1 and eventually leading to the appropriate translation of the desired protein during collateralization will be part of future studies. A more recent study showed that by applying the commonly prescribed angiotensin-converting enzyme inhibitor Ramipril in patients suffering from intermittent claudication led to an alteration in geneexpression of many different players in arteriogenesis and simultaneously improved the patients' walking time.[199] Here we observe that by stimulating a multitude of factors regulating arteriogenesis at the same time can have an effect on the clinical outcome. These results are promising, however the future will tell if this treatment can be applied to daily clinical routine. To clinically employ arteriogenesis, we still need to analyze the different interplay between signaling pathways that modulate the distinct "levels" of communication between cells orchestrating collateral artery growth. This knowledge will provide us with the basis to develop new, modern and safe pharmaceuticals to induce arteriogenesis in patients and maybe even to prevent the incidence of arterial occlusive disease.

VII. SUMMARY

The number of patients suffering from obstructive arterial disease is still increasing. Stimulation of a patient's collateralization (arteriogenesis), though an auspicious therapeutic approach, is still not part of current therapy regimes. Further studies on the molecular level are needed to understand the genetic regulation in this process. The transcription factor early growth response 1 (Egr1) was shown to participate in leukocyte recruitment and cell proliferation *in vitro*. This work contributes to the acquisition of new insights into its mode of action *in vivo*.

Using a model of peripheral arteriogenesis, Egr1 was found significantly upregulated in growing collaterals of wild-type mice (WT), both on mRNA (2.24fold) and protein level (2.3fold). Egr1 stained positive in EC and vSMCs of collaterals as well as in nerves. In LDI measurements conducted over the period of 21 days evidenced a delayed perfusion recovery after femoral artery ligation in $Egr1^{-/-}$ mice compared to WT mice (day7: 0.46±0.05 in $Egr1^{-/-}$ vs. WT (0.73±0.04), day 14: 0.65±0.02 in $Egr1^{-/-}$ vs. 0.88±0.04 in WT and day 21: 0.79 ±0.03 in $Egr1^{-/-}$ vs. 0.96±0.02 in WT). Under baseline conditions, $Egr1^{-/-}$ showed increased levels of monocytes (521.89±52.9 cells/µl vs. 326.56±21.6 cells/µl in WT) and granulocytes (811.79±79.96 cells/µl vs. WT 559.88±34.57 cells/µl) in the circulation but reduced levels in adductor muscles (18.14±2.73 cells/µl vs. 51.22±4.38 cells/µl in WT) as evidenced by FACS analyses. After femoral artery ligation, more macrophages were detected in the perivascular space of collateral arteries in $Egr1^{-/-}$ (8.10±0.99 per vessel) vs. WT (6.12±0.45 per vessel) mice. The mRNA of leukocyte recruitment mediators monocyte chemoattractant protein 1 (MCP-1), intercellular adhesion molecule 1 (ICAM-1) and urokinase plasminogen activator (uPA) were found upregulated in both groups. Whereas other Egr family members (Egr2-4) did not show an upregulation in WT collateral arteries, they were found significantly upregulated in $Egr1^{-/-}$ mice suggesting a mechanism of counterbalancing Egr1 deficiency. A closer look at cell cycle regulators revealed that cyclin E and cdc20 were found upregulated in WT as well as in $Egr1^{-/-}$ mice. However, cyclin D1 was hardly detectable under Egr1 deficiency conferring Egr1 an unique role for cyclin D1 transcription. vSMC phenotype switch is a critical step towards vSMC proliferation and therefore arteriogenesis. In this context, the downregulation of alpha smooth muscle actin (αSM-actin) and of the transcriptional repressor, splicing factor-1 (SF-1) has been shown to be critical *in vitro*. During arteriogenesis, SF-1 has been found downregulated in collaterals of WT mice but was 1.64fold upregulated in $Egr1^{-/-}$. Similar was true for αSM-actin. Whereas in WT mice αSM-actin is downregulated at 12h after ligation Egr1 deficient mice evidenced an upregulation of αSM-actin. The strong upregulation of the nonselective proliferation marker ki67 in WT mice was not detectable under Egr1 deficiency evidencing furthermore a delay in vascular cell proliferation. Conclusion: Compensation for deficiency of Egr1 function in leukocyte recruitment can be mediated by other transcription factors; however, Egr1 is indispensable for effective vascular cell cycle progression and phenotype switch in arteriogenesis.

VIII. ZUSAMMENFASSUNG

Chronische Ischämie von Herz und peripherer Muskulatur stellen für ein epidemiologisch bedeutendes Patientenkollektiv (Diabetiker, Hypertonie- und Arteriosklerosepatienten) oft eine therapeutisch ausweglose Situation dar. Eine Therapieoption für multimorbide Patienten, bei denen eine Bypassoperation des Herzens nötig, aber nicht durchführbar ist, wären natürliche Bypässe, d.h. das Wachstum von präexistenten Kollateralgefäßen (Arteriogenese), die in der Lage sind eine entstandene Stenose funktionell zu kompensieren. Entscheidende Schritte dieses Prozesses sind u.a. die Rekrutierung von Leukozyten, insbesondere Monozyten in den perivaskulären Raum sowie die Proliferation von Endothel- und glatten Gefäßmuskelzellen der wachsenden Kollateralen. Da durch zahlreiche *in vitro*-Studien bekannt ist, dass der Transkriptionsfaktor „early growth response 1“ (Egr1) unter anderem für eben diese Prozesse eine Rolle spielt, war das Ziel dieser Arbeit, die Funktion von Egr1 im Prozess der Arteriogenese zu identifizieren und zu charakterisieren. Zu diesem Zweck wurde das murine Model der peripheren Arteriogenese herangezogen, bei dem Arteriogenese durch Ligatur der Femoralarterie induziert wird. Egr1 war in den wachsenden Kollateralarterien sowohl auf RNA- (2.24fach) als auch auf Proteinebene (2.3fach) differentiell exprimiert und konnte immunhistologisch in Endothel- und glatten Gefäßmuskelzellen wachsender Kollateralerterien sowie in den perivaskulär liegenden Nerven lokalisiert werden. Laser Doppler Analysen von Egr1 defizienten ($Egr1^{-/-}$) im Vergleich zu Wildtyp (WT)-Tieren zeigten eine verlangsamte Arteriogenese über den Zeitraum von 21 Tagen (Tag 7: 0.46±0.05 in $Egr1^{-/-}$ vs. WT (0.73±0.04), Tag 14: 0.65±0.02 in $Egr1^{-/-}$ vs. WT (0.88±0.04) und an Tag 21: 0.79 ±0.03 in $Egr1^{-/-}$ vs. WT (0.96±0.02)). Mittels FACS konnte gezeigt werden, dass $Egr1^{-/-}$ Mäuse unter Ruhebedingungen eine vermehrte Anzahl von Monozyten (521.89±52.9 Zellen/µl vs. WT (326.56±21.6 Zellen/µl)) und Granulozyten (811.79±79.96 Zellen/µl vs. WT 559.88±34.57 Zellen/µl) im Blut haben, aber eine reduzierte Anzahl an Makrophagen im Adduktorgewebe (18.14±2.73 Zellen/µl vs. 51.22±4.38 WT Zellen/µl) zeigen. Nach Ligatur jedoch, konnte eine größere Anzahl Makrophagen um die Kollateralgefäße von $Egr1^{-/-}$ Mäusen (8.10±0.99 pro Gefäß) im Vergleich zu WT (6.12±0.45 pro Gefäß) detektiert werden, ein Hinweis auf eine Beeinträchtigung der Leukozytenrekrutierung unter Ruhebedingungen und eine Überkompensation mit verstärkter Anhäufung nach Setzens eines Stimulus. Bekannte Mediatoren der Monozytenrekrutierung „monocyte chemoattractant protein 1“ (MCP-1), „intercellular adhesion molecule 1“ (ICAM-1) und „urokinase plasminogen activator“ (uPa), die in diesem Modell differentiell exprimiert sind, werden in der Literatur immer wieder mit Egr1 als potentielle „downstream“ Gene in Zusammenhang gebracht, zum Einen aufgrund ihrer Expressionsmuster (bei MCP-1 und ICAM-1), zum Anderen aufgrund ihrer strukturellen Promotercharakteristika (bei uPa). Aber auch in Egr1 defizienten Tieren waren diese Mediatoren hochreguliert. Um der Frage nachzugehen, inwieweit Egr1 Funktionen von anderen Transkriptionsfaktoren über-

nommen werden können, wurde mittels qRT-PCR die Expression anderer Egr-Familienmitglieder überprüft. Es zeigte sich, dass in WT Tieren die Egr Transkriptionsfaktoren Egr2-4 nicht hochreguliert waren, jedoch in Egr1 defizienten Tieren eine starke Hochregulation aller drei Faktoren, was für eine Teilkompensation durch Egr2-4 spricht. Neben der Monozytenrekrutierung ist die Proliferation von Endothel- und glatten Gefäßmuskelzellen ein zentraler Mechanismus der Arteriogenese. Egr1 kontrolliert die Zellproliferation über Expressionskontrolle der Zellzyklusregulatoren cyclin D1, E und cdc20 *in vitro*. Cyclin E und cdc20 waren in WT und $Egr1^{-/-}$ Mäusen exprimiert. Allerdings war cyclin D1 in Kollateralgefäßen Egr1 defizienter Mäuse unterhalb der Nachweisgrenze. Grundvorraussetzung für die Proliferation glatter Gefäßmuskelzellen ist die Phänotypveränderung, der so genannte „phenotype switch", vom kontraktilen zum synthetischen Typ. In diesem Zusammenhang ist bekannt, dass das zytoskelettäre Protein „alpha smooth muscle actin" (αSM-actin) und der Transkriptionsrepressor „splicing factor-1" (SF-1) charakteristischerweise herunterreguliert werden. In dieser Arbeit konnte gezeigt werden, dass dies auch in den wachsenden Kollateralen von WT Tieren der Fall ist. Jedoch zeigte sich in $Egr1^{-/-}$ Mäusen, dass SF-1 hochreguliert (1.64fach) und αSM-actin 12h nach Ligatur nicht mehr differentiell exprimiert war. In diesem Kontext konnte gezeigt werden, dass der Proliferationsmarker ki67, der in WT deutlich hochreguliert ist, in Egr1 defizienten Tieren nicht mehr differentiell exprimiert wird.

Dies zeigt, dass die Egr1 Funktion im Bezug auf die Leukozytenrekrutierung durchaus durch andere Transkriptionsfaktoren und andere Mitglieder der Egr-Familie kompensiert werden kann, jedoch ist Egr1 entscheidend an der Transkription von cyclin D1 im Gefäß beteiligt und kontrolliert entscheidend die Regulation des „phenotype switch". Aufgrund dieser Ergebnisse ist Egr1 unentbehrlich für eine funktionierende Zellproliferation und damit für die Arteriogenese.

IX. REFERENCES

1. World-Health-Organisation. Who fact sheet n°317 : Cardiovascular diseases (cvds). 2013
2. Libby P. Inflammation in atherosclerosis. *Nature*. 2002;420:868-874
3. Shammas NW. Epidemiology, classification, and modifiable risk factors of peripheral arterial disease. *Vasc Health Risk Manag*. 2007;3:229-234
4. Rathore SS, Curtis JP, Chen J, Wang Y, Nallamothu BK, Epstein AJ, Krumholz HM. Association of door-to-balloon time and mortality in patients admitted to hospital with st elevation myocardial infarction: National cohort study. *BMJ*. 2009;338:b1807
5. Desch S, de Waha S, Eitel I, Koch A, Gutberlet M, Schuler G, Thiele H. Effect of coronary collaterals on long-term prognosis in patients undergoing primary angioplasty for acute st-elevation myocardial infarction. *Am J Cardiol*. 2010;106:605-611
6. Lower R. *Tractatus de corde : Item de motu & colore sanguinis, et chyli in eum transitu*. Amstelodami: Apud Danielem Elzevirium; 1669.
7. Haller Av. *Elementa physiologiae corporis humani*. Lausannae: Sumptibus Marci-Michael. Bousquet; 1757.
8. Murley R. John hunter, velvet and vascular surgery. *Ann R Coll Surg Engl*. 1984;66:214-218
9. Buschmann I, Schaper W. The pathophysiology of the collateral circulation (arteriogenesis). *J Pathol*. 2000;190:338-342
10. Spalteholz W. *Die Arterien der Herzwand; anatomische Untersuchungen an Menschen- und Tierherzen, nebst Erörterung der Voraussetzungen für die Herstellung eines Kollateralkreislaufes*. Leipzig: S. Hirzel; 1924.
11. Spalteholz W. *Über das Durchsichtigmachen von menschlichen und tierischen Präparaten und seine theoretischen Bedingungen*. Leipzig: S. Hirzel; 1914.
12. Jamin F, Merkel H. *Die Koronararterien des menschlichen Herzens unter normalen und pathologischen Verhältnissen*. Jena,: G. Fischer; 1907.
13. Longland CJ. Collateral circulation in the limb. *Postgrad Med J*. 1953;29:456-458
14. Fulton WF. Arterial anastomoses in the coronary circulation. I. Anatomical features in normal and diseased hearts demonstrated by stereoarteriography. *Scott Med J*. 1963;8:420-434
15. Shalaby F, Ho J, Stanford WL, Fischer KD, Schuh AC, Schwartz L, Bernstein A, Rossant J. A requirement for flk1 in primitive and definitive hematopoiesis and vasculogenesis. *Cell*. 1997;89:981-990
16. Flamme I, Risau W. Induction of vasculogenesis and hematopoiesis in vitro. *Development*. 1992;116:435-439
17. Carmeliet P. Mechanisms of angiogenesis and arteriogenesis. *Nat Med*. 2000;6:389-395
18. Shalaby F, Rossant J, Yamaguchi TP, Gertsenstein M, Wu XF, Breitman ML, Schuh AC. Failure of blood-island formation and vasculogenesis in flk-1-deficient mice. *Nature*. 1995;376:62-66
19. Fong GH, Klingensmith J, Wood CR, Rossant J, Breitman ML. Regulation of flt-1 expression during mouse embryogenesis suggests a role in the establishment of vascular endothelium. *Dev Dyn*. 1996;207:1-10
20. Liu W, Peng Y, Wu B, Li Q, Chai H, Ren X, Wang X, Zhao Z, Chen M, Huang DJ. A meta-analysis of the impact of epc capture stent on the clinical outcomes in patients with coronary artery disease. *Journal of interventional cardiology*. 2013
21. Hertig AT. Angiogenesis in the early human chorion and in the primary placenta of the macaque monkey. *Contrib. Embryol. Carnegie Inst.* 1935;25:37-81
22. Kutryk MJ, Stewart DJ. Angiogenesis of the heart. *Microsc Res Tech*. 2003;60:138-158
23. Vincent KA, Feron O, Kelly RA. Harnessing the response to tissue hypoxia: Hif-1 alpha and therapeutic angiogenesis. *Trends Cardiovasc Med*. 2002;12:362-367
24. Risau W. Mechanisms of angiogenesis. *Nature*. 1997;386:671-674
25. Mignatti P, Rifkin DB. Plasminogen activators and matrix metalloproteinases in angiogenesis. *Enzyme Protein*. 1996;49:117-137
26. Cooke JP, Losordo DW. Nitric oxide and angiogenesis. *Circulation*. 2002;105:2133-2135
27. Griffioen AW, Molema G. Angiogenesis: Potentials for pharmacologic intervention in the treatment of cancer, cardiovascular diseases, and chronic inflammation. *Pharmacol Rev*. 2000;52:237-268
28. Folkman J. Angiogenesis in cancer, vascular, rheumatoid and other disease. *Nat Med*. 1995;1:27-31

29. Bergers G, Benjamin LE. Tumorigenesis and the angiogenic switch. *Nat Rev Cancer*. 2003;3:401-410
30. Folkman J. Angiogenesis inhibitors generated by tumors. *Mol Med*. 1995;1:120-122
31. Gao D, Nolan DJ, Mellick AS, Bambino K, McDonnell K, Mittal V. Endothelial progenitor cells control the angiogenic switch in mouse lung metastasis. *Science*. 2008;319:195-198
32. Ramalingam SS, Belani CP, Mack PC, Vokes EE, Longmate J, Govindan R, Koczywas M, Ivy SP, Gandara DR. Phase ii study of cediranib (azd 2171), an inhibitor of the vascular endothelial growth factor receptor, for second-line therapy of small cell lung cancer (national cancer institute #7097). *J Thorac Oncol*. 2010;5:1279-1284
33. US-Food-and-Drug-Administration. Bevaczumab prescribing and label information *U.S. BL 125085/168*. 2009;
34. Eitenmuller I, Volger O, Kluge A, Troidl K, Barancik M, Cai WJ, Heil M, Pipp F, Fischer S, Horrevoets AJ, Schmitz-Rixen T, Schaper W. The range of adaptation by collateral vessels after femoral artery occlusion. *Circ Res*. 2006;99:656-662
35. Schaper W, De Brabander, M. , Lewi, P. DNA synthesis and mitoses in coronary collateral vessels of the dog. *Circ Res*. 1971;28:671-679
36. Buschmann I, Schaper W. Arteriogenesis versus angiogenesis: Two mechanisms of vessel growth. *News Physiol Sci*. 1999;14:121-125
l37. Scholz D, Cai WJ, Schaper W. Arteriogenesis, a new concept of vascular adaptation in occlusive disease. *Angiogenesis*. 2001;4:247-257
38. Langille BL. Remodeling of developing and mature arteries: Endothelium, smooth muscle, and matrix. *J Cardiovasc Pharmacol*. 1993;21 Suppl 1:S11-17
39. Schaper W, Scholz D. Factors regulating arteriogenesis. *Arterioscler Thromb Vasc Biol*. 2003;23:1143-1151
40. Ayyaswamy PS. *Modelling of flow in blood vessels. in: Fluid Mechanics 4th Ed.* (Kundu PK, Cohen IM). Amsterdam ; Boston: Academic Press; 2008.
41. Wang QQ, Ping BH, Xu QB, Wang W. Rheological effects of blood in a nonplanar distal end-to-side anastomosis. *J Biomech Eng*. 2008;130:051009
42. Thoma R. *Untersuchungen über die Histogenese und Histomechanik des Gefäßsystems.* Stuttgart: Enke; 1893.
43. Holtz J, Forstermann U, Pohl U, Giesler M, Bassenge E. Flow-dependent, endothelium-mediated dilation of epicardial coronary arteries in conscious dogs: Effects of cyclooxygenase inhibition. *J Cardiovasc Pharmacol*. 1984;6:1161-1169
44. Ben Driss A, Benessiano J, Poitevin P, Levy BI, Michel JB. Arterial expansive remodeling induced by high flow rates. *Am J Physiol*. 1997;272:H851-858
45. Pipp F, Boehm S, Cai WJ, Adili F, Ziegler B, Karanovic G, Ritter R, Balzer J, Scheler C, Schaper W, Schmitz-Rixen T. Elevated fluid shear stress enhances postocclusive collateral artery growth and gene expression in the pig hind limb. *Arterioscler Thromb Vasc Biol*. 2004;24:1664-1668
46. Braddock M, Schwachtgen JL, Houston P, Dickson MC, Lee MJ, Campbell CJ. Fluid shear stress modulation of gene expression in endothelial cells. *News Physiol Sci*. 1998;13:241-246
47. Galbraith CG, Skalak R, Chien S. Shear stress induces spatial reorganization of the endothelial cell cytoskeleton. *Cell Motil Cytoskeleton*. 1998;40:317-330
48. Tzima E, Irani-Tehrani M, Kiosses WB, Dejana E, Schultz DA, Engelhardt B, Cao G, DeLisser H, Schwartz MA. A mechanosensory complex that mediates the endothelial cell response to fluid shear stress. *Nature*. 2005;437:426-431
49. Topper JN, Cai J, Falb D, Gimbrone MA, Jr. Identification of vascular endothelial genes differentially responsive to fluid mechanical stimuli: Cyclooxygenase-2, manganese superoxide dismutase, and endothelial cell nitric oxide synthase are selectively up-regulated by steady laminar shear stress. *Proc Natl Acad Sci U S A*. 1996;93:10417-10422
50. Schwachtgen JL, Houston P, Campbell C, Sukhatme V, Braddock M. Fluid shear stress activation of egr-1 transcription in cultured human endothelial and epithelial cells is mediated via the extracellular signal-related kinase 1/2 mitogen-activated protein kinase pathway. *J Clin Invest*. 1998;101:2540-2549
51. Scholz D, Ito W, Fleming I, Deindl E, Sauer A, Wiesnet M, Busse R, Schaper J, Schaper W. Ultrastructure and molecular histology of rabbit hind-limb collateral artery growth (arteriogenesis). *Virchows Arch*. 2000;436:257-270
52. Heil M, Ziegelhoeffer T, Pipp F, Kostin S, Martin S, Clauss M, Schaper W. Blood monocyte concentration is critical for enhancement of collateral artery growth. *Am J Physiol Heart Circ Physiol*. 2002;283:H2411-2419

53. Hoefer IE, Grundmann S, van Royen N, Voskuil M, Schirmer SH, Ulusans S, Bode C, Buschmann IR, Piek JJ. Leukocyte subpopulations and arteriogenesis: Specific role of monocytes, lymphocytes and granulocytes. *Atherosclerosis*. 2005;181:285-293
54. Schaper J, Konig R, Franz D, Schaper W. The endothelial surface of growing coronary collateral arteries. Intimal margination and diapedesis of monocytes. A combined sem and tem study. *Virchows Arch A Pathol Anat Histol.* 1976;370:193-205
55. Arras M, Ito WD, Scholz D, Winkler B, Schaper J, Schaper W. Monocyte activation in angiogenesis and collateral growth in the rabbit hindlimb. *J Clin Invest*. 1998;101:40-50
56. Deindl E, Hoefer IE, Fernandez B, Barancik M, Heil M, Strniskova M, Schaper W. Involvement of the fibroblast growth factor system in adaptive and chemokine-induced arteriogenesis. *Circ Res*. 2003;92:561-568
57. Surmi BK, Hasty AH. The role of chemokines in recruitment of immune cells to the artery wall and adipose tissue. *Vascul Pharmacol*. 2010;52:27-36
58. Ley K. Arrest chemokines. *Microcirculation*. 2003;10:289-295
59. Ito WD, Arras M, Winkler B, Scholz D, Schaper J, Schaper W. Monocyte chemotactic protein-1 increases collateral and peripheral conductance after femoral artery occlusion. *Circ Res*. 1997;80:829-837
60. Hoefer IE, van Royen N, Rectenwald JE, Deindl E, Hua J, Jost M, Grundmann S, Voskuil M, Ozaki CK, Piek JJ, Buschmann IR. Arteriogenesis proceeds via icam-1/mac-1- mediated mechanisms. *Circ Res*. 2004;94:1179-1185
61. Giancotti FG, Ruoslahti E. Integrin signaling. *Science*. 1999;285:1028-1032
62. Buschmann I HI, Heil M, Schaper W. Anti-adhesion monoclonal antibodies against icam inhibit arteriogenesis. *J Am Coll Cardiol*. 1999;33
63. Cai W, Vosschulte R, Afsah-Hedjri A, Koltai S, Kocsis E, Scholz D, Kostin S, Schaper W, Schaper J. Altered balance between extracellular proteolysis and antiproteolysis is associated with adaptive coronary arteriogenesis. *J Mol Cell Cardiol*. 2000;32:997-1011
64. Gyetko MR, Todd RF, 3rd, Wilkinson CC, Sitrin RG. The urokinase receptor is required for human monocyte chemotaxis in vitro. *J Clin Invest*. 1994;93:1380-1387
65. Kusch A, Tkachuk S, Lutter S, Haller H, Dietz R, Lipp M, Dumler I. Monocyte-expressed urokinase regulates human vascular smooth muscle cell migration in a coculture model. *Biol Chem*. 2002;383:217-221
66. Reichel CA, Uhl B, Lerchenberger M, Puhr-Westerheide D, Rehberg M, Liebl J, Khandoga A, Schmalix W, Zahler S, Deindl E, Lorenzl S, Declerck PJ, Kanse S, Krombach F. Urokinase-type plasminogen activator promotes paracellular transmigration of neutrophils via mac-1, but independently of urokinase-type plasminogen activator receptor. *Circulation*. 2011;124:1848-1859
67. Deindl E, Ziegelhoffer T, Kanse SM, Fernandez B, Neubauer E, Carmeliet P, Preissner KT, Schaper W. Receptor-independent role of the urokinase-type plasminogen activator during arteriogenesis. *FASEB J*. 2003;17:1174-1176
68. Cai W, Schaper W. Mechanisms of arteriogenesis. *Acta Biochim Biophys Sin (Shanghai)*. 2008;40:681-692
69. Cattaruzza M, Schafer K, Hecker M. Cytokine-induced down-regulation of zfm1/splicing factor-1 promotes smooth muscle cell proliferation. *J Biol Chem*. 2002;277:6582-6589
70. Boengler K, Pipp F, Broich K, Fernandez B, Schaper W, Deindl E. Identification of differentially expressed genes like cofilin2 in growing collateral arteries. *Biochem Biophys Res Commun*. 2003;300:751-756
71. Cai WJ, Kocsis E, Scholz D, Luo X, Schaper W, Schaper J. Presence of cx37 and lack of desmin in smooth muscle cells are early markers for arteriogenesis. *Mol Cell Biochem*. 2004;262:17-23
72. Demicheva E, Hecker M, Korff T. Stretch-induced activation of the transcription factor activator protein-1 controls monocyte chemoattractant protein-1 expression during arteriogenesis. *Circ Res*. 2008;103:477-484
73. Boengler K, Pipp F, Fernandez B, Ziegelhoeffer T, Schaper W, Deindl E. Arteriogenesis is associated with an induction of the cardiac ankyrin repeat protein (carp). *Cardiovasc Res*. 2003;59:573-581
74. Milbrandt J. A nerve growth factor-induced gene encodes a possible transcriptional regulatory factor. *Science*. 1987;238:797-799
75. Christy B, Nathans D. DNA binding site of the growth factor-inducible protein zif268. *Proc Natl Acad Sci U S A*. 1989;86:8737-8741

76. Pagel JI, Deindl E. Concepts of egr-1 activation- a hub for signal transduction cascades. *Curr Signal Transduct Ther*. 2010;5:149-160
77. Sukhatme VP, Kartha S, Toback FG, Taub R, Hoover RG, Tsai-Morris CH. A novel early growth response gene rapidly induced by fibroblast, epithelial cell and lymphocyte mitogens. *Oncogene Res*. 1987;1:343-355
78. Cao XM, Koski RA, Gashler A, McKiernan M, Morris CF, Gaffney R, Hay RV, Sukhatme VP. Identification and characterization of the egr-1 gene product, a DNA-binding zinc finger protein induced by differentiation and growth signals. *Mol Cell Biol*. 1990;10:1931-1939
79. Khachigian LM, Anderson KR, Halnon NJ, Gimbrone MA, Jr., Resnick N, Collins T. Egr-1 is activated in endothelial cells exposed to fluid shear stress and interacts with a novel shear-stress-response element in the pdgf a-chain promoter. *Arterioscler Thromb Vasc Biol*. 1997;17:2280-2286
80. Pines A, Bivi N, Romanello M, Damante G, Kelley MR, Adamson ED, D'Andrea P, Quadrifoglio F, Moro L, Tell G. Cross-regulation between egr-1 and ape/ref-1 during early response to oxidative stress in the human osteoblastic hobit cell line: Evidence for an autoregulatory loop. *Free Radic Res*. 2005;39:269-281
81. Tsai-Morris CH, Cao XM, Sukhatme VP. 5' flanking sequence and genomic structure of egr-1, a murine mitogen inducible zinc finger encoding gene. *Nucleic Acids Res*. 1988;16:8835-8846
82. Huang RP, Fan Y, deBelle I, Ni Z, Matheny W, Adamson ED. Egr-1 inhibits apoptosis during the uv response: Correlation of cell survival with egr-1 phosphorylation. *Cell Death Differ*. 1998;5:96-106
83. Christy B, Nathans D. Functional serum response elements upstream of the growth factor-inducible gene zif268. *Mol Cell Biol*. 1989;9:4889-4895
84. Schwachtgen JL, Campbell CJ, Braddock M. Full promoter sequence of human early growth response factor-1 (egr-1): Demonstration of a fifth functional serum response element. *DNA Seq*. 2000;10:429-432
85. Sakamoto KM, Bardeleben C, Yates KE, Raines MA, Golde DW, Gasson JC. 5' upstream sequence and genomic structure of the human primary response gene, egr-1/tis8. *Oncogene*. 1991;6:867-871
86. Cao X, Mahendran R, Guy GR, Tan YH. Detection and characterization of cellular egr-1 binding to its recognition site. *J Biol Chem*. 1993;268:16949-16957
87. Pavletich NP, Pabo CO. Zinc finger-DNA recognition: Crystal structure of a zif268-DNA complex at 2.1 a. *Science*. 1991;252:809-817
88. Matheny C, Day ML, Milbrandt J. The nuclear localization signal of ngfi-a is located within the zinc finger DNA binding domain. *J Biol Chem*. 1994;269:8176-8181
89. Gashler AL, Swaminathan S, Sukhatme VP. A novel repression module, an extensive activation domain, and a bipartite nuclear localization signal defined in the immediate-early transcription factor egr-1. *Mol Cell Biol*. 1993;13:4556-4571
90. Thiel G, Kaufmann K, Magin A, Lietz M, Bach K, Cramer M. The human transcriptional repressor protein nab1: Expression and biological activity. *Biochim Biophys Acta*. 2000;1493:289-301
91. Svaren J, Sevetson BR, Apel ED, Zimonjic DB, Popescu NC, Milbrandt J. Nab2, a corepressor of ngfi-a (egr-1) and krox20, is induced by proliferative and differentiative stimuli. *Mol Cell Biol*. 1996;16:3545-3553
92. Kumbrink J, Gerlinger M, Johnson JP. Egr-1 induces the expression of its corepressor nab2 by activation of the nab2 promoter thereby establishing a negative feedback loop. *J Biol Chem*. 2005;280:42785-42793
93. Houston P, Campbell CJ, Svaren J, Milbrandt J, Braddock M. The transcriptional corepressor nab2 blocks egr-1-mediated growth factor activation and angiogenesis. *Biochem Biophys Res Commun*. 2001;283:480-486
94. Fukuda T, Kanomata K, Nojima J, Urakawa I, Suzawa T, Imada M, Kukita A, Kamijo R, Yamashita T, Katagiri T. Fgf23 induces expression of two isoforms of nab2, which are corepressors of egr-1. *Biochem Biophys Res Commun*. 2007;353:147-151
95. Liao Y, Shikapwashya ON, Shteyer E, Dieckgraefe BK, Hruz PW, Rudnick DA. Delayed hepatocellular mitotic progression and impaired liver regeneration in early growth response-1-deficient mice. *J Biol Chem*. 2004;279:43107-43116
96. Sarateanu CS, Retuerto MA, Beckmann JT, McGregor L, Carbray J, Patejunas G, Nayak L, Milbrandt J, Rosengart TK. An egr-1 master switch for arteriogenesis: Studies in egr-1 homozygous negative and wild-type animals. *J Thorac Cardiovasc Surg*. 2006;131:138-145

97. Lee YS, Jang HS, Kim JM, Lee JS, Lee JY, Li Kim K, Shin IS, Suh W, Choi JH, Jeon ES, Byun J, Kim DK. Adenoviral-mediated delivery of early growth response factor-1 gene increases tissue perfusion in a murine model of hindlimb ischemia. *Mol Ther*. 2005;12:328-336

98. Kharbanda S, Nakamura T, Stone R, Hass R, Bernstein S, Datta R, Sukhatme VP, Kufe D. Expression of the early growth response 1 and 2 zinc finger genes during induction of monocytic differentiation. *J Clin Invest*. 1991;88:571-577

99. Nguyen HQ, Hoffman-Liebermann B, Liebermann DA. The zinc finger transcription factor egr-1 is essential for and restricts differentiation along the macrophage lineage. *Cell*. 1993;72:197-209

100. Guha M, O'Connell MA, Pawlinski R, Hollis A, McGovern P, Yan SF, Stern D, Mackman N. Lipopolysaccharide activation of the mek-erk1/2 pathway in human monocytic cells mediates tissue factor and tumor necrosis factor alpha expression by inducing elk-1 phosphorylation and egr-1 expression. *Blood*. 2001;98:1429-1439

101. Khachigian LM, Lindner V, Williams AJ, Collins T. Egr-1-induced endothelial gene expression: A common theme in vascular injury. *Science*. 1996;271:1427-1431

102. Bain G, Cravatt CB, Loomans C, Alberola-Ila J, Hedrick SM, Murre C. Regulation of the helix-loop-helix proteins, e2a and id3, by the ras-erk mapk cascade. *Nat Immunol*. 2001;2:165-171

103. Yan SF, Fujita T, Lu J, Okada K, Shan Zou Y, Mackman N, Pinsky DJ, Stern DM. Egr-1, a master switch coordinating upregulation of divergent gene families underlying ischemic stress. *Nat Med*. 2000;6:1355-1361

104. Kang JH, Kim MJ, Ko SH, Jeong IK, Koh KH, Rhie DJ, Yoon SH, Hahn SJ, Kim MS, Jo YH. Upregulation of rat ccnd1 gene by exendin-4 in pancreatic beta cell line ins-1: Interaction of early growth response-1 with cis-regulatory element. *Diabetologia*. 2006;49:969-979

105. Fahmy RG, Khachigian LM. Suppression of growth factor expression and human vascular smooth muscle cell growth by small interfering rna targeting egr-1. *J Cell Biochem*. 2007;100:1526-1535

106. Cattaruzza M. Role of zfm1 in smooth muscle cell phenotype regulation. *Joint meeting of the German and Scandinavian Physiological Societies*. 2010;198:95

107. Joseph LJ, Le Beau MM, Jamieson GA, Jr., Acharya S, Shows TB, Rowley JD, Sukhatme VP. Molecular cloning, sequencing, and mapping of egr2, a human early growth response gene encoding a protein with "zinc-binding finger" structure. *Proc Natl Acad Sci U S A*. 1988;85:7164-7168

108. Sukhatme VP, Cao XM, Chang LC, Tsai-Morris CH, Stamenkovich D, Ferreira PC, Cohen DR, Edwards SA, Shows TB, Curran T, et al. A zinc finger-encoding gene coregulated with c-fos during growth and differentiation, and after cellular depolarization. *Cell*. 1988;53:37-43

109. Topilko P, Schneider-Maunoury S, Levi G, Baron-Van Evercooren A, Chennoufi AB, Seitanidou T, Babinet C, Charnay P. Krox-20 controls myelination in the peripheral nervous system. *Nature*. 1994;371:796-799

110. Tourtellotte WG, Keller-Peck C, Milbrandt J, Kucera J. The transcription factor egr3 modulates sensory axon-myotube interactions during muscle spindle morphogenesis. *Dev Biol*. 2001;232:388-399

111. Safford M, Collins S, Lutz MA, Allen A, Huang CT, Kowalski J, Blackford A, Horton MR, Drake C, Schwartz RH, Powell JD. Egr-2 and egr-3 are negative regulators of t cell activation. *Nature immunology*. 2005;6:472-480

112. Collins S, Lutz MA, Zarek PE, Anders RA, Kersh GJ, Powell JD. Opposing regulation of t cell function by egr-1/nab2 and egr-2/egr-3. *Eur J Immunol*. 2008;38:528-536

113. Taillebourg E, Buart S, Charnay P. Conditional, floxed allele of the krox20 gene. *Genesis*. 2002;32:112-113

114. Ramon HE, Cejas PJ, LaRosa D, Rahman A, Harris JE, Zhang J, Hunter C, Choi Y, Turka LA. Egr-2 is not required for in vivo cd4 t cell mediated immune responses. *PLoS ONE*. 2010;5:e12904

115. Suehiro J, Hamakubo T, Kodama T, Aird WC, Minami T. Vascular endothelial growth factor activation of endothelial cells is mediated by early growth response-3. *Blood*. 2011;115:2520-2532

116. Hogarth CA, Mitchell D, Small C, Griswold M. Egr4 displays both a cell- and intracellular-specific localization pattern in the developing murine testis. *Dev Dyn*. 2010;239:3106-3114

117. Hadziselimovic F, Hadziselimovic NO, Demougin P, Krey G, Hoecht B, Oakeley EJ. Egr4 is a master gene responsible for fertility in cryptorchidism. *Sex Dev*. 2009;3:253-263

118. Tourtellotte WG, Nagarajan R, Auyeung A, Mueller C, Milbrandt J. Infertility associated with incomplete spermatogenic arrest and oligozoospermia in egr4-deficient mice. *Development*. 1999;126:5061-5071
119. Tourtellotte WG, Nagarajan R, Bartke A, Milbrandt J. Functional compensation by egr4 in egr1-dependent luteinizing hormone regulation and leydig cell steroidogenesis. *Mol Cell Biol*. 2000;20:5261-5268
120. Lee SL, Sadovsky Y, Swirnoff AH, Polish JA, Goda P, Gavrilina G, Milbrandt J. Luteinizing hormone deficiency and female infertility in mice lacking the transcription factor ngfi-a (egr-1). *Science*. 1996;273:1219-1221
121. Lee SL, Tourtellotte LC, Wesselschmidt RL, Milbrandt J. Growth and differentiation proceeds normally in cells deficient in the immediate early gene ngfi-a. *J Biol Chem*. 1995;270:9971-9977
122. Chomczynski P, Sacchi N. Single-step method of rna isolation by acid guanidinium thiocyanate-phenol-chloroform extraction. *Anal Biochem*. 1987;162:156-159
123. Deindl E, Boengler K, van Royen N, Schaper W. Differential expression of gapdh and beta3-actin in growing collateral arteries. *Mol Cell Biochem*. 2002;236:139-146
124. Pfaffl MW. A new mathematical model for relative quantification in real-time rt-pcr. *Nucleic Acids Res*. 2001;29:e45
125. Laemmli UK. Cleavage of structural proteins during the assembly of the head of bacteriophage t4. *Nature*. 1970;227:680-685
126. Limbourg A, Korff T, Napp LC, Schaper W, Drexler H, Limbourg FP. Evaluation of postnatal arteriogenesis and angiogenesis in a mouse model of hind-limb ischemia. *Nat Protoc*. 2009;4:1737-1746
127. Herzog S, Sager H, Khmelevski E, Deylig A, Ito WD. Collateral arteries grow from preexisting anastomoses in the rat hindlimb. *Am J Physiol Heart Circ Physiol*. 2002;283:H2012-2020
128. Ito WD, Arras M, Scholz D, Winkler B, Htun P, Schaper W. Angiogenesis but not collateral growth is associated with ischemia after femoral artery occlusion. *Am J Physiol.* 1997;273:H1255-1265
129. Unthank JL, Fath SW, Burkhart HM, Miller SC, Dalsing MC. Wall remodeling during luminal expansion of mesenteric arterial collaterals in the rat. *Circ Res*. 1996;79:1015-1023
130. Schierling W, Troidl K, Mueller C, Troidl C, Wustrack H, Bachmann G, Kasprzak PM, Schaper W, Schmitz-Rixen T. Increased intravascular flow rate triggers cerebral arteriogenesis. *J Cereb Blood Flow Metab*. 2009
131. Deindl E, Buschmann I, Hoefer IE, Podzuweit T, Boengler K, Vogel S, van Royen N, Fernandez B, Schaper W. Role of ischemia and of hypoxia-inducible genes in arteriogenesis after femoral artery occlusion in the rabbit. *Circ Res*. 2001;89:779-786
132. Baffour R, Berman J, Garb JL, Rhee SW, Kaufman J, Friedmann P. Enhanced angiogenesis and growth of collaterals by in vivo administration of recombinant basic fibroblast growth factor in a rabbit model of acute lower limb ischemia: Dose-response effect of basic fibroblast growth factor. *J Vasc Surg*. 1992;16:181-191
133. Pipp F, Heil M, Issbrucker K, Ziegelhoeffer T, Martin S, van den Heuvel J, Weich H, Fernandez B, Golomb G, Carmeliet P, Schaper W, Clauss M. Vegfr-1-selective vegf homologue plgf is arteriogenic: Evidence for a monocyte-mediated mechanism. *Circ Res*. 2003;92:378-385
134. Sayed A, Schierling W, Troidl K, Ruding I, Nelson K, Apfelbeck H, Benli I, Schaper W, Schmitz-Rixen T. Exercise linked to transient increase in expression and activity of cation channels in newly formed hind-limb collaterals. *Eur J Vasc Endovasc Surg*. 2010;40:81-87
135. Degabriele NM, Griesenbach U, Sato K, Post MJ, Zhu J, Williams J, Jeffery PK, Geddes DM, Alton EW. Critical appraisal of the mouse model of myocardial infarction. *Exp Physiol*. 2004;89:497-505
136. Unger EF. Experimental evaluation of coronary collateral development. *Cardiovasc Res*. 2001;49:497-506
137. Tuzun E, Oliveira E, Narin C, Khalil H, Jimenez-Quevedo P, Perin E, Silva G. Correlation of ischemic area and coronary flow with ameroid size in a porcine model. *J Surg Res*. 2010;164:38-42
138. Scholz D, Ziegelhoeffer T, Helisch A, Wagner S, Friedrich C, Podzuweit T, Schaper W. Contribution of arteriogenesis and angiogenesis to postocclusive hindlimb perfusion in mice. *J Mol Cell Cardiol*. 2002;34:775-787

139. Helisch A, Wagner S, Khan N, Drinane M, Wolfram S, Heil M, Ziegelhoeffer T, Brandt U, Pearlman JD, Swartz HM, Schaper W. Impact of mouse strain differences in innate hindlimb collateral vasculature. *Arterioscler Thromb Vasc Biol*. 2006;26:520-526
140. Kyriakides ZS, Petinakis P, Kaklamanis L, Lyras T, Sbarouni E, Karayannakos P, Iliopoulos D, Kremastinos DT. Gender does not influence angiogenesis and arteriogenesis in a rabbit model of chronic hind limb ischemia. *Int J Cardiol*. 2003;92:83-91
141. Peng X, Wang J, Lassance-Soares RM, Najafi AH, Sood S, Aghili N, Alderman LO, Panza JA, Faber JE, Wang S, Epstein SE, Burnett MS. Gender differences affect blood flow recovery in a mouse model of hindlimb ischemia. *Am J Physiol Heart Circ Physiol*. 2011;300:H2027-2034
142. Brevetti G, Bucur R, Balbarini A, Melillo E, Novo S, Muratori I, Chiariello M. Women and peripheral arterial disease: Same disease, different issues. *J Cardiovasc Med (Hagerstown)*. 2008;9:382-388
143. Wolf C, Cai WJ, Vosschulte R, Koltai S, Mousavipour D, Scholz D, Afsah-Hedjri A, Schaper W, Schaper J. Vascular remodeling and altered protein expression during growth of coronary collateral arteries. *J Mol Cell Cardiol*. 1998;30:2291-2305
144. Cai WJ, Kocsis E, Wu X, Rodriguez M, Luo X, Schaper W, Schaper J. Remodeling of the vascular tunica media is essential for development of collateral vessels in the canine heart. *Mol Cell Biochem*. 2004;264:201-210
145. Bergmann CE, Hoefer IE, Meder B, Roth H, van Royen N, Breit SM, Jost MM, Aharinejad S, Hartmann S, Buschmann IR. Arteriogenesis depends on circulating monocytes and macrophage accumulation and is severely depressed in op/op mice. *J Leukoc Biol*. 2006;80:59-65
146. Chen Z, Rubin J, Tzima E. Role of pecam-1 in arteriogenesis and specification of preexisting collaterals. *Circ Res*. 2010
147. Belin de Chantemele EJ, Vessieres E, Dumont O, Guihot AL, Toutain B, Loufrani L, Henrion D. Reactive oxygen species are necessary for high flow (shear stress)-induced diameter enlargement of rat resistance arteries. *Microcirculation*. 2009;16:391-402
148. Dumont O, Loufrani L, Henrion D. Key role of the no-pathway and matrix metalloprotease-9 in high blood flow-induced remodeling of rat resistance arteries. *Arterioscler Thromb Vasc Biol*. 2007;27:317-324
149. Hemish J, Nakaya N, Mittal V, Enikolopov G. Nitric oxide activates diverse signaling pathways to regulate gene expression. *J Biol Chem*. 2003;278:42321-42329
150. Nose K, Ohba M. Functional activation of the egr-1 (early growth response-1) gene by hydrogen peroxide. *Biochem J*. 1996;316 (Pt 2):381-383
151. Huang RP, Adamson ED. Characterization of the DNA-binding properties of the early growth response-1 (egr-1) transcription factor: Evidence for modulation by a redox mechanism. *DNA Cell Biol*. 1993;12:265-273
152. Tell G, Quadrifoglio F, Tiribelli C, Kelley MR. The many functions of ape1/ref-1: Not only a DNA repair enzyme. *Antioxid Redox Signal*. 2009;11:601-620
153. Izumi T, Henner WD, Mitra S. Negative regulation of the major human ap-endonuclease, a multifunctional protein. *Biochemistry*. 1996;35:14679-14683
154. Khachigian LM. Early growth response-1: Blocking angiogenesis by shooting the messenger. *Cell Cycle*. 2004;3:10-11
155. Grundmann S, Hoefer I, Ulusans S, Bode C, Oesterle S, Tijssen JG, Piek JJ, Buschmann I, van Royen N. Granulocyte-macrophage colony-stimulating factor stimulates arteriogenesis in a pig model of peripheral artery disease using clinically applicable infusion pumps. *J Vasc Surg*. 2006;43:1263-1269
156. Cullen EM, Brazil JC, O'Connor CM. Mature human neutrophils constitutively express the transcription factor egr-1. *Mol Immunol*. 2010;47:1701-1709
157. Schmidt J, Stoffels B, Moore BA, Chanthaphavong RS, Mazie AR, Buchholz BM, Bauer AJ. Proinflammatory role of leukocyte-derived egr-1 in the development of murine postoperative ileus. *Gastroenterology*. 2008;135:926-936, 936 e921-922
158. Krishnaraju K, Hoffman B, Liebermann DA. Early growth response gene 1 stimulates development of hematopoietic progenitor cells along the macrophage lineage at the expense of the granulocyte and erythroid lineages. *Blood*. 2001;97:1298-1305
159. Gururajan M, Simmons A, Dasu T, Spear BT, Calulot C, Robertson DA, Wiest DL, Monroe JG, Bondada S. Early growth response genes regulate b cell development, proliferation, and immune response. *J Immunol*. 2008;181:4590-4602

160. Lohoff M, Giaisi M, Kohler R, Casper B, Krammer PH, Li-Weber M. Early growth response protein-1 (egr-1) is preferentially expressed in t helper type 2 (th2) cells and is involved in acute transcription of the th2 cytokine interleukin-4. *J Biol Chem*. 2010;285:1643-1652
161. Forlow SB, White EJ, Barlow SC, Feldman SH, Lu H, Bagby GJ, Beaudet AL, Bullard DC, Ley K. Severe inflammatory defect and reduced viability in cd18 and e-selectin double-mutant mice. *J Clin Invest*. 2000;106:1457-1466
162. Lee SL, Wang Y, Milbrandt J. Unimpaired macrophage differentiation and activation in mice lacking the zinc finger transplantation factor ngfi-a (egr1). *Mol Cell Biol*. 1996;16:4566-4572
163. Kubosaki A, Tomaru Y, Tagami M, Arner E, Miura H, Suzuki T, Suzuki M, Suzuki H, Hayashizaki Y. Genome-wide investigation of in vivo egr-1 binding sites in monocytic differentiation. *Genome Biol*. 2009;10:R41
164. Wieland GD, Nehmann N, Muller D, Eibel H, Siebenlist U, Suhnel J, Zipfel PF, Skerka C. Early growth response proteins egr-4 and egr-3 interact with immune inflammatory mediators nf-kappab p50 and p65. *J Cell Sci*. 2005;118:3203-3212
165. Heil M, Ziegelhoeffer T, Wagner S, Fernandez B, Helisch A, Martin S, Tribulova S, Kuziel WA, Bachmann G, Schaper W. Collateral artery growth (arteriogenesis) after experimental arterial occlusion is impaired in mice lacking cc-chemokine receptor-2. *Circ Res*. 2004;94:671-677
166. Patwardhan S, Gashler A, Siegel MG, Chang LC, Joseph LJ, Shows TB, Le Beau MM, Sukhatme VP. Egr3, a novel member of the egr family of genes encoding immediate-early transcription factors. *Oncogene*. 1991;6:917-928
167. Crosby SD, Puetz JJ, Simburger KS, Fahrner TJ, Milbrandt J. The early response gene ngfi-c encodes a zinc finger transcriptional activator and is a member of the gcgggggcg (gsg) element-binding protein family. *Mol Cell Biol*. 1991;11:3835-3841
168. Tourtellotte WG, Milbrandt J. Sensory ataxia and muscle spindle agenesis in mice lacking the transcription factor egr3. *Nat Genet*. 1998;20:87-91
169. Kumbrink J, Kirsch KH, Johnson JP. Egr1, egr2, and egr3 activate the expression of their coregulator nab2 establishing a negative feedback loop in cells of neuroectodermal and epithelial origin. *J Cell Biochem*. 2010;111:207-217
170. Swirnoff AH, Milbrandt J. DNA-binding specificity of ngfi-a and related zinc finger transcription factors. *Mol Cell Biol*. 1995;15:2275-2287
171. Zipfel PF, Decker EL, Holst C, Skerka C. The human zinc finger protein egr-4 acts as autoregulatory transcriptional repressor. *Biochim Biophys Acta*. 1997;1354:134-144
172. Weinberg RA. The retinoblastoma protein and cell cycle control. *Cell*. 1995;81:323-330
173. Coqueret O. Linking cyclins to transcriptional control. *Gene*. 2002;299:35-55
174. Witzel, II, Koh LF, Perkins ND. Regulation of cyclin d1 gene expression. *Biochem Soc Trans*. 2010;38:217-222
175. Xiao D, Chinnappan D, Pestell R, Albanese C, Weber HC. Bombesin regulates cyclin d1 expression through the early growth response protein egr-1 in prostate cancer cells. *Cancer Res*. 2005;65:9934-9942
176. Han W, Liu GN. Egr-1 decoy odns inhibit vascular smooth muscle cell proliferation and neointimal hyperplasia of balloon-injured arteries in rat. *Life Sci*. 2010;86:234-243
177. Amano M, Chihara K, Kimura K, Fukata Y, Nakamura N, Matsuura Y, Kaibuchi K. Formation of actin stress fibers and focal adhesions enhanced by rho-kinase. *Science*. 1997;275:1308-1311
178. Olson MF, Ashworth A, Hall A. An essential role for rho, rac, and cdc42 gtpases in cell cycle progression through g1. *Science*. 1995;269:1270-1272
179. Whitmarsh AJ, Shore P, Sharrocks AD, Davis RJ. Integration of map kinase signal transduction pathways at the serum response element. *Science*. 1995;269:403-407
180. Vickers ER, Kasza A, Kurnaz IA, Seifert A, Zeef LA, O'Donnell A, Hayes A, Sharrocks AD. Ternary complex factor-serum response factor complex-regulated gene activity is required for cellular proliferation and inhibition of apoptotic cell death. *Mol Cell Biol*. 2004;24:10340-10351
181. Li S, Wang DZ, Wang Z, Richardson JA, Olson EN. The serum response factor coactivator myocardin is required for vascular smooth muscle development. *Proc Natl Acad Sci U S A*. 2003;100:9366-9370
182. Wang DZ, Li S, Hockemeyer D, Sutherland L, Wang Z, Schratt G, Richardson JA, Nordheim A, Olson EN. Potentiation of serum response factor activity by a family of myocardin-related transcription factors. *Proc Natl Acad Sci U S A*. 2002;99:14855-14860

183. Guettler S, Vartiainen MK, Miralles F, Larijani B, Treisman R. Rpel motifs link the serum response factor cofactor mal but not myocardin to rho signaling via actin binding. *Mol Cell Biol*. 2008;28:732-742

184. Hinson JS, Medlin MD, Lockman K, Taylor JM, Mack CP. Smooth muscle cell-specific transcription is regulated by nuclear localization of the myocardin-related transcription factors. *Am J Physiol Heart Circ Physiol*. 2007;292:H1170-1180

185. Morita T, Mayanagi T, Sobue K. Reorganization of the actin cytoskeleton via transcriptional regulation of cytoskeletal/focal adhesion genes by myocardin-related transcription factors (mrtfs/mal/mkls). *Exp Cell Res*. 2007;313:3432-3445

186. Yang N, Higuchi O, Ohashi K, Nagata K, Wada A, Kangawa K, Nishida E, Mizuno K. Cofilin phosphorylation by lim-kinase 1 and its role in rac-mediated actin reorganization. *Nature*. 1998;393:809-812

187. Vazquez-Padron RI, Mateu D, Rodriguez-Menocal L, Wei Y, Webster KA, Pham SM. Novel role of egr-1 in nicotine-related neointimal formation. *Cardiovasc Res*. 2010;88:296-303

188. Seiler C, Pohl T, Wustmann K, Hutter D, Nicolet PA, Windecker S, Eberli FR, Meier B. Promotion of collateral growth by granulocyte-macrophage colony-stimulating factor in patients with coronary artery disease: A randomized, double-blind, placebo-controlled study. *Circulation*. 2001;104:2012-2017

189. van Royen N, Schirmer SH, Atasever B, Behrens CY, Ubbink D, Buschmann EE, Voskuil M, Bot P, Hoefer I, Schlingemann RO, Biemond BJ, Tijssen JG, Bode C, Schaper W, Oskam J, Legemate DA, Piek JJ, Buschmann I. Start trial: A pilot study on stimulation of arteriogenesis using subcutaneous application of granulocyte-macrophage colony-stimulating factor as a new treatment for peripheral vascular disease. *Circulation*. 2005;112:1040-1046

190. Simons M, Annex BH, Laham RJ, Kleiman N, Henry T, Dauerman H, Udelson JE, Gervino EV, Pike M, Whitehouse MJ, Moon T, Chronos NA. Pharmacological treatment of coronary artery disease with recombinant fibroblast growth factor-2: Double-blind, randomized, controlled clinical trial. *Circulation*. 2002;105:788-793

191. Grines CL, Watkins MW, Mahmarian JJ, Iskandrian AE, Rade JJ, Marrott P, Pratt C, Kleiman N. A randomized, double-blind, placebo-controlled trial of ad5fgf-4 gene therapy and its effect on myocardial perfusion in patients with stable angina. *J Am Coll Cardiol*. 2003;42:1339-1347

192. Seiler C, Fleisch M, Garachemani A, Meier B. Coronary collateral quantitation in patients with coronary artery disease using intravascular flow velocity or pressure measurements. *J Am Coll Cardiol*. 1998;32:1272-1279

193. Meier P, Gloekler S, Zbinden R, Beckh S, de Marchi SF, Zbinden S, Wustmann K, Billinger M, Vogel R, Cook S, Wenaweser P, Togni M, Windecker S, Meier B, Seiler C. Beneficial effect of recruitable collaterals: A 10-year follow-up study in patients with stable coronary artery disease undergoing quantitative collateral measurements. *Circulation*. 2007;116:975-983

194. Pagonas N, Utz W, Schulz-Menger J, Busjahn A, Monti J, Thierfelder L, Dietz R, Klauss V, Gross M, Buschmann IR, Buschmann EE. Assessment of the effect of external counterpulsation on myocardial adaptive arteriogenesis by invasive functional measurements--design of the arteriogenesis network trial 2. *International journal of cardiology*. 2010;145:432-437

195. Vogel R, Traupe T, Steiger VS, Seiler C. Physical coronary arteriogenesis: A human "model" of collateral growth promotion. *Trends Cardiovasc Med*. 2010;20:129-133

196. Buschmann EE, Utz W, Pagonas N, Schulz-Menger J, Busjahn A, Monti J, Maerz W, le Noble F, Thierfelder L, Dietz R, Klauss V, Gross M, Buschmann IR. Improvement of fractional flow reserve and collateral flow by treatment with external counterpulsation (art.Net.-2 trial). *Eur J Clin Invest*. 2009;39:866-875

197. Shin IS, Kim JM, Kim KL, Jang SY, Jeon ES, Choi SH, Kim DK, Suh W, Kim YW. Early growth response factor-1 is associated with intraluminal thrombus formation in human abdominal aortic aneurysm. *J Am Coll Cardiol*. 2009;53:792-799

198. Vogel S, Kubin T, von der Ahe D, Deindl E, Schaper W, Zimmermann R. Mek hyperphosphorylation coincides with cell cycle shut down of cultured smooth muscle cells. *J Cell Physiol*. 2006;206:25-34

199. Ahimastos AA, Latouche C, Natoli AK, Reddy-luthmoodoo M, Golledge J, Kingwell BA. Potential vascular mechanisms of ramipril induced increases in walking ability in patients with intermittent claudication. *Circ Res.* 2014;114(7):1144-55.

X. LIST OF ABBREVIATIONS

A./a.	arteria
ADP	adenosine diphosphate
AMP	adenosine monophosphate
AMV-RT	avian myeloblastosis virus reverse transcriptase
Ang-1	Angiopoietin-1
AP1	APETALA1/activating protein 1
APE1	apurinic/apyrimidinic endonuclease 1
ATP	adenosine triphosphate
αSM-actin	alpha-smooth muscle actin
BCA	bicinchoninic acid
bp	base pairs
BSA	bovine serum albumine
cAMP	cyclic adenosine monophosphate
carp	cardiac ankyrin repeat protein
CCD	charge-coupled device
CCL2	CC-chemokine ligand 2
CCR-2	CC-chemokine receptor 2
CD	cluster of differentiation
Cdc20	cell division cycle 20
CDK	cyclin dependent kinase
CFIp	pressure- derived collateral flow index
CP	crossing point for targets
CpR	crossing point for reference gene
CpT	crossing point for targets
CREB	CRE binding protein
CREs	cyclic adenosine monophosphate (cAMP) response elements
CVDs	cardiovascular diseases
CWS	circumferential wall stress
DAB	3,3′-diaminobencidine
DBD	DNA binding domain
ddH_20	double distilled water
DNA	desoxribonucleic acid
dNTP	desoxyribonukleoside triphosphate
DTT	dithiothreitol
E2F	elongation factor 2
EBS	early growth response binding sequence
EC	endothelial cell
ECG	electrocardiography
ECM	extracellular matrix
ECP	external counter pulsation
EDTA	ethylenediaminetetraacetate
Egr1	early growth response-1 gene symbol in mouse
EGR1	early growth response-1 gene and protein symbol in humans, protein symbol in mouse
$Egr1^{-/-}$	early growth response-1 deficient
EGTA	ethyleneglycoltetraacetate
ELISA	enzyme-linked immunosorbent assay
Elk-1	Ets like gene 1
eNOS	endothelial nitric oxide synthase
EPCs	endothelial precursor cells
ERK1/2	extracellular signal- regulated kinase 1/2
Ets	E-twenty six transcription factor
FACS	fluorescence activated cell
FDA	United States Food and Drug Association
FGF	fibroblast growth factor
FITC	fluorescein isothiocyanate
Flk1	fetal liver kinase 1
Flt1	fms related tyrosine kinase1 (VEGF receptor)
FNA	flumazenile, naloxone, atipamezole
FSS	fluid shear stress
G-actin	globular actin
G-protein	guanine nucleotide-binding protein
GAPDH	glyceraldehyde 3-phosphate dehydrogenase
GF	growth factors
GMCSF	granulocyte macrophage colony stimulating factor
GnRH	gonadotropin-releasing hormone
GTPase	small guanosine triphosphatase
h	hour(s)
HASMC	human aortic smooth muscle cells
HIF-1	inducible transcription factor 1
i.p.	intraperitoneal
ICAM-1	intercellular adhesion molecule 1
ID	inner diameter
IF	immunofluorescence

IHC	immunohistochemistry	PCNA	proliferating cell nuclear antigen
IL	interleukin		
KCL	potassium chloride	PDGF	platelet-derived GF
kDa	kilodalton	PE	phycoerythrin
LAD	left anterior descending	PECAM-1	platelet endothelial cell adhesion molecule 1
LDI	laser Doppler imaging		
LFA-1	lymphocyte function-associated antigen 1	PMSF	phenylmethanesulfonyl fluoride
		qRT-PCR	quantitative real-time polymerase chain reaction
LH	luteinizing hormone		
LIMK-1	LIM-kinase-1	RANTES	regulated upon activation, normal T-cell expressed, and secreted
LPS	lipopolysaccharides		
mAb	monoclonal antibody		
m.	musculus	Rb	retinoblastoma protein
Mac-1	macrophage-1 antigen	RF	risk factor
Mac-3	macrophage-3 antigen	Rho	Ras homologue
MAPKK/MEK	mitogen-activated protein kinase kinase	ROCK	Rho-associated coiled-coil containing protein kinase
MCP-1	monocyte chemoattractant protein 1	ROI	region of interest
		ROS	reactive oxygen species
MCSF	macrophage colony-stimulating factor	RPEL	RPxxxEL-containing motif
		s.c.	subcutaneous
MEK	mitogen-activated protein kinase kinase	Sap 1/2	SRF accessory protein 1/2
		SDS-PAGE	sodium dodecyl sulfate-polyacrylamide gel electrophoresis
min	minute(s)		
MIPs	macrophage inflammatory proteins	sec	second(s)
MKL	myocardin-like protein	SF-1	splicing factor-1
ml	mililiter	sham	sham operated side
mm	millimeter	siRNA	small interfering RNA
mM	millimolar		sorting
MMF	midazolam, medetomidin, fentanyl (anesthesia)	Sp1	gene-specific activator protein 1
MMPs	matrix metalloproteinases	SRE	serum response element
mRNA	messenger ribonucleic acid	SRF	serum response factor
MRTF	myocardin-related transcription factor	STEMI	ST-segment elevation myocardial infarction
NAB	NGFI-A binding protein	TAE	Tris base, acetic acid EDTA
NaCl	sodium chloride	TBS	Tris buffered saline
NaF	sodium fluoride	TCF	ternary complex factor
NFDM	non-fat dry milk	TCF	ternary complex factors
NFκB	nuclear factor kappa-light-chain-enhancer of activated B cells	TF	transcription factor
		TGF-$ß_1$	transforming growth factor beta 1
NGF	neuronal growth factor	Tie-2	angiopoietin receptor 2
NGFI-A	nerve growth factor inducible A	tPA	tissue plasminogen activator
NLS	nuclear localization sequence	Tris	tris (hydroxymethyl) aminomethane
NO	nitric oxide		
occ	occluded side	uPA	urokinase plasminogen activator
OD	optical density		
P/T	PBS/Triton buffer	uPAR	urokinase plasminogen activator receptor
PAD	peripheral arterial disease		
PBS	phosphate buffered saline	µg	microgram
PCI	percutaneous coronary intervention	µl	microliter
		VCAM-1	vascular cell adhesion mocule1

VEGF	vascular endothelial growth factor
vSMC	vascular smooth muscle cell
WB	western blot
WHO	World Health Organization
WT	wild type

XI. DANKSAGUNG

An erster Stelle geht mein Dank an Frau PD Dr. Elisabeth Deindl vom Walter-Brendel-Zentrum für experimentelle Medizin in München für die Vergabe der Arbeit, ihr Vertrauen und ihre Unterstützung. Ich schulde ihr großen Dank für eine wunderbare Betreuung, während der ich neben einer technischen Ausbildung, vor allem auch eigenständiges wissenschaftliches Arbeiten erlernen durfte.

Hierbei möchte ich auch herzlich dem Leiter des Instituts, Herrn Prof. Dr. Ulrich Pohl danken, der es ermöglichte, die Experimente an seinem Institut durchzuführen.

Des Weiteren möchte ich im Labor in Bad Nauheim Herrn Dr. Mathias Heil sowie seiner technischen Assistentin Frau Sandra Rühl danken, die mir die Methode FACS näher gebracht haben und mit deren Unterstützung die Leukozytendaten entstanden sind. Ebenso danke ich Herrn PD Dr. Tibor Ziegelhoeffer, der mir mit vielen praktischen Tips bei der Etablierung des Laser Doppler Messtechnik geholfen hat.
An der UMC in Utrecht danke ich Herrn Prof. Dr. Imo Höfer und Herrn Dr. Sebastian Grundmann, die mir die Technik der Femoralarterienligatur sowie die Aortenkathetertechnik zeigten.

Ebenso möchte ich der Arbeitsgruppe von Herrn Prof. Dr. Steffen Massberg danken, im Besonderen Frau Dr. Marie-Luise von Brühl, die mir eine erste Einführung in tierexperimentelles Arbeiten gegeben hat und mir vor allem neue Narkosetechniken gezeigt hat.

Am Walter-Brendel-Zentrum für experimentelle Medizin gibt es sehr viele Menschen, denen ich ebenso danken möchte. Zunächst vielen Dank an die technischen Assistentinnen der Arbeitsgruppe von Frau PD Dr. Deindl: Frau Christine Csapo und Frau Mei-Ping Wu, nicht nur aufgrund ihrer exzellenten Arbeit, sondern auch weil sie mir immer mit Rat und Tat zur Seite standen. Mein Dank geht auch an Frau Alke Schropp, die mir die Tür zur Immunhistologie geöffnet hat.
Natürlich möchte ich auch den Doktoranden unserer Arbeitsgruppe für eine großartige Zusammenarbeit im Team danken: Frau Julia Borgolte, Frau Teresa Trenkwalder, Herrn Tobias Grantzow, Herrn Philipp Dussmann und Herrn Omary Chillo. Besonders möchte ich hierbei auch Herrn Michael Schubert aus der Arbeitsgruppe von Herrn Prof Dr. Ulrich Pohl danken.

Ebenso danke ich herzlich den gesamten Teammitgliedern von Prof. Dr. Nikolaus Plesnila, die mir gerade am Anfang meiner Arbeit Zugang zu Operationsmikroskopen gewährten und ebenso mit vielen praktischen Tips bei der Modelletablierung halfen.

Schließlich möchte ich gerne den Menschen meine tiefste Dankbarkeit ausdrücken, die mich nicht nur während der Zeit im Labor sondern mein ganzes Leben lang unterstützt und motiviert haben.
Mama, Papa, ihr seid die besten Eltern, die sich ein Kind nur wünschen kann. Habt Dank für all die Liebe, das Vertrauen in mich und die unendliche Unterstützung, die ich von Euch erfahren darf.

XII.EIDESSTATTLICHE VERSICHERUNG

Pagel, Judith-Irina Carola

Ich erkläre hiermit an Eides statt,

dass ich die vorliegende Dissertation mit dem Thema:

“Functional Characterization of the Transcription Factor

Early growth response 1 (Egr1) in Arteriogenesis”

selbstständig verfasst, mich außer der angegebenen keiner weiteren Hilfsmittel bedient und alle Erkenntnisse, die aus dem Schrifttum ganz oder annähernd übernommen sind, als solche kenntlich gemacht und nach ihrer Herkunft unter Bezeichnung der Fundstelle einzeln nachgewiesen habe.

Ich erkläre des Weiteren, dass die hier vorgelegte Dissertation nicht in gleicher oder in ähnlicher Form bei einer anderen Stelle zur Erlangung eines akademischen Grades eingereicht wurde.

München 18.08.2014